Summer 8-6-2018

Coupled Barrier Island Shoreline and Shoreface Dynamics

Benjamin S. Beasley
University of New Orleans, bsbeasle@uno.edu

Coupled Barrier Island Shoreline and Shoreface Dynamics

A Thesis

Submitted to the Graduate Faculty of the
University of New Orleans
in partial fulfillment of the
requirements for the degree of

Master of Science
in
Earth and Environmental Sciences

by

Benjamin Beasley

B.S. University of New Orleans, 2016

August, 2018

Acknowledgements:

Support for this research was provided by the Louisiana Coastal Protection and Restoration Authority (CRPA) through the Coastal Science Assistantship Program (CSAP) administered by the Louisiana Sea Grant (LSA).

First, I would like to thank my major advisor, Dr. Ioannis Georgiou for his encouragement and support throughout the process. Thank you to Dr. Georgiou for believing in me and inspiring me to pursue a graduate degree and for helping to solidify my passion for coastal science in Louisiana. I would also like to thank my committee members, Dr. Michael Miner and Dr. Dirk-Jan Walstra for their kindness, generosity, and thoughtful insights. Thank you to Darin Lee and everyone who has contributed to the Barrier Island Comprehensive Monitoring Program (BICM) which was responsible for the compiling the bathymetric data used in this study. Thank you to Dr. Mark Byrnes and Applied Coastal for providing the most recently available shoreline data for inclusion in this project. I would also like to extend my gratitude to all the faculty and students in the Earth and Environmental Sciences Department at the University of New Orleans for providing a welcoming, collaborative, and inspirational community.

Of course, a very special thank you to my wife and family for their tremendous encouragement, patience, and understanding throughout my academic career.

Table of Contents

List of Figures

ABSTRACT

In Louisiana, barrier islands are undergoing morphological change driven by high rates of relative sea-level rise and interior wetland loss. Previous works utilized historical region-scale bathymetry and shoreline change analyses to assess coastal evolution. However, more localized assessments considering the role of sediment transport processes in regional evolution are lacking. This is essential to predicting coastal change trajectories and allocating limited sand resources for nourishment. Using bathymetric and shoreline data, 100-m spaced shore-normal transects were created to track meter-scale elevation change for 1880s, 1930s, 1980s, 2006, and 2015. An automated framework was used to quantify and track parameters such as shoreline change, barrier island area and width, bathymetric isobath migration, and shoreface slope. Our results illustrate that monitoring subaerial island erosion rates are insufficient for evaluating regional sediment dynamics of transgressive coastal systems. Advances in understanding these processes will facilitate more informed planning, management, and mitigation of transgressive barrier islands.

Keywords: Louisiana, barrier islands, shoreline, shoreface,

INTRODUCTION

Barrier Islands are prominent features along coastlines in many parts of the world and provide significant ecosystem services and economic resources to coastal communities (Barbier et al. 2011). Barrier systems are particularly important in hurricane prone areas by providing protection for the interior marsh and reducing inland flooding through the attenuation of storm surge and the reduction in wave energy arriving inland (Stone and McBride 1998; Georgiou et al. 2005; Bilskie et al. 2016).

Barrier islands worldwide are experiencing transgression, or landward migration, due to shoreface retreat, increasing tidal prism, lack of sediment supply and the rise in relative sea-level (RSL) (Fearnley et al., 2009; FitzGerald et al., 2008; Miner et al., 2009). In response to these factors the barriers islands must either retreat, fragment, or become submerged shoals (Penland et al. 1988a). To mitigate these processes and prolong the subaerial footprint of the barriers, many communities are implementing restoration efforts including beach nourishment, interior and back barrier marsh creation, and the construction of hard structures such as groins, jetties, and levees (Nordstrom 2014). Although some of these efforts are successful in temporarily maintaining or increasing the barrier island or beach footprint, the fundamental processes causing barrier deterioration, continue to be present and having an impact. With the predictions of increases in the rates of sea level rise (Ranasinghe and Stive 2009; Church et al. 2013; Kopp et al. 2016), many barrier systems will require greater level of intervention to continue to serve the important ecological services and physical protection from storm impacts (Aagaard and Sørensen 2012). The understanding of how transgressive barrier islands respond to forcings such as sea level rise and changes in sediment supply is crucial to the

implementation of the appropriate restoration or adaptation strategies (Cooper and Pilkey 2004). Although much of the analysis of barrier systems primarily focused on shoreline and subaerial portions of the island, changes in the geometry of the shoreface can influence the longevity of the barriers (Bruun, 1962; Swift, 1975).

The objectives of this study are to 1) track and quantify historic changes barrier island evolution parameters such as shoreline change, width, bathymetric contour migration, and shoreface slope, from region-scale historic bathymetric and shoreline data over 135-year period along the rapidly transgressing Louisiana coast and 2) to evaluate barrier trajectory within the context of the processes driving regional coastal change.

Chapter 1 will provide background information about the study area to and shoreface/barrier dynamics to establish the basis for this study.

Chapter 2 is an in-depth evaluation of the Late Lafourche delta lobe in terms of the mode of transgression, storm response, and coastal straightening implications on the long-term evolution trajectory and sediment budget of the Caminada Headland and the down-drift Timbalier Island. This chapter will address two key hypotheses:

- **H1: Coastal straightening**
    - Regional coastal straightening influences shoreface trajectory by reducing local erosion and deposition potential resulting in homogenized shoreface geometry.
- **H2: Storm influence**
    - Shoreface geometry is strongly influenced by storm frequency and magnitude.

Chapter 3 will test the coupling of barrier island shoreline and the shoreface. Utilizing a tool developed in this study, barrier island and shoreface metrics provide the basis for the analysis along the Louisiana coast, through use of case studies that span from the delta lobe scale to the barrier island scale. Locations where restoration projects have been implemented are utilized as case studies to gain insight into restoration planning and management, though analysis of historic barrier and shoreface behavior. This chapter will address two hypotheses:

- **H3: Barrier island shoreline / shoreface coupling**
    - Barrier island shoreline trajectory is influenced by the trajectory and geometry of the shoreface.
- **H4: Restoration / management implications**
    - Barrier island restoration and management decisions should consider the long-term regional trajectory and geometry of the shoreface influences on the regional and local sediment budgets.

CHAPTER 1: BACKGROUND

Study Area:

In southeast Louisiana, barriers are found on both sides of the modern Mississippi River on the Mississippi River Delta Plain (MRDP). This region is experiencing rapid geomorphic change including widespread land loss (Barras et al. 2004; Couvillion et al. 2016), and a shrinking barrier island system, with historic average shoreline erosion rates ranging from 1-11m/yr. (Martinez et al. 2009; Byrnes et al. 2017). These barriers are the product of reworked sandy deposits that are the remains of the abandoned distributary lobes of the Mississippi River (Penland et al. 1988a). High rates of RSL (~0.92cm/yr.), an increase in strong storm activity, and reduction of sediment supply, have made this coastline especially vulnerable (Georgiou et al. 2005b; Fearnley et al. 2009; Miner et al. 2009).

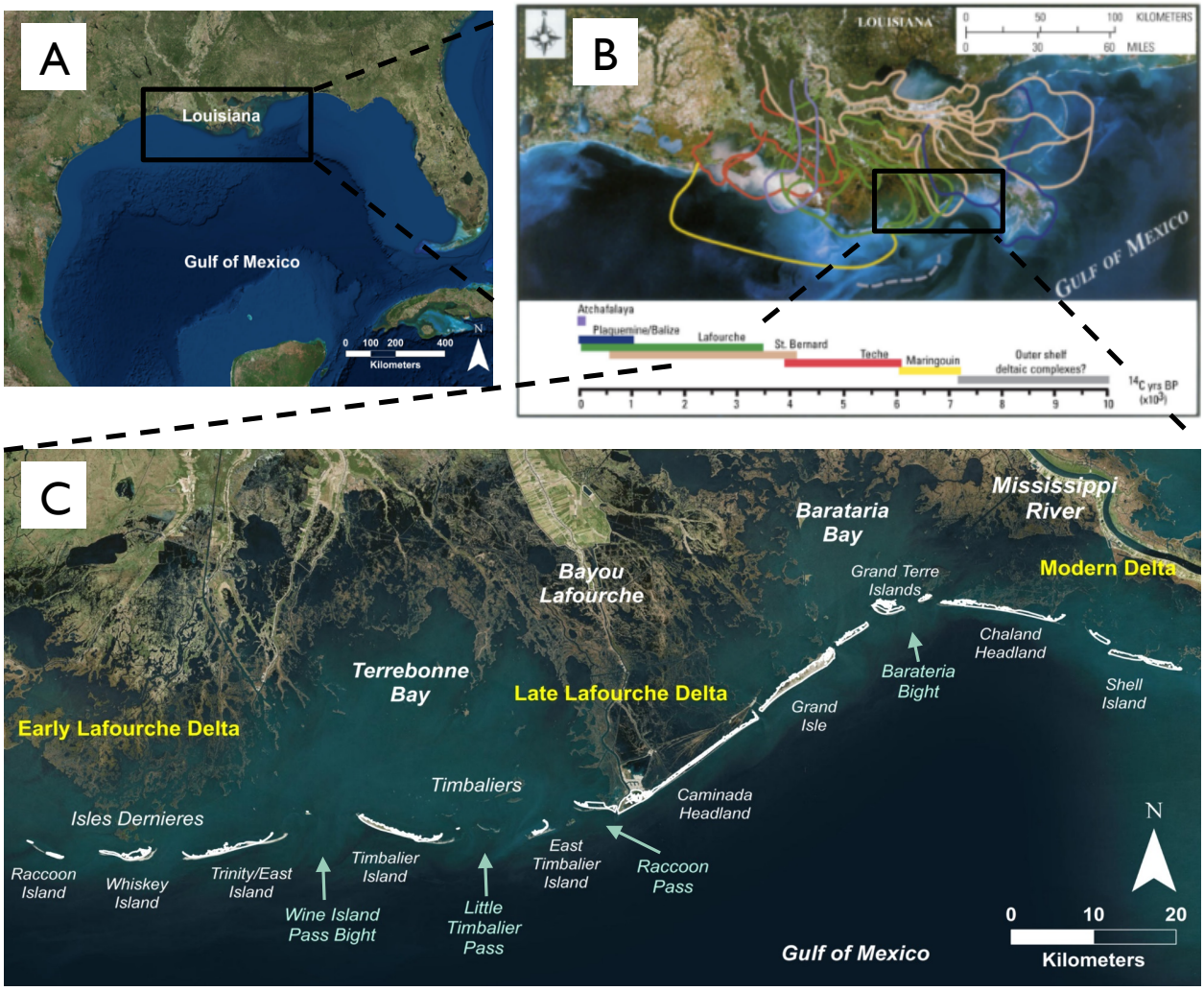

Figure 1: Map showing A) Gulf of Mexico with Mississippi River Delta and B) historic evolution of the delta lobes of Mississippi River (Kulp et al. 2005) and C) barrier island chains west of the modern delta.

This study covers 160 km of the south-central Louisiana coast, west of the Mississippi River, in Terrebonne, Lafourche, Jefferson, and Plaquemines Parishes, including the Isle Dernieres barrier island chain to the west to Pelican Island to the east (Fig. 1). These island chains and headlands are eroding and thinning (transgressive submergence) due to limited sediment supply, interior wetland loss, and high rates of relative sea level rise (FitzGerald et al.

2004; FitzGerald et al. 2007; Miner et al. 2009). The prominent eroding Caminada Headland and flanking barrier islands are the remains of the Bayou Lafourche complex (active 1800-300 years B.P.), while the areas to the east are the result the reworking of the older St. Bernard lobe (3,500-1,800 years B.P.), and the modern Plaquemines/Belize delta lobe (1,000 years B.P. to present) (Fig. 1B) (Frazier, 1967; Kulp et al., 2005; Miner et al., 2009).

Most of these islands have undergone restoration by mechanical introduction of sediment for beach, dune, and back barrier marsh nourishment and enhancement projects using over 3.1×10^7 m^3 of sediment to create an estimated 80 km of barrier islands and berms that have been constructed just since 2007 (CPRA 2017). There have also been attempts at shoreline protection using segmented breakwaters and seawalls along some sectors of coast including Raccoon Island, East Timbalier Island, central Caminada Headland, and Grand Isle.

Table 1: Barrier Island restoration projects for the central coast of Louisiana showing volumes (m3) of material used for each project. Projects are grouped by delta lobe and volumes are totaled for pre/post 2006 (adapted from CPRA 2017).

	Construction Date	Volume m3	Pre 2006	Post 2006
Early Lafourche Delta Region *(Raccoon Island to Wine Island)*				
Raccoon Island Repair and Restoration Project (TE-106)	1994			
Raccoon Island Breakwaters Demonstration (TE-29)	1997			
Whiskey Island Restoration (TE-27)	1999	4.51E+06		
Isles Dernieres Restoration East Island (TE-20)	1999	2.98E+06		
Isles Dernieres Restoration Trinity Island (TE-24)	1999	3.71E+06	**1.12E+07**	
Raccoon Island Shoreline Protection/Marsh Creation (TE-48)	2007	5.62E+05		
New Cut Dune and Marsh Restoration Project (TE-37)	2007	6.56E+05		
Whiskey Island Back Barrier Marsh Creation (TE-50)	2009	2.00E+06		
Raccoon Island Shoreline Protection and Marsh Creation (TE-48, part 2)	2013	5.62E+05		**3.78E+06**
Late Lafourche Delta Region *(Timbalier to East Grand Terre Island)*				
Timbalier Island Planting Demonstration (TE-18)	1996			
East Timbalier Island Sediment Restoration, Phase 1 (TE-25 and 30)	2000	2.02E+06		
Planting of a Dredged Material Disposal Site on Grand Terre Island (BA-28)	2001			
Timbalier Island Dune and Marsh Creation (TE-40)	2004	3.52E+06	**5.54E+06**	
East Grand Terre Island Restoration (BA-30)	2010	2.40E+06		
Bayside Segmented Breakwaters at Grand Isle (BA-50)	2012	2.56E+06		
West Belle Pass Barrier Headland Restoration (Te-52)	2012	3.18E+06		
Caminada Headland Beach and Dune Restoration (BA-45)	2015	2.20E+06		
Caminada Headland Beach and Dune Restoration INCR2 (BA143)	2015	3.78E+06		**1.41E+07**
Modern Delta Region *(East Grand Terre to Sandy Point)*				
Pass La Mer to Chaland Pass Restoration (BA-38, part 1)	2007	2.88E+06		
Pass Chaland to Grand Bayou Pass Barrier Shoreline Restoration (BA-35)	2008	1.90E+06		
Emergency Berms W8,W9,W10	2010-2011			
Pelican Island and Pass (BA-38, part 2)	2012	1.90E+06		
Riverine Sand Mining/Scofield Island Restoration (BA-40)	2013	2.58E+06		**9.25E+06**
	Total =	**4.39E+07**	**1.67E+07**	**2.72E+07**

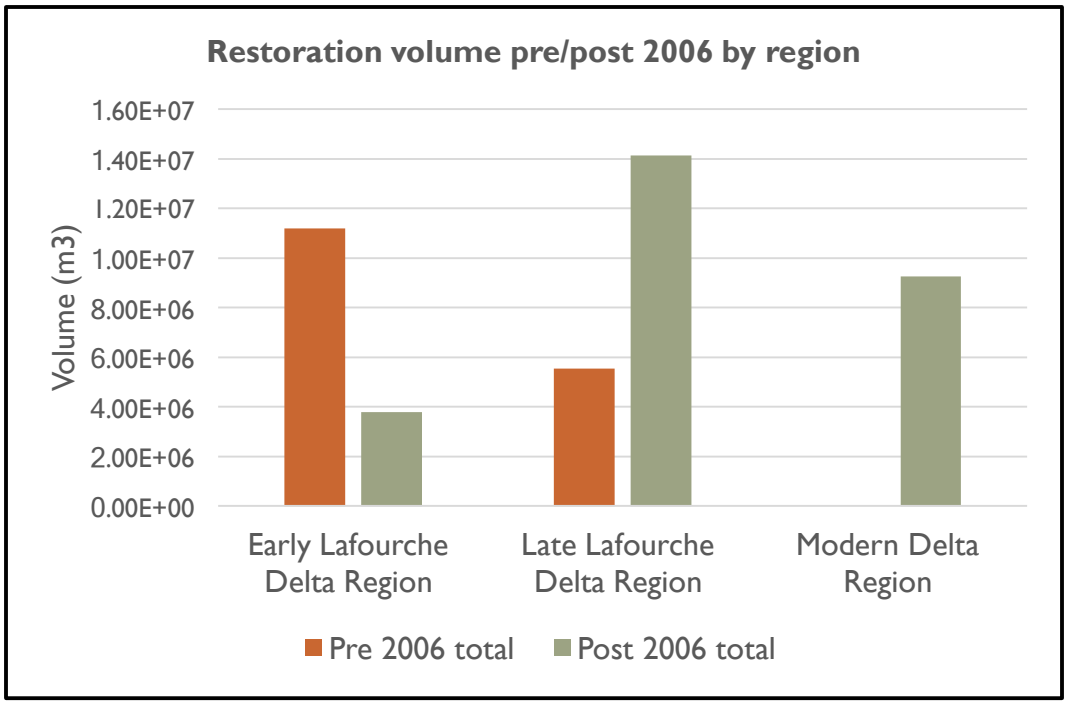

Figure 2: Barrier Island restoration projects for the central coast of Louisiana showing volumes (m3) of material used for each project. Projects are grouped by delta lobe and volumes are totaled for pre/post 2006 (adapted from CPRA 2017).

Barrier Islands:

Barriers islands are accumulations of sediment that are built vertically due to wave action and wind processes. Most barriers are linear features and oriented parallel to the coast and are found on every continent except Antarctica, in every type of geologic setting, and in every kind of climate (Davis and FitzGerald 2004). Barriers are most commonly found on trailing margins in the United States and the rest of the world, and they occupy 15% of the world's coastlines (Cooper and Pilkey 2004). Penland et al. (1988) showed that these landforms are formed from reworked delta deposits, whereby channel sands, mouth bars, natural levees are reworked by wave action to form landscapes that resemble arcuate shapes (headlands) with flanking barrier splits. Storms and other oceanographic processes may cause barrier breaching, overwash and/or continue to grow these landscapes (laterally and vertically) until

they detach from mainland by widespread subsidence and wetland loss within the back barrier setting. Meanwhile, the accumulation of sands comprising the developing barrier island, lag this process and maintain subaerial exposure through further reworking to form a robust subaerial landform (a barrier island).

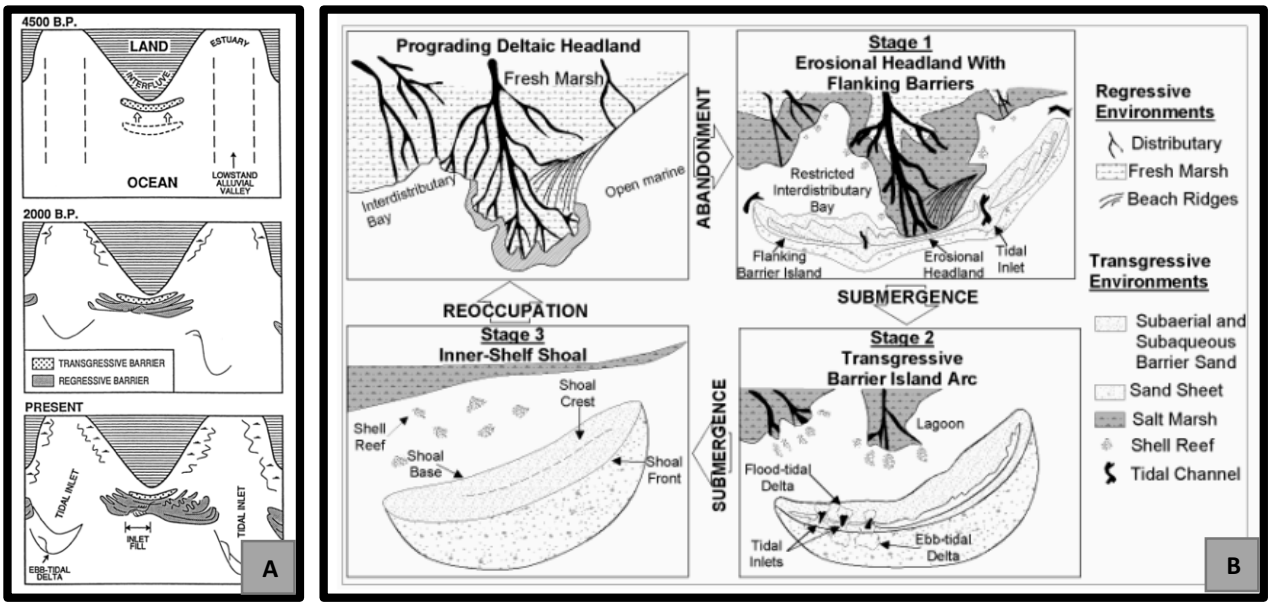

Figure 3**:** Barrier island origin models for transgressive barriers. A) Interfluve model shows the evolution for 4500 years from interfluve and estuary to barriers and inlet system (Hayes, 1994) B) Deltaic headland to inner-shelf shoal model describing the evolution of Louisiana barrier islands (Penland et al. 1988b).

Although there are several theories describing how barrier islands are formed, some early theories include the idea of the erosion and reworking of a prominent headland or interfluve, separating estuaries or bays, giving way to barrier, inlets and tidal deltas (Fig.3A) (Hayes 1994). The Transgressive Mississippi Delta Barrier Model describes a similar process has taken place in Louisiana and shows the specific stages related to how the evolution from a prograding deltaic headland, to an erosional headland with flanking barriers (following an

avulsion event relocating the riverine input of sediment), to a barrier island arc, and finally an inner shelf shoal (Fig. 3B) (Penland et al. 1988b).

Recent analysis using observations spanning a century have increased our understanding of shoreline dynamics and barrier island area response to storms and long-term subsidence (Fearnley et al. 2009). The diminishing supply of sand to the MRDP system - without additional nourishment or opportunities to recycle local or proximal sand from the system – eventually forces barriers to become submerged shoals (Penland et al. 1988b).

Previous Work:

Shoreface:

Previous work has investigated the process of barrier island transgression through the study of the relationship between barrier migration and the morphology of the shoreface (Bruun 1962; Swift 1975; Moore et al. 2010; Wolinsky and Murray 2009; Jaffe et al. 1997; List et al. 1997; Aagaard and Sørensen 2012). The shoreface describes the zone between the shoreline and the continental shelf that is influenced by wave action, from the upper surf-zone to the depth of closure (Swift, 1975; Ortiz et al., 2016). Bruun (1962) established the theory that there is a shoreface profile equilibrium that will remain constant, translating landward and upward, during transgression and there is a linear relationship between sea level rise and shoreline migration rates (Bruun 1962). The Bruun Rule relationship in the simplest form can be written as:

$$s = \frac{al}{h}$$

where *s* is shoreline retreat, *a* is sea level rise, *l* is the distance offshore, and *h* is depth offshore (Bruun 1962; List et al. 1997). Dean (1977) expanded this concept through the application on over 500 locations along the Atlantic coast and used these data derive a coefficient to create the modified Bruun rule (Dean 1977; List et al. 1997). This rule has been used by engineers and coastal planners as a method to predict the rate of shoreline change based on the rate of relative sea level rise (Cooper and Pilkey 2004; Ranasinghe and Stive 2009). However, Cooper and Pilkey (2004) argue that the Bruun rule should be altogether abandoned due to the restrictions inherent in the essential assumptions and the lack of evidence that it will accurately be able to predict shoreline change based on sea level rise. Complicating factors for the viability of implementation of the Bruun rule include: scarcity of long-term consistent data to accurately define the Bruun parameters, insufficient understanding of antecedent geology, and the absence of sediment budget to define the quantities of sediment transferring into and out of the system (List et al. 1997; Moore et al. 2010).

In response to the limitations of the Bruun Rule, researchers have explored how the shoreface/shoreline relationship varies when the profile is not in equilibrium (Wolinsky and Murray 2009; Moore et al. 2010; Lorenzo-Trueba and Ashton 2014). Wolinsky and Murray (2009) discuss the limitations in the application of the Bruun rule and explore the inclusion of and inland topography and shoreface slope variations, it's relationship to the shoreline as well as the inclusion of the morphokinematic Exner equation. The authors modify the Bruun rule theory to create two new scenarios to model gentle slopes or the "barrier Bruun rule" by including the barrier and back-barrier in the slope calculations, and steep slopes "cliff Bruun rule" by accounting for the cliff height in slope calculations, concluding that barrier island slope

is the key factor influencing barrier island trajectories and migration rates instead of the shoreface slope described in the Bruun model (Wolinsky and Murray 2009). Moore et al. (2010) utilized the GEOMBEST model to compare various controls on barrier migration and found that substrate slope, RSL rates, and sediment supply are the main factors. On muddier coasts substrate sediment composition was found to be the dominating control. The combination of average barrier slope and sediment availability, known as the effective barrier island slope determines barrier island trajectory (Moore et al. 2010). The authors also concluded that the rate of migration and shoreface erosion must be balanced so that the amount of sediment liberated from the shoreface is sufficient for the barriers to maintain subaerial exposure, otherwise the barrier is susceptible to transgressive submergence (Penland et al. 1988b; Moore et al. 2010). Aagaard and Sorensen (2014) included sediment transport across the shoreface as a key to improving the ability to model coastal response to RSL and found that the steepness of the profile is essential to determining the direction of cross-shore sediment transport and therefore erosional and transgressive responses (Aagaard and Sørensen 2012). Lorenzo-Trueba and Ashton (2014) explored out of equilibrium shoreface geometry by modeling several modes of barrier behavior as a response to sea level rise including; dynamic equilibrium, height drowning, width drowning and periodic retreat. Their finding suggest that periodic retreat behavior can occur around an equilibrium, and although at millennial time scales barrier systems might be able to return to equilibrium, faced with geologically rapid changes in RSL rates, barrier drowning will become more frequent (Lorenzo-Trueba and Ashton 2014).

These advances have been incorporated in various numerical models, some of which (e.g. UNIBEST-CL) also include the effects of wave driven sediment transport and erosion and

deposition on cross-shore profile dynamics and corresponding coastline response (Rijn et al. 2017). Most models evaluate barrier evolution over millennial scales and field data to validate predictions are lacking due to erosion, retrogradation and other processes driven by sea level cycles. The underlying hypothesis of many models suggests various modes of barrier evolution as a function of the geometry of the shoreface, yet at best only datasets spanning engineering and centennial timescales are available for comparisons. Extrapolating model results from millennial to centennial shoreface behavior may be a risky endeavor without observations. Despite increased understanding from modeling studies at the engineering and millennial timescales, barrier island and shoreface dynamics at the centennial timescale using observations is still lacking. Here we compile bathymetry and shorelines spanning over 135 years, and develop a quantitative framework to analyze and assess the coupling of barrier islands and the shoreface, to test if behaviors reported by modeling studies at the millennial timescale still hold at the centennial timescale.

Shoreface on the MRDP

List et al. (1997) investigated the viability of applying the Bruun rule in predicting shoreline change in the Mississippi River Delta Plain (MRDP) along the central coast of Louisiana west of the modern delta. This site was chosen because high shoreline retreat rates and relative sea level rise have contributed to the rapid morphological change of the barrier islands. The existence of historic bathymetric and shoreline data provided an opportunity to investigate these relationships on barriers at variety of stages of transgression. The authors used sequential bathymetry from NOAA and utilized cross-shore profiles to test the Bruun

equilibrium response. Their results showed that only 50% of the profiles studied showed the Bruun equilibrium criteria and they did not show any statistical significance for hindcasting or predicting shoreline change (List et al. 1997). They also determined that although relative sea level rise plays a role in shoreline change throughout the area, one of the most complicating factors is the inability to define and constrain an accurate enough sediment budget to account for longshore transport and other sediment distribution processes that drive changes in the shoreface and therefore the applicability of the Bruun rule (List et al. 1997).

Jaffe et al. (1997) utilized the same bathymetric and shoreline data for the Louisiana coast to investigate these sediment transport processes such as the offshore sediment bypassing between two barrier systems resulting in a large area of deposition that effectively slowed the erosion rates of the proximal shoreface and shorelines. This offshore shoreface bypassing illustrates a pathway for sediment to naturally nourish downdrift barriers and supports the theory that the amount of sediment on the shoreface plays a role in determining the erosion rates of the proximal shoreline (Jaffe et al. 1997).

Building on the work of List et al. (1994; 1997) and Jaffe et al. (1997), Miner et al. (2009) analyzed seafloor change and documented volumes of sediment eroded from proximal (barrier platform, inlets, ebb-deltas) and distal (shoreface) environments, and highlighted key processes governing sediment loss from the barrier system during transgression. The authors concluded that coastal straightening along the Caminada Headland, mostly in the form of lower shoreface erosion driven by storm induced waves and currents, has been the dominant source of liberated sediment that has been available for reworking and deposition in sinks such as ebb-tidal deltas (Miner et al. 2009).

Despite the advancements by List et al. (1997), Jaffe et al. (1997) and Miner et al. (2009), all of which illustrated the importance of a regional understanding of sediment transport processes and identified the increasing erosion of the Caminada Headlands, the regional implications of a reduction in available sand due to continued shoreface ravinement into fine-grained sediments and variations in shoreface geometry in this transgressive system are not well defined. Localized assessments considering the role of sediment transport pathways and processes in regional evolution are lacking and are essential to predicting coastal change trajectories and allocating limited sand resources for nourishment.

References:

Aagaard, T., & Sørensen, P. (2012). Coastal profile response to sea level rise: A process-based approach. *Earth Surface Processes and Landforms*, *37*(3), 354–362. https://doi.org/10.1002/esp.2271

Barbier, E. B., Hacker, S. D., Kennedy, C., Koch, E. W., Stier, A. C., & Silliman, B. R. (2011). The value of estuarine and coastal ecosystem services. *Ecological Monographs*, *81*(2), 169–193.

Barras, J., Beville, S., Britsch, D., Hartley, S., Hawes, S., Johnston, J., … Suhayda, J. (2004). Historical and Projected Coastal Louisiana Land Changes : 1978-2050. *World*, *334*(January), 45. Retrieved from http://www.louisianaspeaks-parishplans.org/projectattachments/001246/NewHistoricalland.pdf

Bilskie, M. V., Hagen, S. C., Alizad, K., Medeiros, S. C., Passeri, D. L., Needham, H. F., & Cox, A. (2016). Dynamic simulation and numerical analysis of hurricane storm surge under sea level rise with geomorphologic changes along the northern Gulf of Mexico. *Earth's Future*, (April), n/a-n/a. https://doi.org/10.1002/2015EF000347

Bruun, P. (1962). *Sea-level Rise as a Cause of Shore Erosion*. Florida Engineering and Industrial Experiment Station. Retrieved from https://books.google.com/books?id=UJ_iHAAACAAJ

Byrnes, M. R., Berlinghoff, J. L., Griffee, S. F., Underwood, S. G., & Lee, D. M. (2017). Louisiana Barrier Island Comprehensive Monitoring Program (BICM): Phase 2 - Shoreline Compilation and Change Assessment. Prepared for : Louisiana Coastal Protection and Restoration Authority Prepared by : Louisiana Barrier Island Comprehensive Monitorin, (February), 41 p. plus appendices.

Church, J. A., Clark, P. U., Cazenave, A., Gregory, J. M., Jevrejeva, S., Levermann, A., … Unnikrishnan, A. S. (2013). *Sea Level Change. In: Climate Change 2013: The Physical Science Basis. Contribution of Working Group I to the Fifth Assessment Report of the Intergovernmental Panel on Climate Change [Stocker, T.F., D. Qin, G.-K. Plattner, M. Tignor, S.K. Allen, J. Boschu*. Cambridge, UK and New York, NY, USA.

Cooper, J. A. G., & Pilkey, O. H. (2004). Sea-level rise and shoreline retreat: Time to abandon the Bruun Rule. *Global and Planetary Change*, *43*(3–4), 157–171. https://doi.org/10.1016/j.gloplacha.2004.07.001

Couvillion, B. R., Beck, H. J., Schoolmaster, D., & Fischer, M. R. (2016). *Land Area Change in Coastal Louisiana (1932 to 2016)*.

Coastal Protection and Restoration Authority of Louisiana. (2017). *Louisiana's Comprehensive Master Plan for a Sustainable Coast.* Coastal Protection and Restoration Authority of Louisiana. Baton Rouge, LA.

Davis, R. A., & FitzGerald, D. M. (2004). *Beaches and Coasts*. *Estuarine, Coastal and Shelf Science*. Blackwell Science, Oxford, England. https://doi.org/10.1016/j.ecss.2004.11.006

Dean, R. G. (1977). *Equilibrium Beach Profiles: U.S. Atlantic and Gulf Coasts*. Center for Apllied Coastal Research. Retrieved from https://books.google.com/books?id=_bMRywAACAAJ

Fearnley, S. M., Miner, M. D., Kulp, M., Bohling, C., & Penland, S. (2009). Hurricane impact and recovery shoreline change analysis of the Chandeleur Islands, Louisiana, USA: 1855 to 2005. *Geo-Marine Letters*, *29*(6), 455–466. https://doi.org/10.1007/s00367-009-0155-5

FitzGerald, D. M., Fenster, M. S., Argow, B. A., & Buynevich, I. V. (2008). *Coastal Impacts Due to*

Sea-Level Rise. *Annual Review of Earth and Planetary Sciences* (Vol. 36). https://doi.org/10.1146/annurev.earth.35.031306.140139

FitzGerald, D. M., Kulp, M. A., Hughes, Z. J., Georgiou, I. Y., Miner, M. D., Penland, S., & Howes, N. (2007). IMPACTS OF RISING SEA LEVEL TO BACKBARRIER WETLANDS, TIDAL INLETS, AND BARRIER ISLANDS: BARATARIA COAST, LOUISIANA. *Coastal Sediments 07*, *53*(9), 1689–1699. https://doi.org/10.1017/CBO9781107415324.004

Fitzgerald, D. M., Kulp, M., Penland, S., Flocks, J., & Kindinger, J. (2004). Morphologic and stratigraphic evolution of muddy ebb-tidal deltas along a subsiding coast: Barataria Bay, Mississippi River delta. *Sedimentology*, *51*(6), 1157–1178. https://doi.org/10.1111/j.1365-3091.2004.00663.x

Frazier, D. (1967). *Recent Deltaic Deposits of Mississippi River: Their Development and Chronology*. *Aapg Bulletin - AAPG BULL* (Vol. 51). https://doi.org/10.1306/5D25C219-16C1-11D7-8645000102C1865D

Georgiou, I. Y., FitzGerald, D. M., & Stone, G. W. (2005). The Impact of Physical Processes along the Louisiana Coast. *Journal of Coastal Research*, *Sp. Issue*(Figure 1), 72–89. Retrieved from http://www.jstor.org/stable/10.2307/25737050

Hayes, M. O. (1994). The Georgia Bight Barrier System BT - Geology of Holocene Barrier Island Systems. In R. A. Davis (Ed.) (pp. 233–304). Berlin, Heidelberg: Springer Berlin Heidelberg. https://doi.org/10.1007/978-3-642-78360-9_7

Jaffe, B. E., List, J. H., & Sallenger, A. H. (1997). Massive sediment bypassing on the lower shoreface offshore of a wide tidal inlet - Cat Island Pass, Louisiana. *Marine Geology*, *136*(3–4), 131–149. https://doi.org/10.1016/S0025-3227(96)00050-3

Kopp, R. E., Kemp, A. C., Bittermann, K., Horton, B. P., Donnelly, J. P., Gehrels, W. R., … Rahmstorf, S. (2016). Temperature-driven global sea-level variability in the Common Era. *Proceedings of the National Academy of Sciences*, *113*(11), E1434–E1441. https://doi.org/10.1073/pnas.1517056113

Kulp, M. A., Fitzgerald, D. M., & Penland, S. (2005). Sand-rich Lithosomes of the Holocene Mississippi River Delta Plain. In *River Deltas* (pp. 277–294).

List, J. H., Sallenger, A. H., Hansen, M. E., & Jaffe, B. E. (1997). Accelerated relative sea-level rise and rapid coastal erosion: testing a causal relationship for the Louisiana barrier islands. *Marine Geology*, *140*(3–4), 347–365. https://doi.org/10.1016/S0025-3227(97)00035-2

Lorenzo-Trueba, J., & Ashton, A. D. (2014). Rollover, drowning, and discontinuous retreat: Distinct modes of barrier response to sea-level rise arising from a simple morphodynamic model. *Journal of Geophysical Research: Earth Surface*, *119*(6), 1310–1321. https://doi.org/10.1002/2013JF003034.Received

Martinez, L., Brien, S. O., Bethel, M., & Penland, S. (2009). Louisiana Barrier Island Comprehensive Monitoring Program (BICM) Volume 2 : Shoreline Changes and Barrier Island Land Loss 1800 ' s - 2005, *2*.

Miner, M. D., Kulp, M. A., FitzGerald, D. M., Flocks, J. G., & Weathers, H. D. (2009). Delta lobe degradation and hurricane impacts governing large-scale coastal behavior, South-central Louisiana, USA. *Geo-Marine Letters*, *29*(6), 441–453. https://doi.org/10.1007/s00367-009-0156-4

Miner, M. D., Kulp, M. A., Penland, S., Weathers, H. D., Motti, J., Mccarty, P., … Torres, J. (2009). *Louisiana Barrier Island Comprehensive Monitoring Program (BICM) Volume 3: Bathymetry*

and Historical Seafloor Change 1869-2007.
Moore, L. J., List, J. H., Williams, S. J., & Stolper, D. (2010). Complexities in barrier island response to sea level rise: Insights from numerical model experiments, North Carolina Outer Banks. *Journal of Geophysical Research*, *115*(F3), F03004 1-27. https://doi.org/10.1029/2009JF001299
Nordstrom, K. F. (2014). Living with shore protection structures: A review. *Estuarine, Coastal and Shelf Science*, *150*(PA), 11–23. https://doi.org/10.1016/j.ecss.2013.11.003
Ortiz, A. C., & Ashton, A. D. (2016). Exploring shoreface dynamics and a mechanistic explanation for a morphodynamic depth of closure. *Journal of Geophysical Research F: Earth Surface*, *121*(2), 442–464. https://doi.org/10.1002/2015JF003699
Penland, S., Boyd, R., & Suter, J. R. (1988a). Delta Plain : a Model for Barrier Shoreline and. *Journal of Sedimentary Petrology*, *58*(6), 932–949.
Penland, S., Boyd, R., & Suter, J. R. (1988b). Transgressive depositional systems of the Mississippi Delta plain; a model for barrier shoreline and shelf sand development. *Journal of Sedimentary Research*. https://doi.org/10.1306/212F8EC2-2B24-11D7-8648000102C1865D
Ranasinghe, R., & Stive, M. J. F. (2009). Rising seas and retreating coastlines. *Climatic Change*, *97*(3), 465–468. https://doi.org/10.1007/s10584-009-9593-3
Rijn, L. C. Van, Tonnon, P. K., & Walstra, D. J. R. (2017). Numerical modelling of erosion and accretion of plane sloping beaches at different scales. *Coastal Engineering*, (July 2011). https://doi.org/10.1016/j.coastaleng.2011.01.009
Stone, G. W., & McBride, R. A. (1998). Louisiana barrier islands and their importance in wetland protection: forecasting shoreline change and subsequent response of wave climate. *Journal of Coastal Research*. Retrieved from http://www.jstor.org/stable/10.2307/4298843
Swift, D. J. P. (1975b). Barrier-island genesis: evidence from the central atlantic shelf, eastern U.S.A. *Sedimentary Geology*, *14*(1), 1–43. https://doi.org/10.1016/0037-0738(75)90015-9
Wolinsky, M. A., & Murray, A. B. (2009). A unifying framework for shoreline migration: 2. Application to wave-dominated coasts. *Journal of Geophysical Research: Earth Surface*, *114*(1), 1–13. https://doi.org/10.1029/2007JF000856

CHAPTER 2: THE ROLE OF STORMS AND COASTAL STRAIGHTENING ON SHOREFACE SEDIMENT BUDGET AND BARRIER ISLAND EVOLUTION

Introduction:

Barrier islands are the first line of defense for the rapidly changing Louisiana coast by providing protection for the interior marsh and reducing inland flooding through the attenuation of storm surge and waves reduction (Stone and McBride 1998; Georgiou et al. 2005; Bilskie et al. 2016). High rates of relative sea level rise RSLR (~0.92cm/yr.), an increase in strong storm activity, and constriction of sediment supply due to anthropogenic controls on the Mississippi river, have made this coastline especially vulnerable (Georgiou et al. 2005b; Fearnley et al. 2009; Miner et al. 2009).

The Late Lafourche delta complex in the Mississippi River Delta Plain (MRDP), Louisiana is the most recently abandoned occupation of the Mississippi River (active 1,800-300 years B.P) and provides an example of the early stage deltaic barrier development in which a distributary channel of the Mississippi river created a headland and subsequent abandonment and reworking have produced flanking barrier islands (Penland et al. 1988b). Since abandonment, the Caminada Headland and flanking barriers just to the west of the Mississippi river have seen some of the highest rates of shoreline retreat (>14m^3/yr.) and shoreface erosion (>10 x10^7 m^3) over the last century (Miner, Kulp, FitzGerald, Flocks, et al. 2009; Byrnes et al. 2017). This transgressive headland has been identified as central to the long-term evolution of this area and key to understanding regional sediment budget and barrier island evolution (List et al. 1994; List et al. 1997; Miner, Kulp, FitzGerald, Flocks, et al. 2009).

Previous works utilized historical region-scale bathymetry change and shoreline change analyses to assess large-scale coastal evolution. However, more localized assessments considering the role of sediment transport processes in regional evolution are lacking.

Massive land loss and shoreface erosion due to the relatively active 2005 hurricane season illustrated the importance of storm activity to accurately evaluating the rates of transgression, yet the relationship of the historic data to frequency and magnitude of storms is not well defined. Evaluating these processes is essential to predicting coastal change trajectories and allocating limited sand resources for nourishment.

The objective of this study is to evaluate the evolution of the Late Lafourche delta complex over a 135-year period within the context of the shoreface processes driving regional coastal change and the early stages of barrier chain emergence. Specifically, this study focusses on the mode of transgression through the evaluation of contour migration rates at key locations to determine the trajectory of the system relative to the role of regional coastal straightening and the distribution, frequency, and magnitude of historical storms and on evolution of the shoreface. Two key hypotheses will be addressed.

- **H1: Coastal straightening**
    - Regional coastal straightening influences shoreface trajectory by reducing local erosion and deposition potential resulting in homogenized shoreface geometry.
- **H2: Storm influence**
    - Shoreface geometry and trajectory are strongly influenced by storm frequency and magnitude.

Study Area:

In southeast Louisiana, barriers are located on both sides of the modern Mississippi River Delta (MRD). This region is experiencing rapid geomorphic change including widespread land loss (Barras et al. 2004; Couvillion et al. 2016), and a shrinking barrier island system, with historic average shoreline erosion rates ranging from 1-11m/yr. (Martinez et al. 2009; Byrnes et al. 2017). These barriers are the product of reworked sandy sediments that are the remains of the abandoned distributary lobes of the Mississippi River (Penland et al. 1988a).

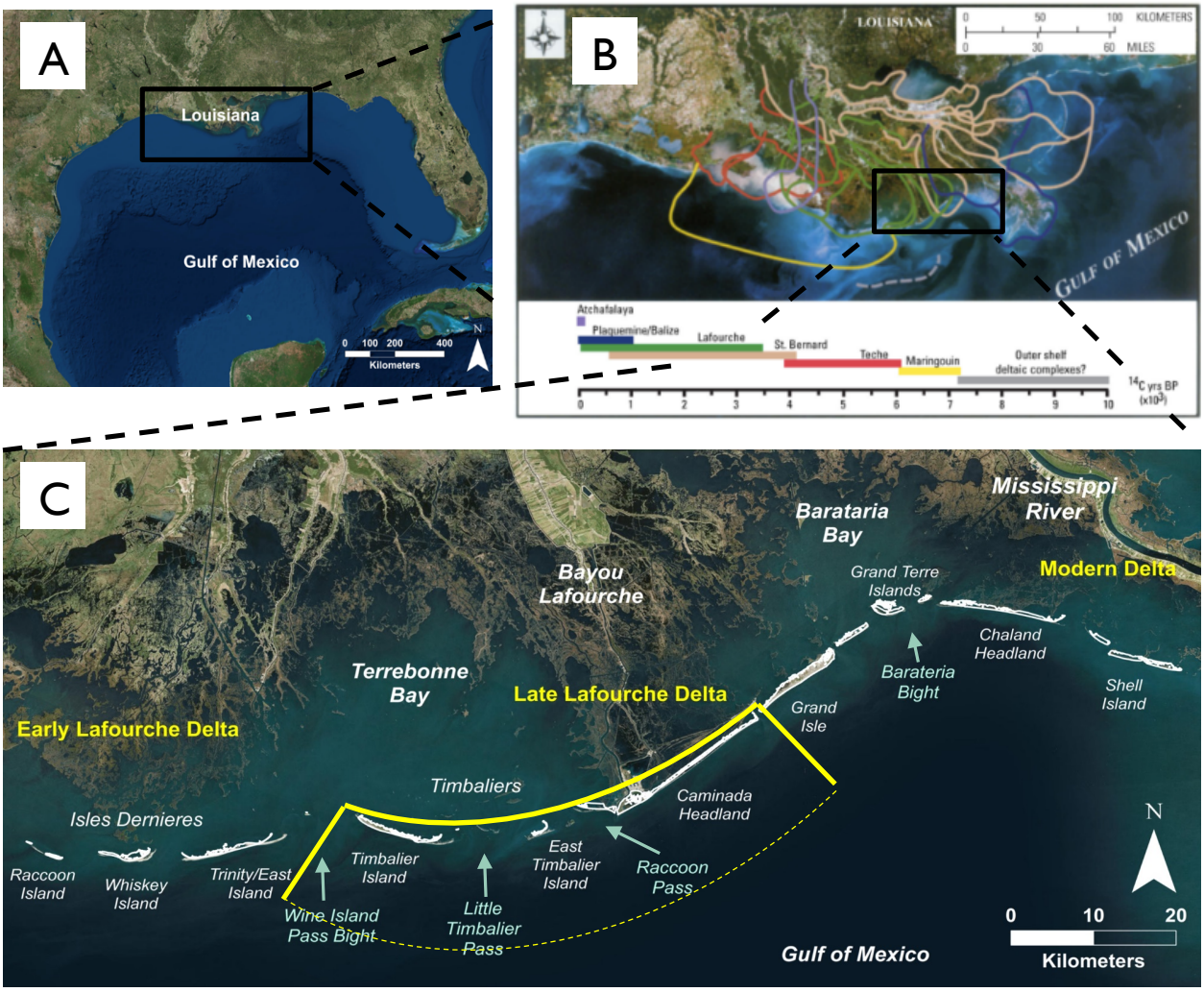

Figure 3: Map showing A) Gulf of Mexico with Mississippi River Delta and B) historic evolution of the delta lobes of Mississippi River (Kulp et al. 2005) and C) barrier island chains west of the modern delta. Approximate Late Lafourche study area in yellow.

This study covers 75 km. of the Louisiana coast, just to the west of the Mississippi River, in Lafourche and Jefferson Parishes, including the Timbalier Island and East Timbalier Island to the west to Grand Isle to the east (Fig. 1). The prominent eroding Caminada Headland and flanking barrier islands are the remains of the abandoned Bayou Lafourche delta lobe complex (active 1,800-300 years B.P.) (Fig. 1) (Frazier 1967; Kulp et al. 2005; Miner, Kulp, FitzGerald, Flocks, et al. 2009).

These island and headland represent stage 1 of the transgressive barrier model which describes the evolution of deltaic barriers in terms of the relationship between the abandonment of delta lobes resulting from avulsion events of the river, leaving sediments to be reworked eventually forming barrier islands (Penland et al. 1988a). Stage 1 is characterized by a central erosional headland and flanking barrier islands and spits in which the headland serves as the sediment source for island migration away from the headlands and inlets increase in size (Penland et al. 1988a).

The history of the evolution of the Late Lafourche coastal zone has also been influenced by various anthropogenic alterations that have had some influence on the morphology in the recent past. Beginning in 1904, with the construction of a dam on Bayou Lafourche, construction of jetties in 1935 at Belle Pass, followed be the relocation of Belle Pass and the construction of new jetties in 1960's and their extension in 1969, as well as periodic dredging to maintain navigation (Poff et al. 2015).

East Timbalier Island became the site of oil and gas infrastructure and therefore efforts to control its erosion and landward migration date back to the 1950s followed by groins in the 1960's and which were altered and integrated into a rock seawall in the 1970s, yet the island has since separated from the revetment migrating landward (Poff et al. 2015).

Subsequent efforts have been made to restore and stabilize the area by Coastal Wetlands Planning, Protection, and Restoration Act (CWPPRA) and the Louisiana Coastal Protection and Restoration Authority (CPRA) including some unsuccessful early attempts, followed by the Bell Pass Barrier Headland Restoration project (TE-52) in 2012 covering 441 acres of beach and marsh restoration. Caminada Headland restoration project (BA-45) was completed in 2015 and

is the site of one of the largest beach/dune of restoration projects completed in Louisiana, consisting of the enhancement of 303 acres of beach with 3.3 million cubic yards of sand (CEC, 2015).

Background:

Previous Work

List et al. (1994) compiled historical bathymetric maps from the 1880s, 1930s, and 1980s for the Louisiana coast and performed assessment of erosion and deposition and regional trends for this transgressive coast and provided the early datasets for this study (List et al. 1994).

Subsequent studies have utilized this data (e.g. List et al. 1997), where they investigated of the viability of applying the Bruun rule - which predicts shoreline migration rates based on sea-level rise and a assumed shoreface profile equilibrium - in the Mississippi River Delta Plain (MRDP), but the results showed that only 50% of the profiles studied met equilibrium criteria and that they did not show any statistical significance for hindcasting or predicting shoreline change (List et al. 1997). They also determined that one of the most complicating factors in determining shoreline and shoreface trajectories, is the inability to define and/or constrain an accurate sediment budget to account for longshore transport and other sediment distribution processes that drive changes in the shoreface (List et al. 1997).

Jaffe et al. (1997) utilized the same dataset and documented sediment transport processes which have contributed to offshore sediment bypassing between two barrier island

chains (Caminada/Timbalier and Isle Dernieres) resulting in a large area of deposition that effectively slowed the erosion rates of the proximal shoreface and shorelines. This shoreface bypassing illustrates a pathway for sediment to naturally nourish down drift barriers and supports the theory that the amount of sediment on the shoreface plays a role in determining the erosion rates of the proximal shoreline (Jaffe, List, and Sallenger, 1997).

Building on the work of List et al. (1994; 1997) and Jaffe et al. (1997), Miner et al. (2009) analyzed seafloor change and documented volumes of sediment eroded from proximal (barrier platform, inlets, ebb-deltas) and distal (shoreface) environments, and highlighted key processes governing sediment loss from the barrier system during transgression. The authors concluded that coastal straightening along the Caminada Headland, mostly in the form of lower and middle shoreface erosion driven by storm induced waves and currents, has been the dominant source of liberated sediment that has been available for reworking and deposition in sinks such as ebb-tidal deltas (Miner et al. 2009).

Although List et al. (1997), Jaffe et al. (1997) and Miner et al. (2009) all illustrated the importance of a regional understanding of sediment transport processes and identified the increasing erosional area of the Caminada Headland, the implications of storm impacts and regional coastal straightening on sediment budgets and barrier evolution are not fully understood.

Coastal Straightening

Coastal straightening has been described as a function of wave refraction where wave energy (and thus wave power) is concentrated on the protruding headland and a reduction in

power in the bays, which causes erosion of the headland, longshore transport of sediment, and deposition in the bays eventually leading to a straighter coast (Swift 1975a). May and Turner (1973) modified the idea of sediment continuity and littoral transport to model straightening as a function of the increase and decrease of wave power based on concave and convex sections of the coastline (Fig. 2A) and showed that sediment transport across the shoreface would convert to deposition proportional to the rate of change of the coast line angle (May and Tanner 1973; Swift 1975a).

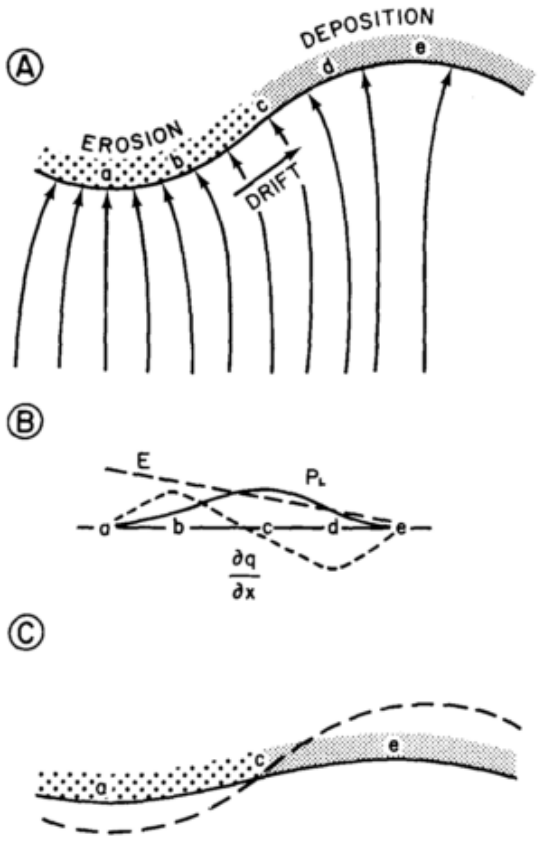

Figure 2: Model for littoral sediment transport from Swift (1975) after May and Tanner (1973) describing the (A) wave-refraction pattern and zones of erosion and deposition and direction of longshore transport (drift) along a curved section of coast analogous to the early stage of the abandoned Late Lafourche delta lobe. (B) Based on the curved geometry changes in energy density at the breaker wave energy density *E* (larger dashed line); longshore component of littoral wave power *PL (*solid line); and the littoral-discharge gradient ~q/~x (smaller dashed line) results in (C) a straighter coast over time as the headland is preferentially eroded and the bays are infilled.

The straightening process can be observed at the local scale in fairly short time periods but the same concept applies to regional scale and will result in the reduction of longshore transport rates as the headland retreats, becomes straighter and attains more homogenized shoreface geometry.

This regional straightening has occurred along the Late Lafourche shore and has been recognized as a dominant process contributing to the transgressive evolution of the area as the largest areas of shoreface erosion and highest rates of landward shoreline migration (List et al. 1994; Miner, et al. 2009). Although straightening is attributed to littoral processes, the Late Lafourche straightening has also taken place at depths greater than would be attributed to average wave breaking processes and therefore are likely the result of storm induced processes, which are consequently key to forecasting trends in shoreface sediment budgets (List et al. 1994).

Storms

The passage of tropical cyclones plays a major role in the erosion of shoreline, reworking of sediments, and the rate of transgression of barrier islands (Stone et al. 1997). Powerful storms can cause massive erosional events including significant shoreline migration, island breaching, and inlet migration and multiple storms in succession can have a cumulative effect (Komar and McDougal 1994). Storm frequency and magnitude are key components of the impact of storms on the coast and have periodic fluctuation on various time scales form annual, decadal, to multi-century (Masselink and Van Heteren 2014).

The Louisiana coast is wave dominated and morphological change is mostly driven by storm activity, yet a lower energy regime is typical in the absence of storm activity (Ritchie and Penland 1988; Stone et al. 1997). During the 2005 hurricane season Miner et al. (2009) reported that the volume of sediment eroded was 8.94 ($\pm$2.33) x $10^7 m^3$ from the Caminada Headland shoreface and identified the erosion of lower shoreface by storm driven currents as the key process contributing to the high rates of historic landward migration (Miner et al. 2009).

Data and Methods:

To determine the influence of coastal straightening and storm frequency and magnitude on the shoreface evolution of the Late Lafourche delta lobe, 100-m spaced shore-normal transects were created to track meter-scale elevation change for 1880s, 1930s, 1980s, 2006, and 2015 from historic bathymetric and shoreline data. An automated framework was used to quantify and track barrier island evolution parameters such as shoreline change, island width, bathymetric contour migration, and shoreface slopes.

To evaluate the influence of coastal straightening a simple straightening index based on the ratio of the curvature of the shoreline and isobaths to a straight line from the endpoints on the east and west was calculated to quantify the relative straightness of the shoreline and shoreface for each time-period. For example, when the Cartesian shoreline length is shorter than the actual curved coast, the index is greater than 1, while for a straighter the coast the index approaches 1.

To determine the role of storms on the observed shoreface change, individual storm power was estimated using the Power Dissipation Index (PDI) method (Emanuel 2005) and the frequency and distribution of the historical storm impacts evaluated with a modified Cumulative PDI (CPDI). The CPDI is defined as the sum the annual PDI combined with a reduction factor to account for the diminishing influence of a storm while still retaining the influence of frequency and magnitude resulting from multiple storms. Spatially explicit maps of CPDI were generated based on the actual storm track for each storm and for each of the periods of interest.

The straightness index and CPDI were then compared to the shoreface slopes and migration rates.

Data sets

This work utilizes historic bathymetric and shoreline data for the south-central Louisiana coast that was originally compiled as a part of the Louisiana Barrier Island Erosion Study, (Williams et al. 1992; List et al., 1994; Miner et al. 2009a,b). These data are available in the form of interpolated bathymetric grids at 100m resolution compiled from U.S. Coast and Geodetic Survey hydrographic survey smooth sheets (H-sheets) for the 1880s and 1930s and data collected by the U.S. Geological Survey for the 1980s (List et al., 1994). Corresponding shoreline data were compiled by McBride et al. (1992) in (Williams et al. 1992) and Martinez et al. (2009) from historic US Coast and Geodetic Survey topographic smooth sheets (T-sheets) and digital aerial imagery.

In the State of Louisiana, the agency responsible for nourishing barrier is presently the Coastal Protection and Restoration Authority (CPRA). In the recent history (~2005) the agency developed the Barrier Island Comprehensive Monitoring (BICM) program in partnership with the U.S. Geological Survey (USGS) and the University of New Orleans (UNO) Pontchartrain Institute for environmental Sciences (PIES) to collect and digitize historical shoreline, bathymetry, topographic, habitat, and sediment data. The idea was (and continues to be) to build a framework where every ~7 years a complete dataset would be collected and added to the database. This effort builds upon the work of List et al. (1994), and added complimentary bathymetry and shoreline data for 2006 and 2015.

For detailed information about original data sources and methods refer to List et al (1994) and Miner et al. (2009).

Bathymetry

Historic bathymetric data compiled by List et al (1994) were adjusted for subsidence and referenced to a common vertical datum (NAVD88) for direct comparison of erosion and accretion with the 2006 data collected by BICM (Miner et al. 2009).

For BICM2 the CPRA and have completed the single beam bathymetric surveys for 2015. Using the methodology established by Miner et al. (2009), a surface for 2015 was created using Golden Software Surfer 13 from the bathymetric point data supplied by the State of Louisiana (Miner et al. 2009). All together there are bathymetric surfaces for 1880s, 1930s, 1980s, 2006, and 2015. To assess changes in the bathymetry, isobath maps, at 1m intervals, were created in Surfer 13 from the bathymetric surfaces and exported as ESRI shapefiles.

Shorelines

The historic shoreline data used for this project was acquired from the first BICM project for the 1880s, 1930s, 1980, and 2006 as polygon shapefiles (Martinez et al. 2009). The current BICM2 effort has just completed the 2015 shorelines and shapefiles were supplied by the State of Louisiana CPRA for this project (Byrnes et al. 2017). All polygons were converted to line shapefiles using QGIS.

Transects

To create a quantitative framework for measuring changes to the shoreface and shorelines through time a series of 30km long, cross-shore transects was created at a 100m alongshore interval. These transects were created using ERSI ArcMap and the Digital Shoreline Assessment Tool (DSAS) tool created by USGS (Thieler et al. 2009). A baseline was derived from the 1880's shoreline by using the buffer tool to draw a line offshore and parallel to the shoreline and far enough from the shore to cover the entire bathymetry study area. The line was smoothed and adjusted to create a balance between maintaining a shore-parallel (for 90^{o} transect orientation) and a smooth curvature to avoid the crossing of transects. This resulted in a series of 1600 transects that serve as the framework for the metrics used in the study. An additional baseline and series of transects were created for Timbalier island to produce profiles that are closer to shore normal orientation.

Shoreface Metrics

For each of the dates, the bathymetry isobaths and the corresponding shoreline data were combined into a single file consisting of a line/isobath for every 1m of elevation

difference. QGIS was used to intersect the transects with each of these isobath line files for each date, resulting in a series of points that correspond to the location where the transects crossed each of the isobaths. From the resulting point data, a series of parameters were derived that characterize the shoreface and shoreline relationships.

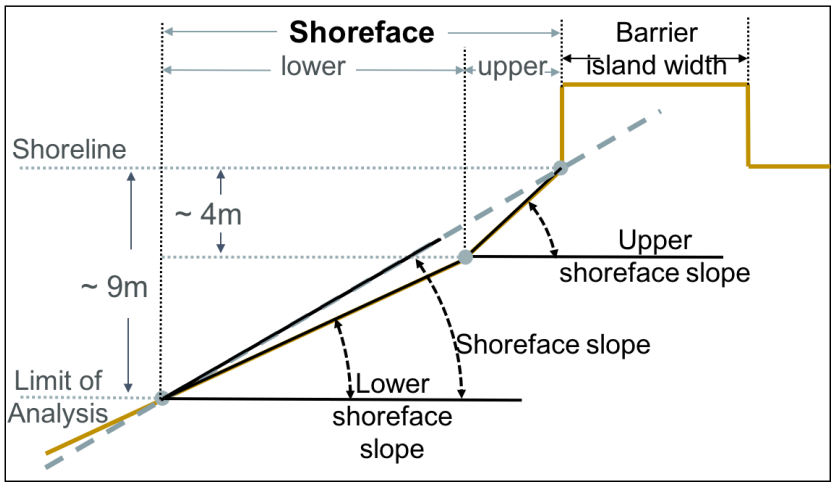

Figure 3. Barrier island geomorphic parameters for used evaluate changes in the geometry of the shoreface including the limit of analysis (LOA), shoreface break, and shoreline position, barrier island width, shoreface slope, and upper/lower shoreface slopes.

1880s, 1930s, 1980s, 2006, 2015

For each of the dates in the time series, as series of static metrics (fig. 3) were calculated including and shoreface slope, upper shoreface slope, and lower shoreface slope consistent with the definitions in previous work (Wolinsky and Murray 2009). These measurements create the basis for quantitative comparisons between each of the dates and allow for the estimation of the steepening or relaxing of the shoreface.

Shoreface slope is the angle of slope from the toe at depth of closure to the shoreline on the seaward side. The upper and lower shoreface slopes were also calculated separately by dividing the shoreface into two sections by the shoreface break which was determined by the

average point in which there is an inflection point on the shoreface. For this area, the 4m isobath was used as the shoreface break. To avoid discrepancies based on the differences in shoreline and bathymetry data collection methods and dates the 1m isobaths were used as the upper limit instead of the shorelines to calculate the slopes. For the lower limit for slope calculations, a limit of analysis (LOA) was substituted for the for the depth of closure limit that is usually used to calculate shoreface slope. Depth of closure (DOC) as defined as the point at which there is no longer observable changes in the profile over the time period, varies greatly over the study area and in some cases, extend beyond the data limits (List et al. 1997). Alternately, depth of closure can be defined as the limit at which waves can entrain sand and therefore have a limited effect on the bed. Using the Hallermeier equation calculated by the Army Corps of Engineers Gulf of Mexico Depth of Closure for Wave Information Studies (WIS) station #73129, which is located just off shore of Caminada Headland, depth of closure was estimated at 9m (Hallermeier 1980).

$$d_l = 2.28H_e - 68.5\left(\frac{H_e^2}{gT_e^2}\right)$$

Using either method to determine depth of closure, the lower limit selection was restricted by data coverage and when necessary the deepest isobaths were substituted as the default boundary. For example, 8m was used for the Timbalier Island shoreface since the 9m was not continuous in all time periods. Although the determination and assessment of depth of closure is critical for many applications, this study uses a limit of analysis as a boundary point for data selection and not as a specific morphological distinction.

Erosion/deposition

To provide a direct linkage from the shoreface and shoreline data to the erosion and deposition data another method for the calculation of seafloor change based on the transects was derived. The Surfer 13 slice function was used to extract elevation change and distance data along each transect. This information was used to calculate the integrals and derive the total negative (erosion) and positive (deposition) change for each selected transect. This method allows for selection of the same geographic area that is used to calculate all other parameters derived from the transect framework.

Bathymetric change

Bathymetric change analysis was done to identify and quantify areas of erosion and deposition where the differencing of two seafloor maps yields the net elevation change. The first two time periods 1880s-1930s and 1930s-1980s were originally computed by List et al (1994), 1980s-2006 was added by Miner et al (2009) and 2006-2015 was add for this study.

Coastal Straightening

To evaluate the role of coastal straightening on the evolution of the shoreface and shoreline, the amount of straightening was quantified using an index that compares the length of a straight line connecting the farthest west point to the farthest east point to the actual distance along the coast. This process is based on the calculation used to evaluate the sinuosity of a meandering river where the distance along the center of the channel (channel length) is compared to the straight-line distance (Cartesian length) from a point upstream to a point

downstream (Mueller 1968). The resulting ratio yields a higher number when the coast is more curved and conversely the lower the number the straighter the coast where a value of one is a perfectly straight coast (ratio = 1:1) and values greater than one indicate increasing curvature. This process was used to test the straightening of the shoreline and averages of the isobaths for the upper and lower shoreface.

$$\frac{\boldsymbol{Distance\ (alongshore)}}{\boldsymbol{Distance\ (straightline)}} = \boldsymbol{straightening\ index}$$

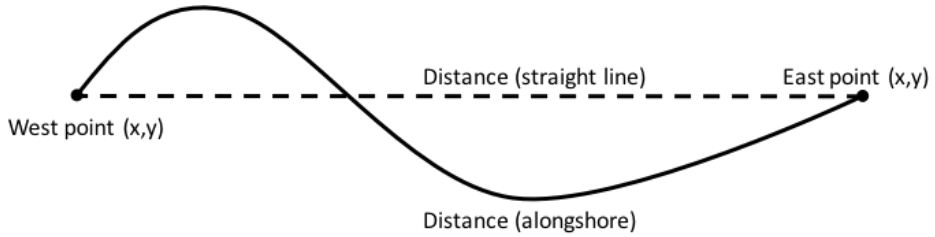

Figure 4: To quantify the amount of straightening that has taken place along the coast, the straightening index takes the ratio of the distance alongshore of the shoreline or isobaths to the straight-line distance from the first point to the last point. A straight coast would result in a 1 and increasing curvature would result in increasing values.

Storms Analysis

To test the relationship of storm frequency and magnitude to the observed changes in the shoreface, a modified Power Dissipation Index (PDI) was used (Emanuel 2005). PDI has been used as a proxy for the power dissipation and therefore the potential destruction of tropical cyclones based on the cube of the maximum wind speeds integrated over the life of the storm (Emanuel 2005).

$$PDI = \int_0^T V^3{}_{max} dt$$

For this study, PDI was used to characterize the power of each storm that passed through the area and a cumulative index was added to evaluate the residual effects of each storm and the cumulative effects of multiple storms in succession. Data from the International Best Track Archive for Climate Stewardship (IBTrACS) database provided storm track coordinates and wind speeds at 6 hour intervals dating back to the 1840s (Knapp et al. 2010).

Regional PDI/CPDI

To estimate the regional temporal variations in frequency and magnitude of historic tropical cyclones, PDI was calculated for all storms that were proximal to the study area over time.

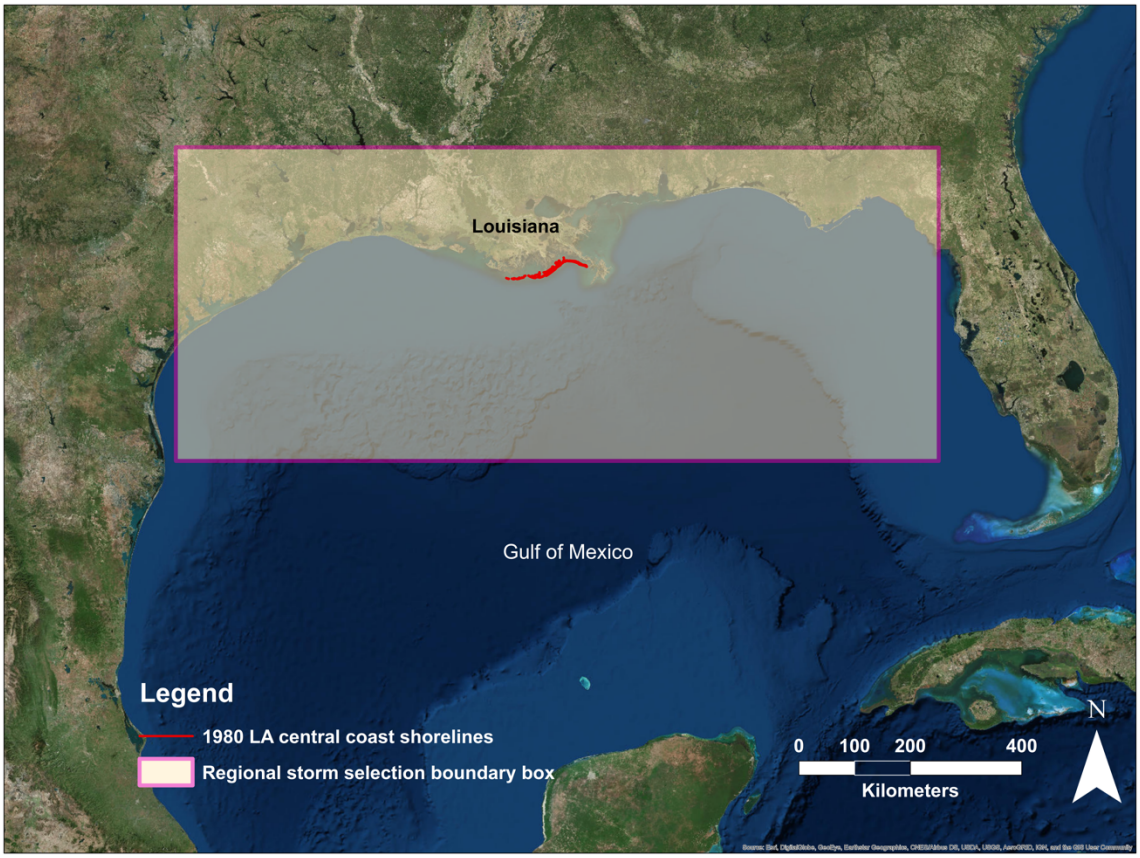

Figure 5: Regional storm selection boundary box (highlighted rectangle) for the selection of storms from the historical storm track data.

Unlike the method used by Emanuel (2005) that calculated the PDI for the entire life of the storm, the storm data was subset based on a regional area of interest that would capture all the storms that would possibly influence the study area; PDI (for each storm) was then calculated only on that segment of the storm track that fell within the regional study area therefore only rating the storms based on the wind speed and time relative to the area (Fig. 5).

Using the regional PDI for the Northern Gulf of Mexico (Fig. 5), a regional cumulative storm impact index (CPDI) was developed to evaluate the patterns of variability in storm frequency and magnitude through time. First, the regional annual PDI resulting from all storm tracks within the area box (Fig.5) was calculated, and each year thereafter, the regional annual

PDI was added to the previous year to produce the CPDI. The CPDI accumulates, but each year, the previous regional PDI is discounted (using a fixed percentage ~5%) to account for "reduced coastal impacts" from past storms. This method allows for evaluation of the temporal relationship of the bathymetry, shorelines and storms.

Local PDI/CPDI

Although the regional PDI and CPDI provide a method for comparison of the datasets to the frequency and magnitude of storms, it does not consider the spatially explicit impacts resulting from storms (e.g. forward speed, storm trajectory/path, incident angle at landfall) which can vary widely across the MRDP. To account for these factors a new PDI analysis was developed utilizing a spatially explicit PDI.

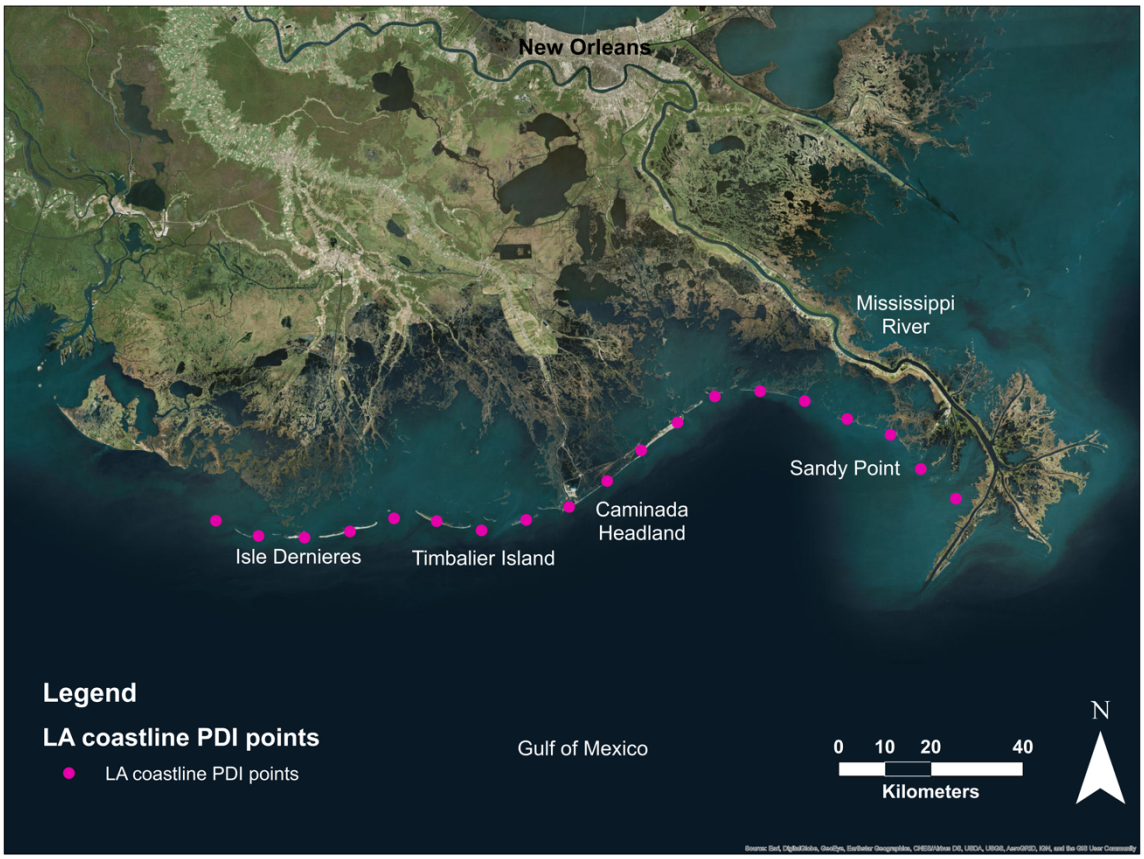

Figure 6: PDI collection points for the Louisiana central coast spaced every 10km.

First, locations every 10km were created along the shoreline to serve as collection points for the PDI (Fig. 6). Utilizing storm data, the 6-hour time integral of PDI (IPDI) was calculated and distributed throughout space based on a predetermined radius informed by the average storm size and reduced by a Gaussian distribution away from the storm center. This allows for maximum weighting locally within the eye of the storm and a reduction distally at the edges of the storm. For each 6-hour time-step the distributed IPDI for each storm that crossed the interest area (Fig 5) was evaluate for all points along the coast (Fig 6) the fell within the Gaussian footprint. This was repeated for every 6-hour period in the dataset and for all storms (from 1840-present) and summed annually for each collection point. This process effectively

provides a method to visualize the spatial distribution of storm impact throughout time and space.

Modeling

To test how the observed trends in barrier shoreline evolution are driven by the shoreface slope and other factors, the UNIBEST-LT+ coastline morphodynamics and longshore sediment transport model was utilized. UNIBEST-LT+ was selected due to the suitability of computing appropriate time scales of decades to centuries and spatial scales relevant to the study area while maintaining efficient run times. UNIBEST utilizes a wave propagation module for wave transformation, based on local wave climate using Simulating Waves in the Nearshore (SWAN) model to covert wave power to surf zone change (Booij et al., 1999; UNIBEST-CL + manual 2011).

Five simulations were run using UNIBEST to test the impacts of regional straightening and the relative effects of the frequency of storms on shoreface and shoreline evolution of the headland and flanking barriers. Two time periods were selected, the earliest (1880s) and the post storm (2006) datasets, and two climate scenarios were run on each. Waves at the offshore boundary for UNIBEST were derived using SWAN northern Gulf Model (Georgiou et al., 2013) which was forced with offshore waves from NOAA 42040 Station and validated using WAVCIS observations (Georgiou et al., 2013). For this analysis, 45 events (with their corresponding return period) were established using data reduction methods (e.g. Lesser et al., 2004) using a 20-year wave records from the Wave Information System (WIS; Corps of Engineers), while water levels and winds were obtained from Grand isle NOAA Station for the

same 20-year window (CEC, 2017). To account for stormier wave climate, selected events from the record were adjusted (both in terms of frequency and magnitude) to reflect higher energy. This allowed for the comparison of the effects of shoreline orientation (straightening) and wave energy (storms) on longshore transport rates along sections of the study area.

1880s – calm

1880s – stormy

2006 – calm

2006 – stormy

1880s- calm with 2006 coastal angles

Results:

To facilitate readability the following nomenclature will be used to describe the time-periods of the study in the results and discussion: Period 1 is (1880s to 1930s), Period 2 is (1930s to 1980s), Period 3 is (1980s to 2006), Period 4 is (2006 to 2015)

Storm analysis

Regional PDI/CPDI

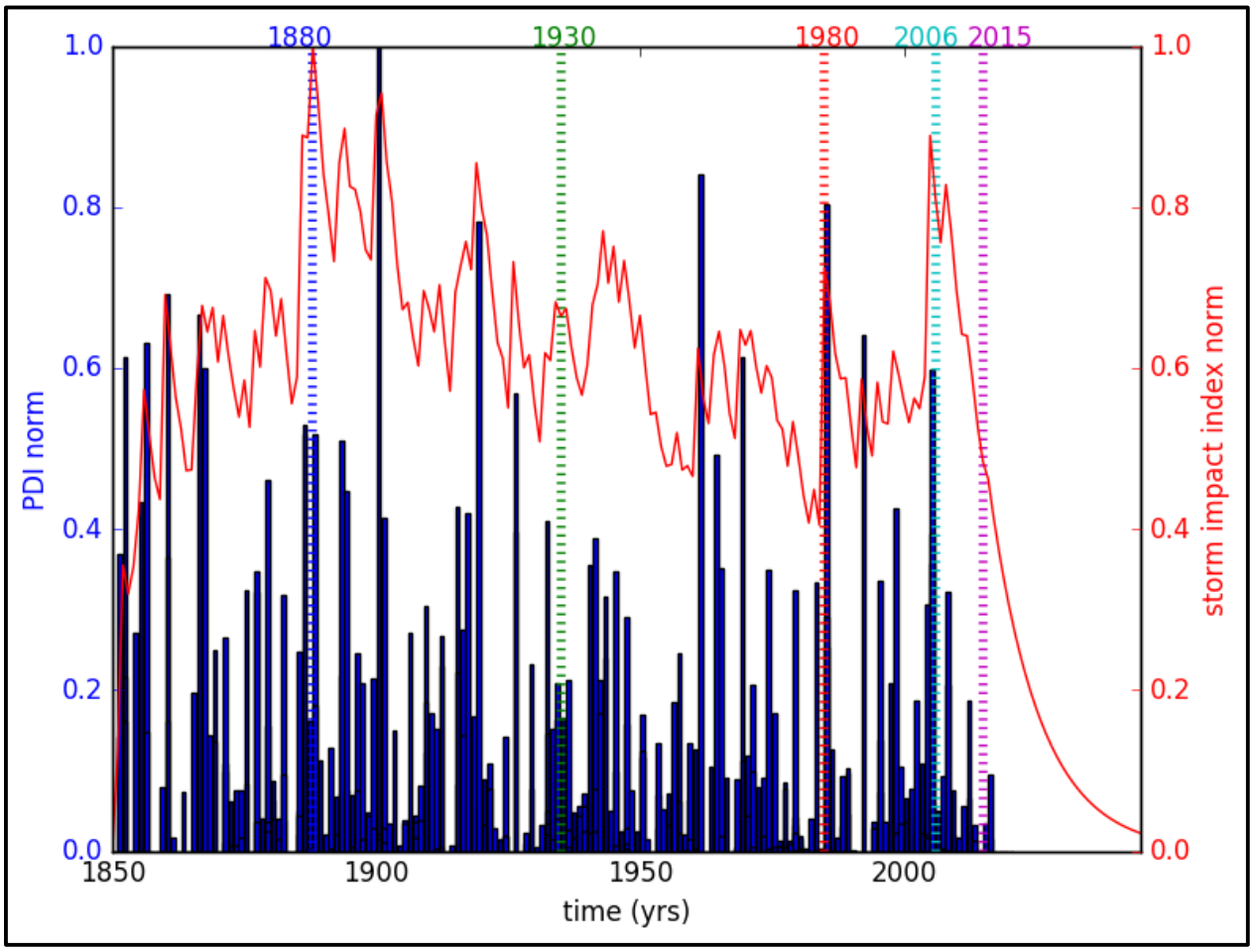

Figure 7: Regional storm impact analysis using the IBTrACS storm track data to calculate the Power Dissipation Index (PDI) (Emanuel 2005) (blue bars) over the time span of the study and the cumulative PDI (CPDI) (red line). The bathymetric survey periods (dashed bars) show the relationship of regional tropical cyclone storm activity and when the bathymetry data was collected. The intersection of these bars and the CPDI (red line) indicate the relative CPDI value for that data set.

To evaluate variations in historic storm activity relative to the bathymetric change data, the Power Dissipation Index (PDI) was plotted showing the relative impact of the storm power for all the storms on record that passed through the region since 1840 (Fig. 7). There are several storms with high PDI in the dataset including the 1900, and 1920, 1965.

Even though PDI shows the relative power of storms, it does not reflect the frequency and grouping of storms that would likely affect how storms would impact an area. The first dataset 1880s has the highest storm impact index of all the datasets, as it follows a tight group of relatively powerful storms in the preceding decade resulting in a spike in the index right before the data acquisition. The Galveston hurricane of 1900 has the highest PDI in the group as it passed parallel to the Louisiana shore and was a storm containing high sustained wind speeds. The next dataset (1930s) shows a lower CPDI even though the preceding decades had several storms with high PDI. The frequency and the clustering of those storms were lower than in the late 1800s. The trend continues in Period 2 with CPDI declines despite strong named storms such as Betsy in 1965; this period had the lowest CPDI on record. Period 3 began with a jump in the index due to a powerful storm just after the 1980's data followed by a moderate period but the 2006 data showed an abrupt increase in the index number due to the clustering of strong storms in 2005 (e.g. Cindy, Rita, and Katrina) immediately preceding the survey data. Period 4 resulted in a falling index number due to the relatively low storm activity over that period and the 2015 dataset having the lowest index score of all the datasets.

Local PDI/CPDI

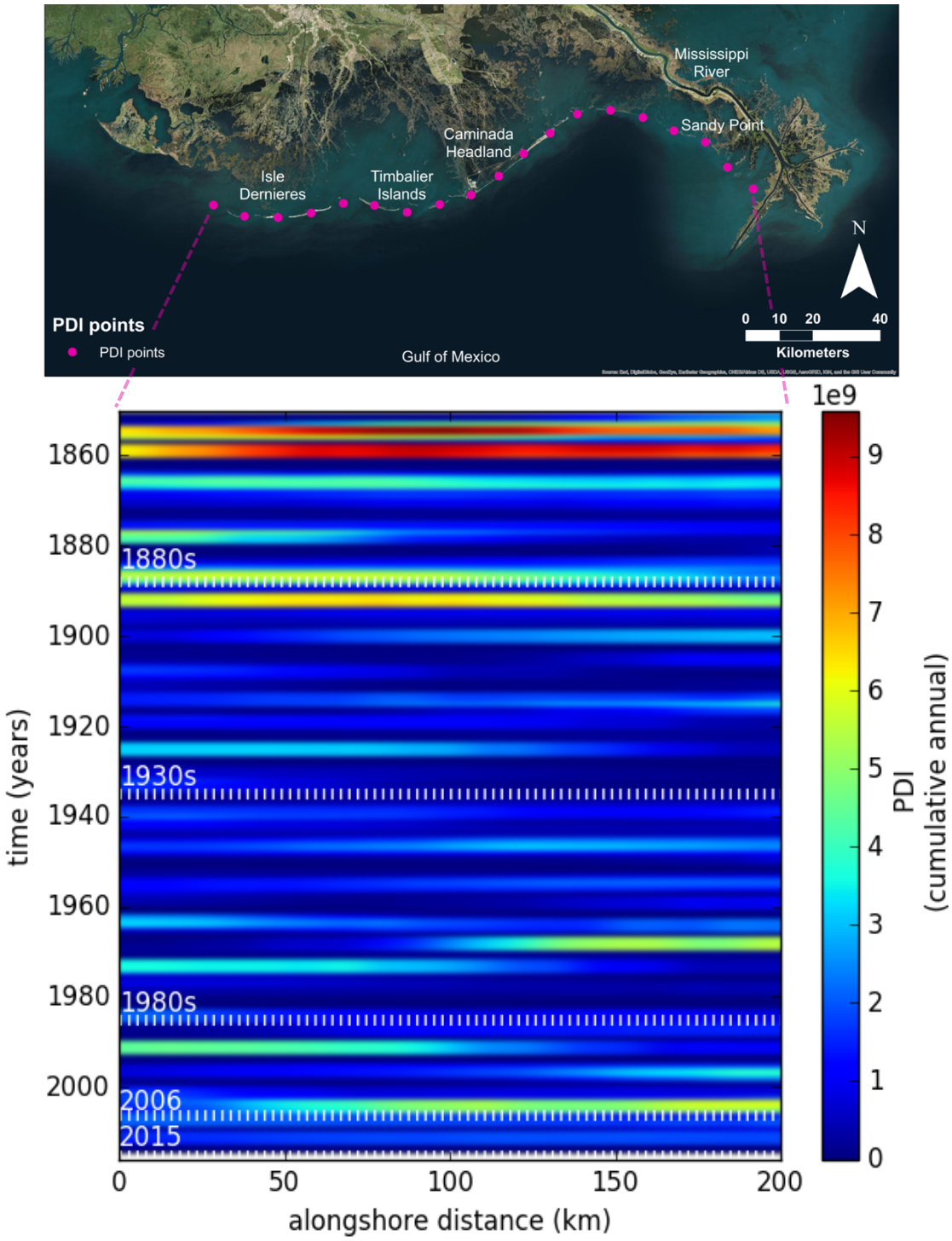

Figure 8: The local PDI relative to the coastline reveals the variations in storm magnitude and frequency distributed spatially across the coast (pink dots served as collection locations) with the time in years with the time of the bathymetry surveys (white dotted lines). The highest levels of PDI were in the 1850s and 1860s and note the values of PDI immediately preceding the survey such as the peaks just before the 1880s and 2006 data and the relatively low PDI for the 1930s and 1980s datasets.

The local PDI results show different results compared to the regional PDI, although retained most of the same trends. One of the most notable results is the highest PDI values in the dataset which takes place in the 1850s-1860s, likely caused by the proximity of the storms to the coast during this period. These intense events were followed by relatively calm conditions and an intense event in the 1880s before the 1880s surveys. Following that event during period 1 there was ~30 years with only one significant event before the 1930s datasets. In period 2, there were only a couple of events in the mid 1960s and 1970s and several years of calm before the 1980s datasets. Period 3 had one event in the 1990s and then a clear increase in the PDI in 2005 right before the 2006 dataset with a lower PDI in period 4.

Bathymetric change

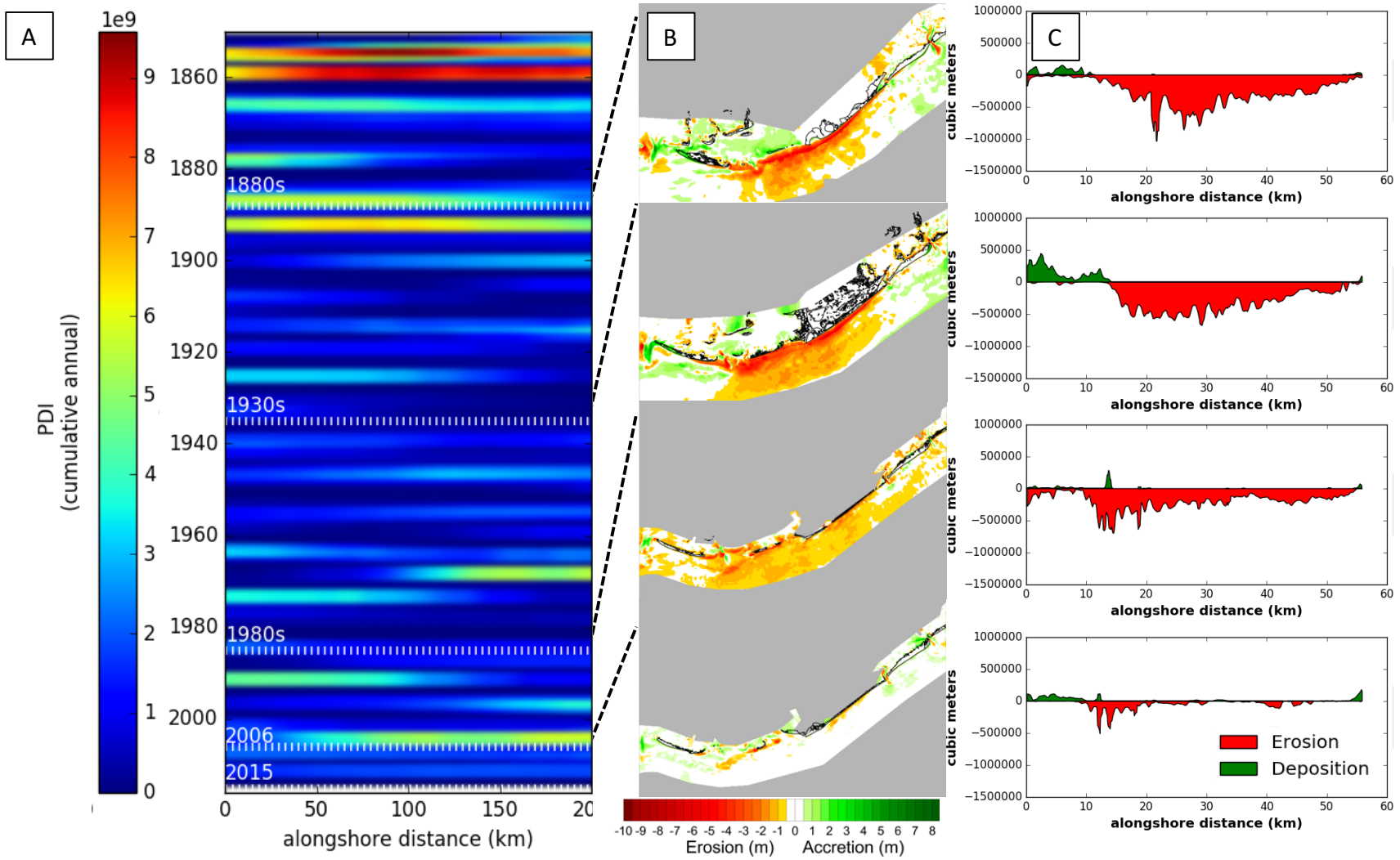

Figure 9: A). Spatially explicit PDI calculated based on IBTrACS historic storm track data. B). Bathymetric change maps for the Late Lafourche lobe showing erosion and deposition for the 1880s-1930s, 1930s-1980s, 1980s-2006, and 2006-2015. Notice the increasing size of the erosional zone along the shoreface in the first three periods an and diminished erosion and deposition in the most recent period. C). Shoreface erosion and deposition for the Late Lafourche lobe per 100m longshore distance from the -8 to the -3m isobaths. Notice the migration of the peak erosional zone to the west through time.

To evaluate erosion and deposition along the shoreface in terms of vertical change, bathymetric change maps were used. In period 1, there was significant erosion along the western side of the Caminada shoreface with higher concentrations of erosion along the upper shoreface and some areas of deposition on the Timbalier and Grand Isle shoreface (Fig. 9B). The focus of the erosional zone was along the shoreface of the Caminada headland and East Timbalier Island (Fig. 9C).

During period 2, the erosion of the headland continued with more erosion of the East Timbalier shoreface and the distal Raccoon pass ebb-tidal delta and along a larger area of the shoreface to the west compared to the previous period (Fig. 9B). During this period, the areas of deposition along the proximal shoreface fronting Timbalier islands continued and became more apparent (Fig. 9B and C). In period 3, widespread erosion occurred across the entire shoreface because of the stormy 2005 hurricane season (Fig. 9C). Period 4 shows very little change compared with the other periods although there is an erosional zone along the nearshore of the headland and another zone along the ebb tidal delta as well as some noticeable deposition on the Timbalier shoreface (Fig. 9B).

Overall the trend in erosion of the shoreface from period 1 through 4 shows a shifting or migration of the peak erosion to the west (Fig. 9C)

Migration rates: Caminada Headland

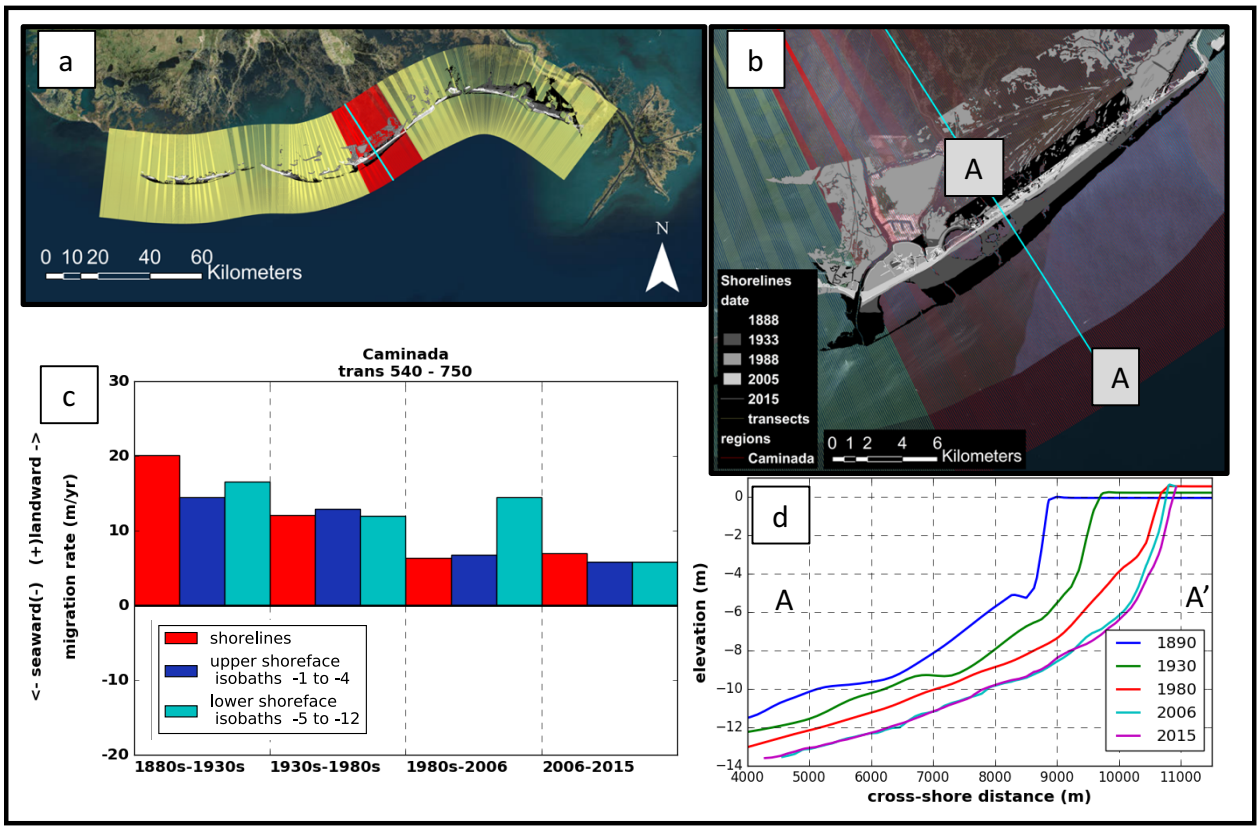

Figure 10: (a) Study area map showing selected transect (red) for calculating mean migration rates. (b) Map of Caminada Headland showing selected transect (A to A') for example profiles (d). (c) Migration rates of the Caminada Headland shorelines (red), upper shoreface (dark blue) and lower shoreface (cyan). Positive numbers signify landward migration and negative numbers signify seaward migration. Representative cross-shore profile showing profile changes through time.

In period 1, the Caminada headland had the highest rates (~20m/yr.) of landward migration at the shoreline with relatively high rates (>10m/yr.) on the upper and lower shoreface with most of the change along the western end of the headland aided by the erosion into the large land-bound bay. In period 2, there were reduced rates of shoreline migration (~10m/yr.) and similar rates on the shoreface. During period 3, there were lower rates on the shoreline and upper shoreface (~5m/yr.) but the lower shoreface increased (~20m/yr.) corresponding to the increased storm activity in the 2005 hurricane season. Period 4 showed slower landward migration with similar rates for the shoreline and shoreface (~5m/yr.) and overall this period had the lowest migration rates over the entire study period.

Migration rates: Timbalier Island

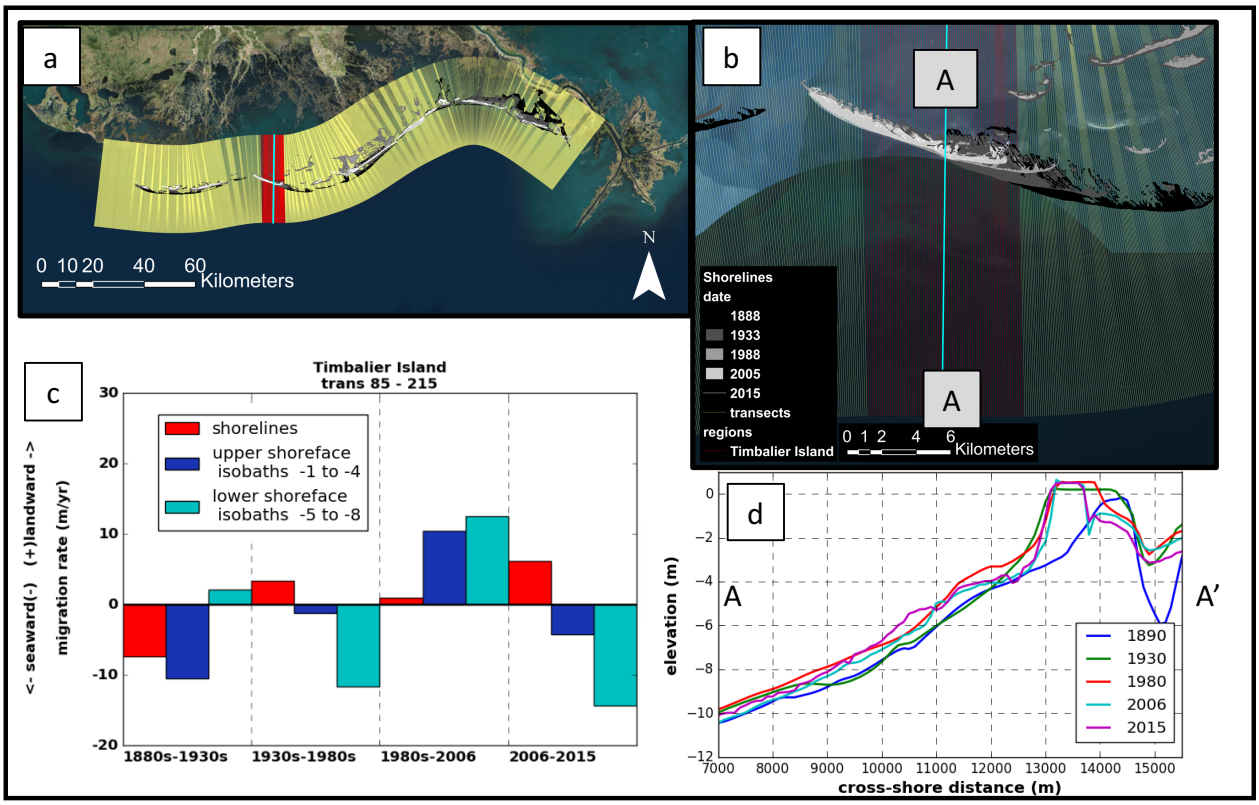

Figure 11: (a) Study area map showing selected transect (red) for calculating mean migration rates. (b) Map of Timbalier Island showing selected transect (A to A') for example profiles (d). (c) Migration rates of the Timbalier Island shorelines (red), upper shoreface (dark blue) and lower shoreface (cyan). Positive numbers signify landward migration and negative numbers signify seaward migration. (d) Representative cross-shore profile showing profile changes through time.

In period 1, Timbalier island was migrating seaward and westward as the shoreline and upper shoreface were eroded from the eastern side of the island but longshore transport delivered sediment to the western portion of the island where spit building to the west resulted in a net mean migration rate in the seaward direction (Fig. 11D). Period 2, the shoreline began to migrate landward while the upper and lower shoreface continued to migrate seaward resulting from more erosion of the shoreline along the eastern end of the island during this period Fig. 11D). The rate of the lower shoreface seaward migration increased due to a growing depositional zone along the middle of the shoreface. In the following period the

shoreline continued to migrate landward (~4m/yr.) and the upper and lower shoreface also migrated landward as a result of the widespread erosion during the 2005 hurricane season (Miner et al., 2009). In the last period, the shoreline migrated landward at the highest rate (~10m/yr.) while the lower shoreface migrated seaward at the highest rate (~12m/yr.). This flip in migration rates indicates the return of the depositional zone on the shoreface but a destabilized shoreline mostly along the eastern end and just to the west of the shoreline revetments.

Coastal Straightening

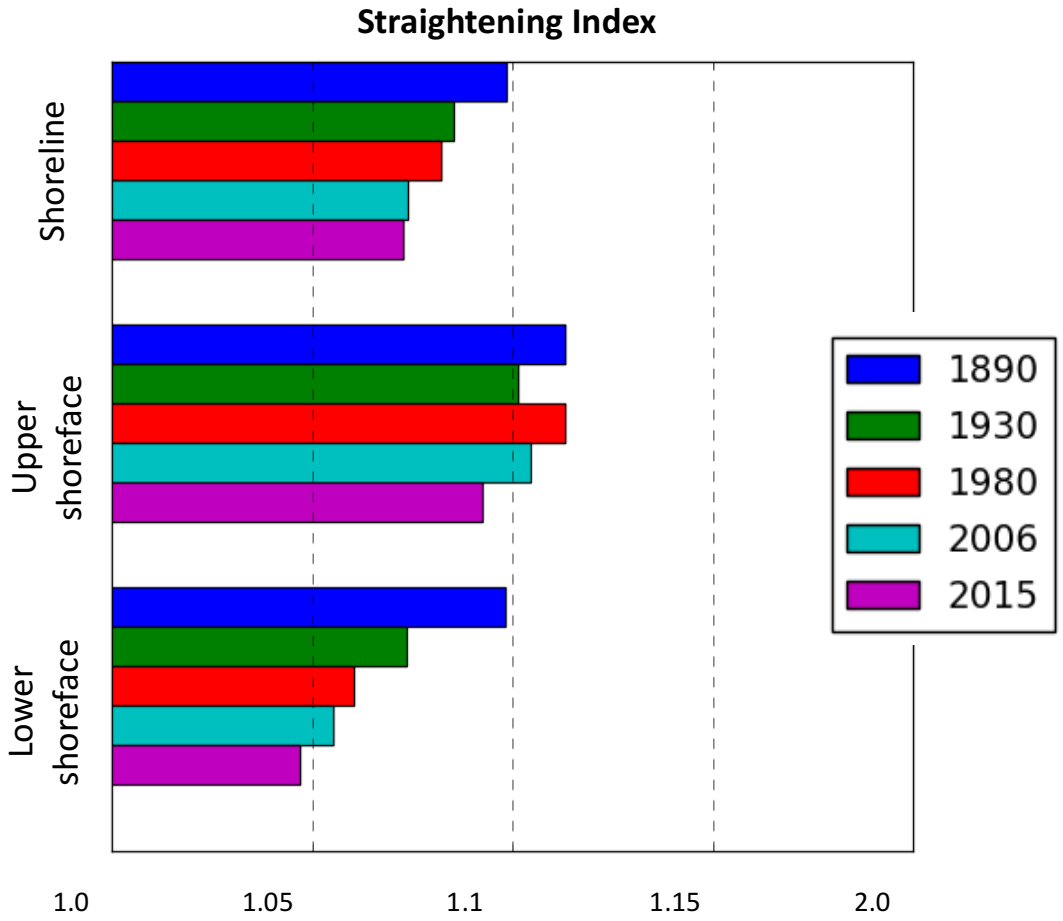

Figure 14: Straightening index for the Late Lafourche delta lobe showing the ratio of the distance along the shoreline, or average distance of groups of isobaths verses the straight-line distance from one end to the other. The lower the straight index number the closer to a straight line the shape of the shoreline of isobaths.

The results of the coastal straightening analysis show that the Late Lafourche section of coast is straightening through time along the shorelines, upper shoreface and the lower shoreface (Fig. 12). The straitening index for the lower shoreface dropped from 1.09 to 1.07 in period 1 with continued reduction in the following periods to 1.04 in 2015.

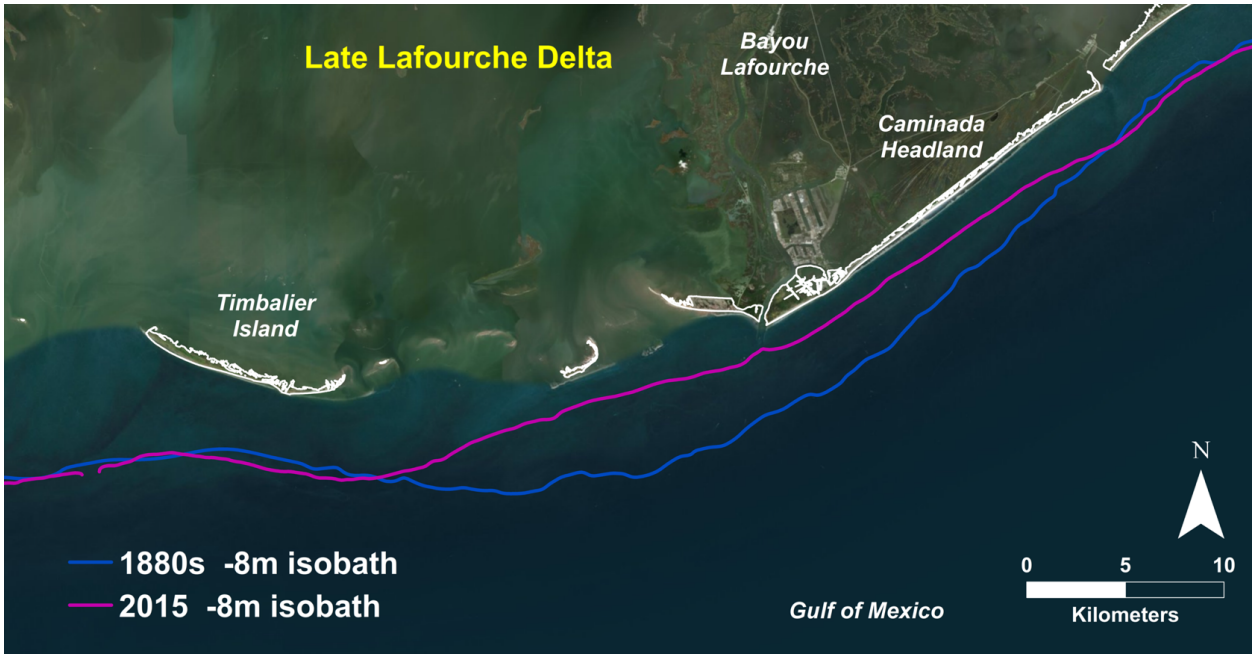

Figure 15: Example of coastal straightening from the 1880s (blue line) to 2015 (magenta line) for a selected isobaths (8m) from the west side of Timbalier Island to the eastern edge of Caminada Headland. Note the amount of straightening that has taken place where the isobaths have not moved very much on either end but the central section has migrated landward ~5 km.

The shoreline straightening analysis results show that the shoreline reduced in curvature from 1.09 to 1.07 from 1880s to 2015 (Fig. 12). Upper shoreface straightened in period 1 and returned to a similar amount of curvature in 1980s followed again by straightening in the next two periods to 1.09 (Fig. 12). Although straightening took place along the shoreline and the shoreface, the lower shoreface showed the most significant change. The amount of straightening indicated in the straightening index is equivalent to 5km of landward migration of the isobaths in the middle and very little change at either end (Fig. 13).

Shoreface homogeny

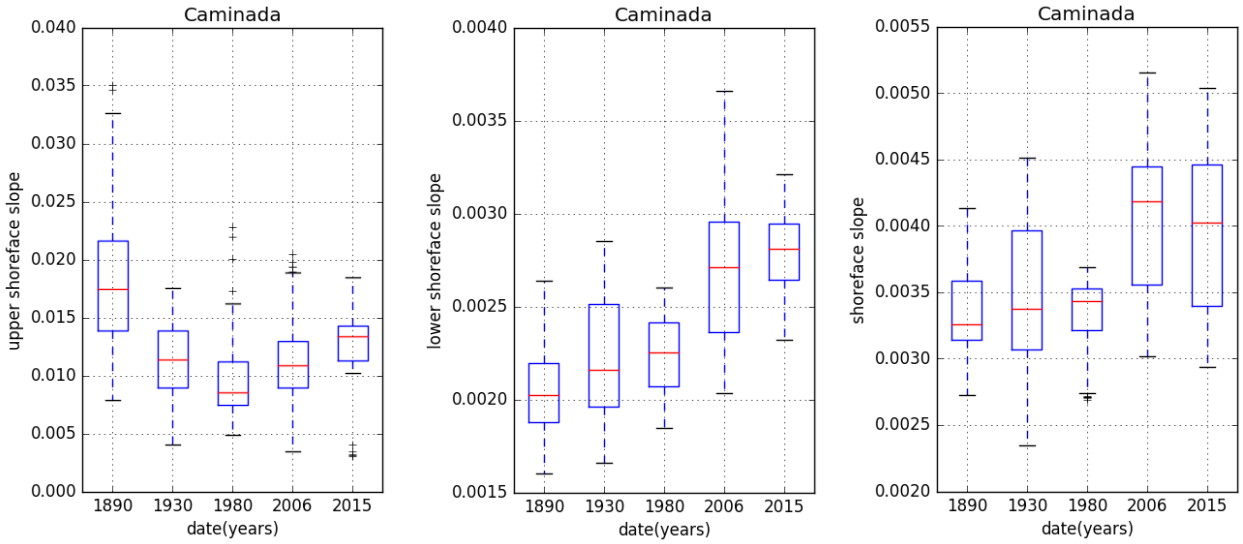

Figure 14: Caminada Headland shoreface slope distributions for each of the bathymetric surveys (1880s-2015) separated into the A). upper shoreface (-1m to -4m), B). the lower shoreface (-4m to -9m), and C). the shoreface slope (-1m to -9m). Notice the tightening of the grouping in the upper shoreface over time, the steepening of the lower shoreface and the tightening of the distribution in the 1980s of the shoreface slope.

To test the if coastal straightening has resulted in a more homogenized shoreface, shoreface slope distributions where compiled to identify the amount of diversity in slopes in each period. Due to the complicating factors of the inlets, the Caminada Headland area is focused on. The results show that the distribution of the upper shoreface has tightened with the most variance in the 1880s and the least variance in 2015 (Fig. 14A). The lower shoreface has increased in slope and the most variance is in 2006 (Fig. 14B). The shoreface slope shows that overall slopes had the least variance in the 1980s and the most in 2015 (Fig. 14C).

UNIBEST LT: Coastal straightening: 1880s vs. 2006

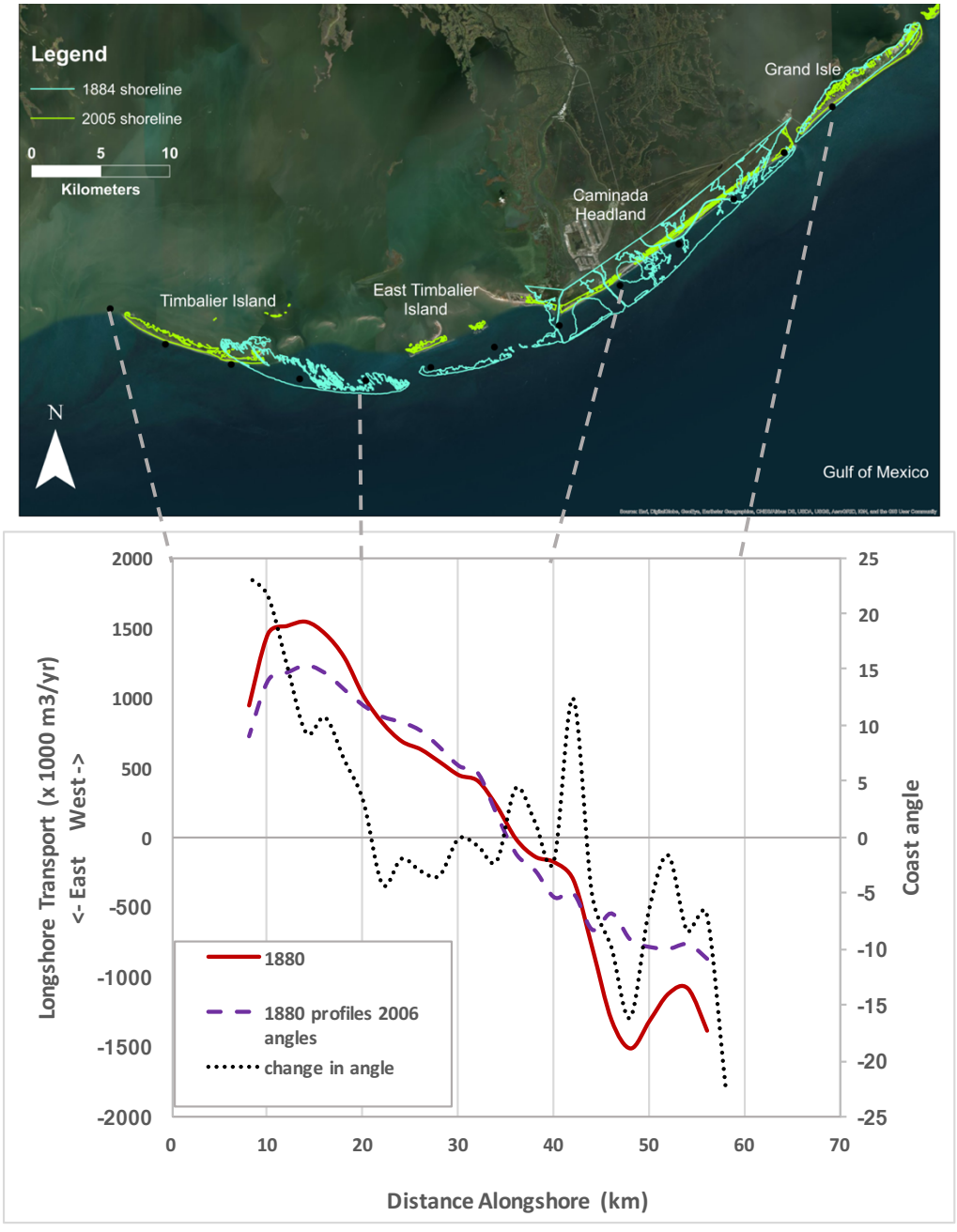

Figure 15: UNIBEST Lt results for the 1880s dataset (red), the 1880s profile data with the 2006 coastal angles (purple) and the corresponding change in coastal angles between the time periods (black dots). Results show the total sediment transport (Qs) (negative values = eastward transport and positive values = westward transport) based on the selected cross-shore transect at 2 km interval and the coastal angle for each dataset. The change to the 2006 angles represents the relative straightening of the coast and the results show a reduction in transport rates at the edges (less than 20km and greater than 40km) and an increase in transport rates in the central section.

To test the influence of coastal straightening on longshore sediment transport flux, a simple test was run with the 1880s and 2006 coastal angles with the same wave scenarios to isolate the variation based only on changes in the orientation of the coast. Results show that the relative straightening of the 2006 shoreline resulted in a decrease in the longshore transport rates to the east and west at the ends (less that 20km and greater than 43km) and an increase in the center of the area (between 20km and 43km) with a slight shift to west of the point between eastward and westward transport (from 37km to 36 km) (Fig. 15).

UNIBEST LT: Storm impacts: 1880s and 2006

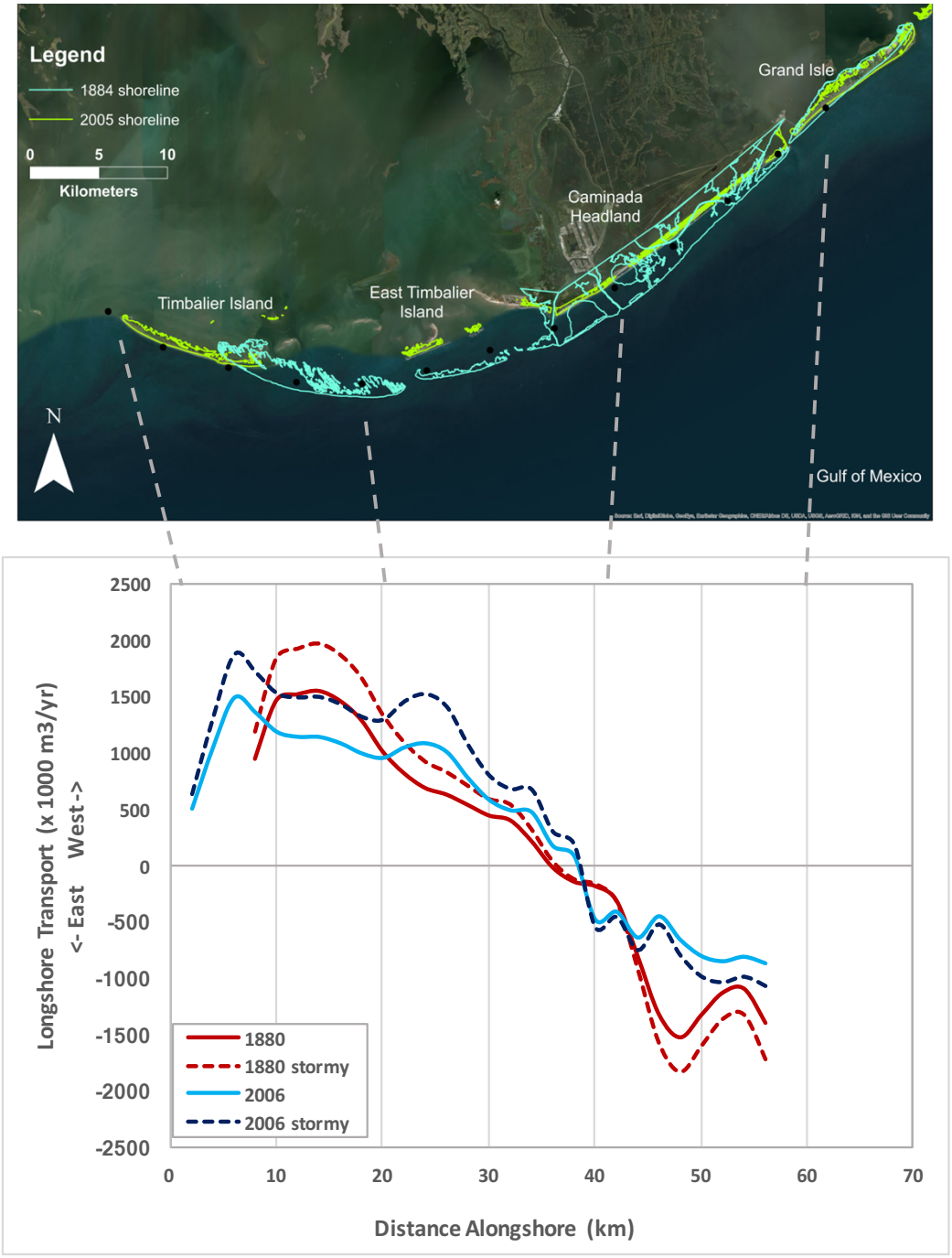

Figure 16: UNIBEST Lt longshore transport results for the 1880s (red) and 2006 (blue) standard waves (solid lines) and stormy (dashed lines) wave climate scenarios. Results illustrate that the more active storm scenarios increase longshore transport rates in both 1880s and 2006 as would be expected.

To test the influence of storm activity on sediment transport flux, a simple test was run with the 1880s and 2006 data with the same wave scenarios for an average year and wave scenarios with the frequency adjusted for a stormier wave climate to isolate the variation based only on changes in wave frequency on the coast. Results show that for both the early period (1880s) and the more recent period (2006) the increase in story activity is reflected in an increase in the longshore transport rates both to the east and west (Fig. 16). The results again show that the transport rates across the center of the study area (18-43km) have increased and both ends (< 18km and >43km) have decreased from the 1880s to 2006.

Discussion:

A key to interpreting the results of this study is to understand the influence of temporal scales on the observed trends in barrier island shoreline and shoreface trajectories. As discussed by Schumm and Lichty (1965), the recognition of the time-scale at which changes in landforms occur determines the understanding of the variables and processes effected by and driving change (Schumm and Lichty 1965). The authors identify three time-scales, which do not have distinct limits and can vary based on the processes or landform of interest. For application in this study the scales could be delineated as; cyclic (millennial), graded (decadal), and steady (less than annual). The limitations of the available data (~10 to ~50 year intervals) spanning over 135 years, prohibit observing the entire cyclic time-scale, but the delta lobe cycle could fit in this framework as well as the process of coastal straightening, where the process of the erosion of the delta lobe is a relatively long-term process. The graded scale fits the dynamic equilibrium behavior of the shoreface slope in response to storm activity where the punctuated erosion of the shoreface temporarily steepens the shoreface followed by relaxation of the slope. The steady scale would be at shorter time frames where significant storm events do not disrupt more moderate erosion regime. This cross-shore dynamic equilibrium of the shoreface is occurring within the context of the longer-term straightening of the delta lobe with storm activity being the main factor driving fluctuation around the equilibrium.

The Late Lafourche delta lobe system represents an example of this periodic retreat model, in which the passage of intense tropical cyclones dominates the erosion of the lower shoreface resulting in a temporary disequilibrium followed by periods of relative quiescence where some recovery or reduced erosion allow for storage of sediments along the shoreface.

This periodic retreat is evident in the erosion of the Caminada Headland as seen in the migration rates of the shoreface (Fig. 10). During period 1, there were higher rates of landward migration of the shoreline and upper shoreface indicating a relaxation of the shoreface. This likely was the result of an over steepening of the shoreface in the 1850s due to the passage of the most intense storms in the region (PDI of ~8 $x10^9$) (Fig. 8). This series of intense storms early in this time-period would have increased the wave-base which can entrain sediments at greater depths causing a more accelerated retreat of the lower shoreface and therefore a steepening of the upper shoreface. This process would explain the relatively steeper upper shoreface slopes of Caminada Headland in 1880s (Fig. 10C).

This steeper shoreface would have reduced the distance which smaller waves would have interacted with the seafloor therefore less erosion of the lower shoreface would have occurred. Wave energy would be transferred onto the upper shoreface and shoreline yielding higher rates migration rates as the shoreface readjusts to the long-term equilibrium. This response is evident in Caminada example profile (Fig. 10B) which shows the relaxation of the shoreface in period 1 and 2. Storm induced erosion of the lower shoreface in period 3 steepened the profile. In period 4 there was not much change in the lower shoreface and yet there was still some erosion of the upper shoreface during the quiescent period. If this pattern continues, wave energy during the relative quiescent times like the most recent period (Fig. 8) will still facilitate erosion of the upper shoreface and shorelines. The shoreface will again retreat at higher short-term rates in a punctuated manner during times of increased storm activity.

For period 3, when comparing the vertical change of the shoreface in the bathymetric change maps, it appears that the erosion along the Caminada Headland was distributed evenly along the cross-shore direction beyond the limits of the data (Fig. 9B). However, when evaluating shoreface response in terms of the rates of isobaths migration, the lower shoreface exhibited the highest rates of landward migration for period 3 (10A). This behavior is likely due to the intensity of storms in 2005 that immediately preceded the survey which had higher wave base and thus had the capacity to liberate sediment from deeper portions of the shoreface.

Offshore sediment availability is key to barrier resilience to storm impacts where barrier thinning and shoreface steepening could slow landward migration but increase the vulnerability of the barriers to storms (Moore et al. 2010; Masselink and Van Heteren 2014). Thinner barriers are ultimately more susceptible to fragmentation during storms and have a diminished capacity to support back barrier marsh which in turn helps to stabilize the barrier. In this way, barriers will become submerged at a faster rate when the lower shoreface is preferentially eroded.

Along the Caminada Headland there is no net deposition on the shoreface in any on the periods meaning the only way the profile remains in equilibrium is an equal landward migration of the shoreface and the shoreline. In other words, the net long-term erosion of the shoreline must balance the long-term erosion of the lower shoreface. List et al. 1997, suggests in locations with a sediment deficit, the return to profile equilibrium must be dominated by erosional processes and deposition is driven mainly by longshore processes (List et al. 1997). Caminada Headland is an example of the erosional process contribute to profile adjustments and the Timbalier Island is an example of the longshore processes aiding in deposition. As the

Caminada Headland is eroded and migrates landward the some of the liberated sediment is transported downdrift to the flanking barrier islands (Timbalier to the west and Grand Isle to the east) and the much of the finer grained material is transported offshore or into the back barrier.

For Timbalier Island, landward migration of the shoreface occurred in all time periods except for period 3 in which the shoreline, upper and lower shoreface all migrated landward. Period 4 had the highest rates of seaward migration of the lower shoreface (Fig. 11). As this is the shortest time-period in the data-set, this suggests that the instantaneous storm erosion is followed by sub-decadal periods of post-storm recovery (Fig. 8). Deposition occurs during this recovery due to a decrease in erosional events and therefore a diminished wave energy allowing sediment to accumulate. These high rates of lower shoreface recovery or seaward migration were likely occurring in the historic periods but are masked in the data by the interspersed large storm events in which the punctuated landward migration occurred (Fig. 11). This depositional period supports the longshore process recovery model that provides a mechanism for the shoreface to maintain an equilibrium profile.

The CPDI analysis attempts to put the data-sets into this context of these oscillations between the passage of intense tropical cyclones and the associated post-storm recovery (Fig. 8). The regional storm patterns reflect this relationship as the periods with the highest CPDI are the 1880 and the 2006 which both have higher rates of erosion along the shoreface resulting in steeper shoreface slopes. The lowest CPDI are in the 1980 and 2015 periods which correspond to the periods of the recovery of the lower shoreface of Timbalier Island (Fig. 11). The same pattern can be observed in the local PDI analysis which shows the highest levels of PDI in the

1850s-1860s and the highly active 2005 season right before the 2006 dataset, followed by the quiescent period 4. It should be noted that there were powerful hurricanes that occurred in this period such as Gustav and Isaac but there impacts on this scale were relatively minor even though there was significant morphological change during those storm events.

The source of the lower shoreface deposits along the Timbalier shoreface is not certain, but the most likely source is the eroding ebb-delta front along at Little Pass Timbalier and likely Raccoon Pass in earlier periods. This area is not only the most proximal it is also the most significant location of erosion in the 2006 to 2015 period. As discussed by Miner et al. 2009, this area had significant storm induced erosion of the ebb-tidal delta during 2005, but this erosion also continued into the relative quiescent most recent period. This could be the result of the straightening of this section of the coast, by which the curvature on the western side of the Caminada Headland in the earlier periods provided some protection for the ebb-delta which diminished as the headland retreated.

Coastal straightening analysis shows that not only has the curvature of the shorelines have straightened over the study period but there was a greater magnitude of straightening on the lower shoreface (Fig. 12). As this straightening has developed the inflection point of the curve has migrated westward. This migration is corroborated in the UNIBEST analysis of longshore transport that shows the elevated transport rates in the 2006 results and by the volumetric erosion results showing the highest magnitude of erosion migrating further to the west in each period (Fig. 9C).

This westward migration is a function of the straightening process as the UNIBEST results show that the adjustment of the coastal angle resulted in an increase in transport

potential across Little Timbalier and Raccoon Pass and a decrease at the west end of Timbalier and the east end of Caminada (Fig. 15). High rates of erosion of East Timbalier Island led to the construction of rock breakwaters to maintain the shoreline position. Ultimately, this method was not successful as the focus of this erosional zone was driving this area of the coastline and shoreface to migrate landward in response to the straightening process (Fig. 13).

This shifting of the erosional hotspot on the shoreface shows how the long-term changes in regional geometry influence the evolution of the system. This has implications for the distribution of wave energy throughout the area, as the refraction around the curve has shifted away from the straighter headland to the ebb-delta. This will eventually lead to a reduction in the available sediment for the down drift barriers as the sediment stored in the ebb-delta becomes exhausted.

In the most recent period this ebb delta erosion corresponds to high rates of seaward migration of the isobaths (recovery) along the Timbalier Island shoreface. Although these processes may have helped to nourish down drift barriers in the past, the effectiveness of the underlying processes that drove them but will diminish. Anthropogenic intervention to protect infrastructure reduces the amount of landward migration and therefore the volume of sediment that may have been liberated with unimpeded transgression. Storm induced shoreface ravinement will continue at comparable rates relative to the frequency and magnitude of storms leading to a regime of over-steepening of the shoreface.

Although regional straightening is generally associated with the littoral processes in the nearshore, the high rates of erosion along the lower shoreface in the period 3 illustrates that the straightening is widespread, and that it is the result of infrequent punctuated large storm

events that erode the lower shoreface of the headland at higher rates than the proximal island shoreface leading to a straightening of the shoreface.

Uncertainty

Each dataset used in this study introduced some amount of uncertainty, but the purpose of this effort was to identify broad trends and trajectories which are generally beyond the margin of error. The amount of uncertainty related to the bathymetry datasets varies and increases with time, but List et al. (1994) conservatively estimated a maximum of +/- 0.5m for calculating elevation change for the historic datasets (Miner et al. 2009). Translating this vertical error to horizontal migration rates results in an estimation of error of +/- 5m/yr. for the most relaxed slopes and oldest bathymetry data. The uncertainty for the shoreline change rates are estimated to be less than 1m/yr. (Byrnes et al. 2017). These uncertainties are reduced by averaging the data over alongshore and cross-shore sections.

The storm impact analysis has some uncertainty related to the methods of data collection and recording of historic storms. The most consequential errors are omission (storms not observed), storm track, and intensity. The earliest data (pre 1885) having up possible omissions of 0-6 storms per year (Atlantic Basin) up to 220km position error and 13 m/s of intensity error, yet reduce to 110km and 8 m/s for storms that made landfall (Landsea et al. 2004). All uncertainty factors significantly reduce as technology has improved and population have increased resulting in modern storms having uncertainty estimates of 45 km position error and 5 m/s intensity error and reduce to 24km for storm that made landfall (Landsea and Franklin 2013). The methods used for the regional PDI analysis are not dependent on the exact

storm position since the entire storm tracks within the regional box are included. The local (spatially explicit) PDI is inherently biased toward the higher certainty landfall storm data as opposed to the open water data and distributes the storm around the track by an average storm radius, so the uncertainties in the exact position may result in east/west errors but are diffused. The main trends observed in the storm data analysis (relatively active early period (pre-1880s), quiescence from 1900 through the 1980s, the highly active 2005 season, followed by the quieter 2006 to 2015 period) are valid even with the significant amount of uncertainty in the dataset.

Implications for long-term evolution and coastal management

The results from this study suggest that the role of storm influence and coastal straightening on the regional sediment budget for the coast should be considered further. Storm analysis suggested that the impacts of storms on the study area were likely the most intense in the 1850s and 1860s (PDI of ~8 $x10^9$) which is 20-30 years before the first data set in this study and therefore the resulting change. However, the steepest upper shoreface along the Caminada Headland was during 1880s which would corroborate these results assuming the underlying theory that the impact of large storms results in greater erosion of the shoreface leading to a steeper shoreface.

The erosion of the Caminada shoreface has served as the main source of sediment for the proximal Timbalier island and has eroded over time leading to a straightening of the coast which has shifted the erosional center to the west. As erosion shifts to the west, the ebb delta across Little Timbalier Pass has continued to erode even during the relative quiescent recent

period. The UNIBEST analysis (Fig 14 and 15) shows an increased zone of transport corresponding to the eastern edge of this ebb delta corroborating that this area is increasingly vulnerable because of changes in shoreface geometry. As coastal straightening continues, the erosional potential will decrease as the sediment sinks, such as the ebb delta, are preferentially eroded. Even though the depositional zone along the shoreface of Timbalier Island will likely remain an area where sediment can accumulate during quiescent periods the erosional center will continue to migrate to the west and further encroach upon this area of the shoreface.

Our results suggest that coastal straightening is a fundamental part of long-term evolution of erosion and deposition patterns on the shoreface of the Late Lafourche delta complex leading to a migration of the erosional zone to the west as that section of coast and shoreface straighten through time. The isobaths migration analysis confirms that the shoreface has eroded in a punctuated retreat mode and correlates with storms induced erosion of the shoreface producing a temporary disequilibrium followed by localized recovery/deposition during relatively quiescent times.

Our analysis suggests that although shoreline erosion rates decreased, overall landward migration of the barrier system increased as the shoreface steepened during the stormy 2005 hurricane season followed by a period of relative quiescence. This illustrates that the shoreface is more sensitive to storm impacts than is evident by the shoreline response and that these fluctuations play a key role in determining sediment budget trajectories. The return of the lower shoreface to progradational in some locations shows zones of post storm recovery possibly indicating areas where restoration would be more resilient. Our results illustrate that monitoring subaerial island erosion rates are insufficient for evaluating regional dynamics of

transgressive coastal systems. To maintain subaerial exposure, barriers islands require nourishment from shoreface sediments, therefore understanding sediment transport pathway and shoreface dynamics is key to evaluating barrier island trajectories. Advances in understanding these processes will facilitate more informed planning, management, and mitigation of transgressive barrier islands.

Conclusions:

- Punctuated storm response suggests periodic retreat type model - temporary disequilibrium caused by the storm.
- Lower shoreface undergoes post-storm recovery to dynamic equilibrium.
- Sediment bypassing mechanism transfers sediment along lower shoreface.
- Sediment is stored in lower shoreface (during quiescent times) mobilized during storm events, ultimately nourishes down drift barriers.
- Coastal straightening has diminished the effectiveness of these processes through the reduction in longshore sediment fluxes across the middle and lower shoreface of Timbalier Island while increasing the longshore transport across the inlets and has transferred the erosional inflection point toward the west continuing to deplete the ebb delta. This will ultimately result in a reduction in nourishment capacity for down-drift barriers.

References:

Barras, J., Beville, S., Britsch, D., Hartley, S., Hawes, S., Johnston, J., … Suhayda, J. (2004). Historical and Projected Coastal Louisiana Land Changes : 1978-2050. *World*, *334*(January), 45. Retrieved from http://www.louisianaspeaks-parishplans.org/projectattachments/001246/NewHistoricalland.pdf

Bilskie, M. V., Hagen, S. C., Alizad, K., Medeiros, S. C., Passeri, D. L., Needham, H. F., & Cox, A. (2016). Dynamic simulation and numerical analysis of hurricane storm surge under sea level rise with geomorphologic changes along the northern Gulf of Mexico. *Earth's Future*, (April), n/a-n/a. https://doi.org/10.1002/2015EF000347

Booij, N., Ris, R. C., & Holthuijsen, L. H. (1999). A third-generation wave model for coastal regions: 1. Model description and validation. *Journal of Geophysical Research*, *104*(C4), 7649–7666. https://doi.org/10.1029/98JC02622

Byrnes, M. R., Berlinghoff, J. L., Griffee, S. F., Underwood, S. G., & Lee, D. M. (2017). Louisiana Barrier Island Comprehensive Monitoring Program (BICM): Phase 2 - Shoreline Compilation and Change Assessment. Prepared for : Louisiana Coastal Protection and Restoration Authority Prepared by : Louisiana Barrier Island Comprehensive Monitorin, (February), 41 p. plus appendices.

Coastal Engineering Consultants, Inc (CEC) (2015). *Caminada Headland Beach and Dune Restoration. Prepared for State of Louisiana (OCPR.*.

Couvillion, B. R., Beck, H. J., Schoolmaster, D., & Fischer, M. R. (2016). *Land Area Change in Coastal Louisiana (1932 to 2016)*.

Emanuel, K. (2005). Increasing destructiveness of tropical cyclones over the past 30 years. *Nature*, *436*(7051), 686–688. https://doi.org/10.1038/nature03906

Fearnley, S. M., Miner, M. D., Kulp, M., Bohling, C., & Penland, S. (2009). Hurricane impact and recovery shoreline change analysis of the Chandeleur Islands, Louisiana, USA: 1855 to 2005. *Geo-Marine Letters*, *29*(6), 455–466. https://doi.org/10.1007/s00367-009-0155-5

Frazier, D. (1967). *Recent Deltaic Deposits of Mississippi River: Their Development and Chronology*. *Aapg Bulletin - AAPG BULL* (Vol. 51). https://doi.org/10.1306/5D25C219-16C1-11D7-8645000102C1865D

Georgiou, I. Y., FitzGerald, D. M., & Stone, G. W. (2005). The Impact of Physical Processes along the Louisiana Coast. *Journal of Coastal Research*, *Sp. Issue*(Figure 1), 72–89. Retrieved from http://www.jstor.org/stable/10.2307/25737050

Hallermeier, R. J. (1980). A profile zonation for seasonal sand beaches from wave climate. *Coastal Engineering*, *4*, 253–277. https://doi.org/https://doi.org/10.1016/0378-3839(80)90022-8

Jaffe, B. E., List, J. H., & Sallenger, A. H. (1997). Massive sediment bypassing on the lower shoreface offshore of a wide tidal inlet - Cat Island Pass, Louisiana. *Marine Geology*, *136*(3–4), 131–149. https://doi.org/10.1016/S0025-3227(96)00050-3

Knapp, K. R., Kruk, M. C., Levinson, D. H., Diamond, H. J., & Neumann, C. J. (2010). The International Best Track Archive for Climate Stewardship (IBTrACS): Unifying tropical cyclone best track data. *Bulletin of the American Meteorological Society, 91*, 363–376. https://doi.org/10.1175/2009BAMS2755.1

Komar, P. D., & McDougal, W. G. (1994). The Analysis of Exponential Beach Profiles. *Journal of Coastal Research*, *10*(1), 59–69.

Kulp, M. A., Fitzgerald, D. M., & Penland, S. (2005). Sand-rich Lithosomes of the Holocene Mississippi River Delta Plain. In *River Deltas* (pp. 277–294).

Landsea, C. W., Anderson, C., Charles, N., Clark, G., Dunion, J., Fernandez-Partagas, J., … Zimmer, M. (2004). The Atlantic hurricane database re-analysis project: Documentation for the 1851-1910 alterations and additions to the HURDAT database. *Hurricanes and Typhoons: Past, Present, and Future*, 177–221.

Landsea, C. W., & Franklin, J. L. (2013). Atlantic Hurricane Database Uncertainty and Presentation of a New Database Format. *Monthly Weather Review*, *141*(10), 3576–3592. https://doi.org/10.1175/MWR-D-12-00254.1

List, J. H., Jaffe, B. E., Sallenger, A. H., Williams, S. J., Mcbride, R. A., & Penland, S. (1994). *Louisiana Barrier Island Erosion Study: Atlas of Sea-Floor Changes from 1878 to 1989*.

List, J. H., Sallenger, A. H., Hansen, M. E., & Jaffe, B. E. (1997). Accelerated relative sea-level rise and rapid coastal erosion: testing a causal relationship for the Louisiana barrier islands. *Marine Geology*, *140*(3–4), 347–365. https://doi.org/10.1016/S0025-3227(97)00035-2

Martinez, L., Brien, S. O., Bethel, M., & Penland, S. (2009). Louisiana Barrier Island Comprehensive Monitoring Program (BICM) Volume 2 : Shoreline Changes and Barrier Island Land Loss 1800 ' s - 2005, *2*.

Masselink, G., & Van Heteren, S. (2014). Response of wave-dominated and mixed-energy barriers to storms. *Marine Geology*, *352*, 321–347. https://doi.org/10.1016/j.margeo.2013.11.004

May, J. P., & Tanner, W. F. (1973). The littoral power gradient and shoreline changes. In D. R. Coates (Ed.), *Publications in Geomorphology* (pp. 43–60). State University, N.Y., Binghamton, N.Y. 404 pp.

Miner, M. D., Kulp, M. A., FitzGerald, D. M., Flocks, J. G., & Weathers, H. D. (2009). Delta lobe degradation and hurricane impacts governing large-scale coastal behavior, South-central Louisiana, USA. *Geo-Marine Letters*, *29*(6), 441–453. https://doi.org/10.1007/s00367-009-0156-4

Miner, M. D., Kulp, M. A., Penland, S., Weathers, H. D., Motti, J., Mccarty, P., … Torres, J. (2009). *Louisiana Barrier Island Comprehensive Monitoring Program (BICM) Volume 3: Bathymetry and Historical Seafloor Change 1869-2007*.

Moore, L. J., List, J. H., Williams, S. J., & Stolper, D. (2010). Complexities in barrier island response to sea level rise: Insights from numerical model experiments, North Carolina Outer Banks. *Journal of Geophysical Research*, *115*(F3), F03004 1-27. https://doi.org/10.1029/2009JF001299

Mueller, J. E. (1968). An introduction to the hydraulic and topographic sinuosity indexes. *Annals of the Association of American Geographers*, *58*(2), 371–385. https://doi.org/10.1111/j.1467-8306.1968.tb00650.x

Penland, S., Boyd, R., & Suter, J. R. (1988a). Delta Plain : a Model for Barrier Shoreline and. *Journal of Sedimentary Petrology*, *58*(6), 932–949.

Penland, S., Boyd, R., & Suter, J. R. (1988b). Transgressive depositional systems of the Mississippi Delta plain; a model for barrier shoreline and shelf sand development. *Journal of Sedimentary Research*. https://doi.org/10.1306/212F8EC2-2B24-11D7-

8648000102C1865D
Poff, M., Georgiou, I., Kulp, M., Leadon, M., Thomson, G., & Walstra, D. J. R. (2015). 2017 Coastal Master Plan Modeling: Attachment C3-4 – Barrier Island Model Development (BIMODE), (July 2015).
Ritchie, W., & Penland, S. (1988). Rapid dune changes associated with overwash processes on the deltaic coast of South Louisiana. *Marine Geology*, *81*(1–4), 97–122. https://doi.org/10.1016/0025-3227(88)90020-5
Schumm, S. A., & Lichty, R. W. (1965). Schumm and Lichty, 1965. *American Journal of Science*, *263*, 110–119. Retrieved from papers2://publication/uuid/8301365A-9F14-44A6-8DB4-00395C001834
Stone, G. W., Grymes, J. M. I., Dingler, J. R., & Pepper, D. . A. (1997). Overview and significance of hurricanes on the Louisiana coast, USA. *Journal of Coastal Research*, *13*(3), 656–669. https://doi.org/10.2307/4298661
Stone, G. W., & McBride, R. A. (1998). Louisiana barrier islands and their importance in wetland protection: forecasting shoreline change and subsequent response of wave climate. *Journal of Coastal Research*. Retrieved from http://www.jstor.org/stable/10.2307/4298843
Swift, D. J. P. (1975). Barrier-island genesis: evidence from the central atlantic shelf, eastern U.S.A. *Sedimentary Geology*, *14*(1), 1–43. https://doi.org/10.1016/0037-0738(75)90015-9
Thieler, E. R., Himmelstoss, E. A., Zichichi, J. L., & Ergul, A. (2009). *The Digital Shoreline Analysis System (DSAS) Version 4.0 - An ArcGIS extension for calculating shoreline change*. *Open-File Report*. Reston. Retrieved from http://pubs.er.usgs.gov/publication/ofr20081278
UNIBEST-CL + manual. (2011).
Williams, S. J., Penland, S., & Sallenger, A. H. (1992). *Louisiana Barrier Island Erosion Study: Atlas of Shoreline Changes in Louisiana from 1878 to 1989*. *USGS/La. State Univ., Misc. Investig. Ser. I-2150-A*.
Wolinsky, M. A., & Murray, A. B. (2009). A unifying framework for shoreline migration: 2. Application to wave-dominated coasts. *Journal of Geophysical Research: Earth Surface*, *114*(1), 1–13. https://doi.org/10.1029/2007JF000856

CHAPTER 3: COUPLED BARRIER ISLAND SHORELINE AND SHOREFACE DYNAMICS AT REGIONAL AND LOCAL SCALES

Introduction:

Barriers islands are accumulations of sediment that are built vertically due to wave action and wind processes are most commonly found on trailing margins, occupying 15% of the world's coastlines (Cooper and Pilkey 2004). The barrier islands on the Mississippi River Delta Plain (MRDP) formed from reworked delta deposits, whereby channel sands, mouth bars, natural levees are reworked by wave action to form landscapes that resemble arcuate shapes (headlands) with flanking barrier splits. Storms and other oceanographic processes may cause barrier breaching, overwash and/or continue to grow these landscapes (laterally and vertically) until they detach from mainland by widespread subsidence and wetland loss within the back barrier setting. Meanwhile, the accumulation of sands comprising the developing barrier island, lag this process and maintain subaerial exposure through further reworking to form a robust subaerial landform (a barrier island).

These islands provide ecosystem services and economic resources to coastal communities (Barbier et al. 2011), and provide protection for the interior marsh by reducing inland flooding through the attenuation of storm surge, and the reduction in wave energy arriving inland (Stone and McBride 1998; Georgiou et al. 2005; Bilskie et al. 2016).

Barrier islands in the MRDP and worldwide are experiencing transgression or landward migration, due to shoreface retreat, increasing tidal prism, lack of sediment supply and other factors including the rise in relative sea-level (RSL) (Davis et al., 2004;Fearnley et al., 2009;

FitzGerald et al., 2008; Miner et al., 2009). In response to these factors barriers must either retreat, fragment, or become submerged shoals (Penland et al. 1988a). To mitigate loss of area due to transgression and to prolong the subaerial footprint of barriers, many coastal communities are implementing restoration efforts and adaptive management strategies including beach nourishment, interior and back barrier marsh creation, and the installation and construction of hard structures such as groins, jetties, and levees (Nordstrom 2014). Although some of these efforts are successful in temporarily maintaining or increasing the barrier island or beach footprint, the fundamental processes that contribute to barrier deterioration continue to be active, and thus transgression, and often accompanied erosion, persists. Much of the monitoring and analysis of barrier islands was historically focused on shoreline and subaerial portions of the island, but changes in the geometry of the shoreface can influence the longevity of the barriers (Bruun, 1962; Swift, 1975). For instance, Bruun (1962) suggested that the shoreface is in a state of dynamic equilibrium where the retreat rate of the barrier is linked to shoreface slope, a result that was revisited by Swift (1975), where he reported that shoreface retreat behavior can vary depending on sediment supply and RSL (Bruun, 1962; Swift, 1975).

In southeast Louisiana, barriers are found on both sides of the modern Mississippi River on the Mississippi River Delta Plain (MRDP). This region is experiencing rapid geomorphic change including widespread land loss (Barras et al. 2004; Couvillion et al. 2016), and a shrinking barrier island system, with historic average shoreline erosion rates ranging from 1-11m/yr. (Martinez et al. 2009; Byrnes et al. 2017). These barriers are the product of reworked sandy deposits that are the remains of the abandoned distributary lobes of the Mississippi River (Penland et al. 1988a). High rates of RSL (~0.92cm/yr.), an increase in strong storm activity, and

reduction of sediment supply have made this coastline especially vulnerable (Georgiou et al. 2005b; Fearnley et al. 2009; Miner et al. 2009).

In the State of Louisiana, the agency responsible for nourishing barrier is presently the Coastal Protection and Restoration Authority (CPRA). In the recent history (~2005) the agency developed the Barrier Island Comprehensive Monitoring (BICM) program in partnership with the U.S. Geological Survey (USGS) and the University of New Orleans (UNO) Pontchartrain Institute for environmental Sciences (PIES) to collect and digitize historical shoreline, bathymetry, topographic, habitat, and sediment data. The idea was (and continues to be) to build a framework where every ~7 years a complete dataset would be collected and added to the database.

The rapid morphological change of the MRDP barriers in conjunction with the BICM data provide an opportunity to evaluate the processes that drive barrier island evolution at decadal and centennial timescales rather than engineering or geologic timescales. The BICM bathymetric and shoreline for 2006 and 2015, in combination with historic data for the 1880s, 1930s, and 1980s, compiled by List et al. (1994) provides over 135 years for the Louisiana coast. An automated framework based on 100-m spaced shore-normal transects was created to quantify and track barrier island evolution though standardized metrics and parameters such as shoreline change, barrier island area and width, bathymetric contour migration at selected intervals, and shoreface slope and geometry.

This study uses this framework and the BICM/historic data to implement barrier island parameter tools created for this project in terms of 1) evaluating the coupling between the trajectories of barrier islands and the shoreface at regional scales along the Louisiana coast and

2) provide historic context and analysis of case study locations where various forms of restoration projects were implemented in the form of shoreline stabilization or beach and dune nourishment/restoration projects. Here we test the following hypothesis:

H3: Barrier island shoreline / shoreface coupling

Barrier island shoreline trajectory is coupled with the trajectory and geometry of the shoreface. Shoreface slope has been linked to the rate of shoreline erosion as barrier islands migrate landward and long-term modeling has indicated that steeper shoreface slopes will correspond to slower rates of shoreline migration and conversely that more gentle slopes will correspond to faster shoreline erosion rates (Moore et al. 2010; Lorenzo-Trueba and Ashton 2014).

H4: Restoration / management implications

Barrier island restoration and management decisions should consider the long-term regional trajectory and geometry of the shoreface and the resulting influences on the regional and local sediment budgets.

Study Area:

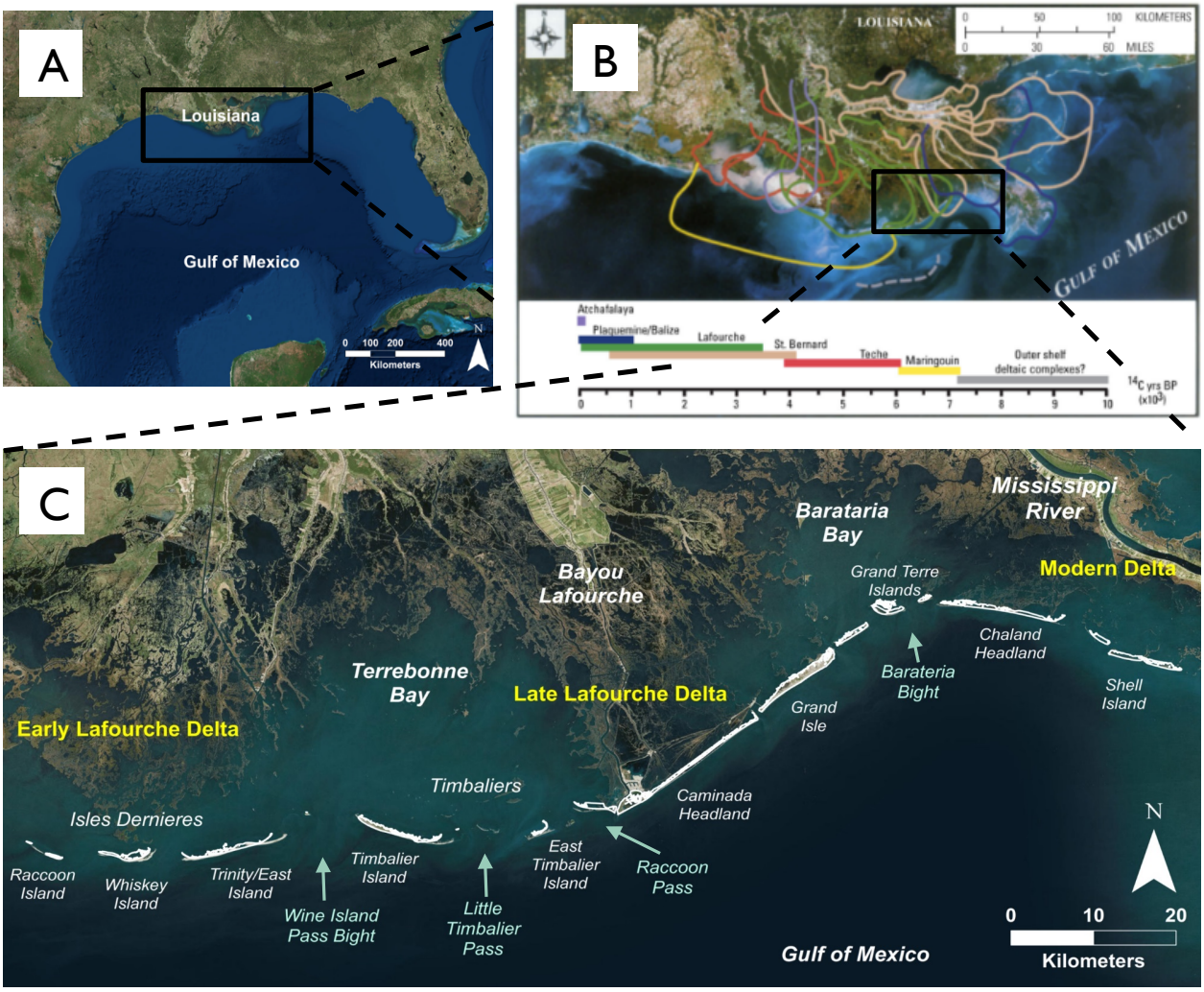

Figure 6: Map showing A) Gulf of Mexico with Mississippi River Delta and B) historic evolution of the delta lobes of Mississippi River (Kulp et al. 2005) and C) barrier island chains west of the modern delta.

This study covers 160 km of the south-central Louisiana coast, west of the Mississippi River, in Terrebonne, Lafourche, Jefferson, and Plaquemines Parishes, including the Isle Dernieres barrier island chain to the west to Shell Island to the east (Fig. 1). The prominent eroding Caminada Headland and flanking barrier islands are the remains of the Bayou Lafourche complex (active 1800-300 years B.P.), while the areas to the east are the result the

reworking of the older St. Bernard lobe (3,500-1,800 years B.P.), and the modern Plaquemines/Belize delta lobe (1,000 years B.P. to present) (Fig. 1B) (Frazier, 1967; Kulp et al., 2005; Miner et al., 2009).

Most of these islands have undergone restoration by mechanical introduction of sediment for beach, dune, and back barrier marsh nourishment and enhancement projects with an estimated 80 km of barrier islands and berms that have been constructed since 2007 (CPRA 2017). There have also been attempts at shoreline protection using segmented breakwaters and seawalls along some sectors of the coast including Raccoon Island, Timbalier and East Timbalier Island, central Caminada Headland, and the eastern portion of Grand Isle.

Background:

Barrier Islands

Barriers islands are accumulations of sediment that are built vertically due to wave action and wind processes are most commonly found on trailing margins, occupying 15% of the world's coastlines (Cooper and Pilkey 2004). The barrier islands on the MRDP formed from reworked delta deposits, whereby channel sands, mouth bars, natural levees are reworked by wave action to form landscapes that resemble arcuate shapes (headlands) with flanking barrier splits. Storms and other oceanographic processes may cause barrier breaching, overwash and/or continue to grow these landscapes (laterally and vertically) until they detach from mainland by widespread subsidence and wetland loss within the back barrier setting. Meanwhile, the accumulation of sands comprising the developing barrier island, lag this process and maintain subaerial exposure through further reworking to form a robust subaerial landform (a barrier island). Transgressive Mississippi Delta Barrier Model describes this process and shows the specific stages related to how the evolution from a prograding deltaic headland, to an erosional headland with flanking barriers (following an avulsion event relocating the riverine input of sediment), to a barrier island arc, and finally an inner shelf shoal (Fig. 2B) (Penland et al. 1988a).

Shoreface

The shoreface describes the portion of the seabed from the shoreline transitioning to the inner continental shelf (Barrell 1912). This seaward limit or often referred to as Depth of Closure (DOC) varies or shoreface toe depending on the timescale of interest. However, a

common convention is to estimate this depth using a relationship that utilizes annualized wave parameters with a return period of ~10% and local grain size to determine the limit of significant cross-shore exchange of sand during a typical year (Hallermeier 1980). The shoreface is then subdivided into upper and lower shoreface to differentiate the more active (seasonal) and less active lower shoreface (decades to centuries) (Hallermeier 1980; Niedoroda and Swift 1991). The shoreface shape is determined by the balance of sediment flux (alongshore and cross-shore) which is a function of grain size and the wave climate; thus over time the shoreface will reach a state of dynamic equilibrium with a concave up profile shape (Dean, 1991).

Previous studies have investigated processes of barrier island transgression by attempting to couple the barrier island migration and the geometry of the shoreface (Bruun 1962; Swift 1975; Moore et al. 2010; Wolinsky and Murray 2009; Jaffe et al. 1997; List et al. 1997; Aagaard and Sørensen 2012). Bruun (1962) proposed a shoreface profile equilibrium that will remain constant, translating landward and upward, during transgression and suggested a linear relationship between sea level rise and shoreline migration rates, which yields the following relationship its simplest:

$$s = \frac{al}{h}$$

where *s* is shoreline retreat, *a* is sea level rise, *l* is the distance offshore, and *h* is depth offshore (Bruun 1962; List et al. 1997). Dean (1977) expanded this concept through the application of the "Bruun rule" on over 500 locations along the Atlantic coast and used these data to derive a coefficient and to develop what is known as the modified Bruun rule (Dean 1977; List et al. 1997). This rule has been used by engineers and coastal planners as a method to predict the

rate of shoreline change based in response to relative sea level rise (Cooper and Pilkey 2004; Ranasinghe and Stive 2009). However, Cooper and Pilkey (2004) argue that the Bruun rule should be altogether abandoned due to the limitation and restrictions inherent in the essential assumptions in the development of this theory, and the lack of evidence to accurately predict shoreline change during sea level rise. Complicating factors for the viability of implementing the Bruun rule include, (a) scarcity of long-term consistent data to accurately define the Bruun parameters, (b) insufficient understanding of antecedent geology, and (c) the absence of a sediment budget to define the quantities of sediment transferring into and out of the system (List et al. 1997; Moore et al. 2010).

In response to the limitations of the Bruun Rule, researchers have explored how the shoreface/shoreline relationship varies when the profile is not in equilibrium (Wolinsky and Murray 2009; Moore et al. 2010; Lorenzo-Trueba and Ashton 2014). For instance, Wolinsky and Murray (2009) discuss the limitations in the application of the Bruun rule and explore the inclusion of and inland topography and shoreface slope variations, they explore it's relationship to the shoreline, and include what they defined as the morphokinematic Exner equation. The authors modify the Bruun rule theory to create two new scenarios to model gentle slopes or the "barrier Bruun rule" by including the barrier and back-barrier in the slope calculations, and for the steep slopes "cliff Bruun rule" by accounting for the cliff height in slope calculations. Their work concludes that barrier island slope (slope from the DOC to the landward shoreline) is the key factor influencing barrier island trajectories and migration rates instead of the shoreface slope described in the Bruun model (Wolinsky and Murray 2009). Moore et al. (2010) utilized the GEOMBEST model to compare various controls on barrier migration and found that

substrate slope, RSL rates, and sediment supply are the main factors. They also found that substrate composition is the dominating control in muddier coasts and that the barrier trajectory is a function of a combination of average barrier slope and sediment availability, known as the effective barrier island slope (Moore et al. 2010). The authors also concluded that the rate of migration and shoreface erosion must be balanced so that the amount of sediment liberated from the shoreface is sufficient for the barriers to maintain subaerial exposure to avoid transgressive submergence (Penland et al. 1988a; Moore et al. 2010). Aagaard and Sorensen (2014) considered sediment transport across the shoreface as a key to improving the ability to model coastal response to RSL and found that the steepness of the profile is essential to determining the direction of cross-shore sediment transport and therefore erosional and transgressive responses (Aagaard and Sørensen 2012). During a modeling study, Lorenzo-Trueba and Ashton (2014) explored shoreface geometry that was out of equilibrium shoreface by modeling several modes of barrier behavior in response to sea level rise including; dynamic equilibrium, height drowning, width drowning and periodic retreat. Their results suggest that periodic retreat behavior can occur around a shoreface equilibrium, and although at millennial time scales barrier systems might be able to return to equilibrium, faced with geologically rapid changes in RSL rates, barrier drowning will become more frequent (Lorenzo-Trueba and Ashton 2014).

Shoreface on the MRDP

List et al. (1994) compiled historical bathymetric maps from the 1880s, 1930s, and 1980s for the Louisiana coast and performed assessment of erosion and deposition and regional sediment transport trends for this transgressive coast and provided the early datasets for this study (List et al. 1994).

Subsequent studies have utilized this data (e.g. List et al. 1997), where they tested the applicability of the Bruun rule - which predicts shoreline migration rates based on sea-level rise and an assumed shoreface profile equilibrium - in the Mississippi River Delta Plain (MRDP). Their results showed that only 50% of the profiles examined met equilibrium criteria and that they did not show any statistical significance for hindcasting or predicting shoreline change (List et al. 1997). They also determined that one of the most complicating factors in determining shoreline and shoreface trajectories, is the inability to define and/or constrain an accurate sediment budget to account for longshore transport and other sediment distribution processes that drive changes in the shoreface (List et al. 1997).

Jaffe et al. (1997) utilized the same dataset and documented sediment transport processes which have contributed to offshore sediment bypassing resulting in a large area of deposition which offset erosion rates of the proximal shoreface and shorelines. This offshore bypassing illustrates a pathway for sediment to naturally nourish down drift (shoreface and) barriers and supports the theory that the volume of coarse grained sediment on the shoreface plays a role in determining the erosion rates of the proximal shoreline (Jaffe et al. 1997).

Building on the work of List et al. (1994; 1997) and Jaffe et al. (1997), Miner et al. (2009) analyzed seafloor change and documented volumes of sediment eroded from proximal (barrier

platform, inlets, ebb-deltas) and distal (shoreface) environments, and highlighted key processes governing sediment loss from the barrier system during transgression. The authors concluded that coastal straightening along the Caminada Headland, mostly in the form of lower and middle shoreface erosion driven by storm induced waves and currents, has been the dominant source of liberated sediment that has been available for reworking and deposition in sinks such as ebb-tidal deltas (Miner et al. 2009).

Although List et al. (1997), Jaffe et al. (1997) and Miner et al. (2009) all illustrated the importance of a regional understanding of sediment transport processes, the changes in shoreface geometry on sediment budgets and barrier evolution are not fully understood.

Part 1: Regional Trends in Shoreface Slope and Barrier Island Migration

Results

To identify long-term trends on the shoreface, shoreface slope, shoreline migration rates, and the average rates and slopes were calculated and compared for five selected regions along the central coast; Isles Dernieres Islands, Timbalier Islands, Caminada Headland, Grand Isle and Grand Terre, and the Modern Delta (Fig. 2). The results show that the mean landward shoreline migration rates have declined for all the regions except for an increase in period 4 for Timbalier Islands. The two regions to the to the east (Grand Isle and Grand Terre, and Modern Delta) switched to progradational (seaward) trajectory in period 4 (Fig 2).

The mean shoreface slopes relaxed in the two western regions (Isles Dernieres, and Timbalier Islands) and near Grand Isle and Grand Terre (Fig 2), while it steepened along the Caminada Headland and Modern Delta, despite experiencing the largest reduction in shoreline migration (>10m/yr). The steepest slopes (~1:250) were found in the Caminada region during times 4 and 5 while the most relaxed slopes were in the Isle Dernieres and Modern Delta (~1:1000).

To evaluate the regional trajectory of the shoreface the mean rate of migration for selected groups of isobaths (upper and lower) were calculated to estimate the shoreface migration rate, and were plotted alongside shoreline migration rates for comparison (Fig 3). The Isles Dernieres upper shoreface experienced landward migration every period with a peak rate in Period 3 (~> 20m/yr) stabilizing in period 4. The lower shoreface was prograding in period 1 and stable in period 2 followed by a landward trajectory in period 3 and a return to seaward migration (~12 m/yr) in period 4 (Fig 3).

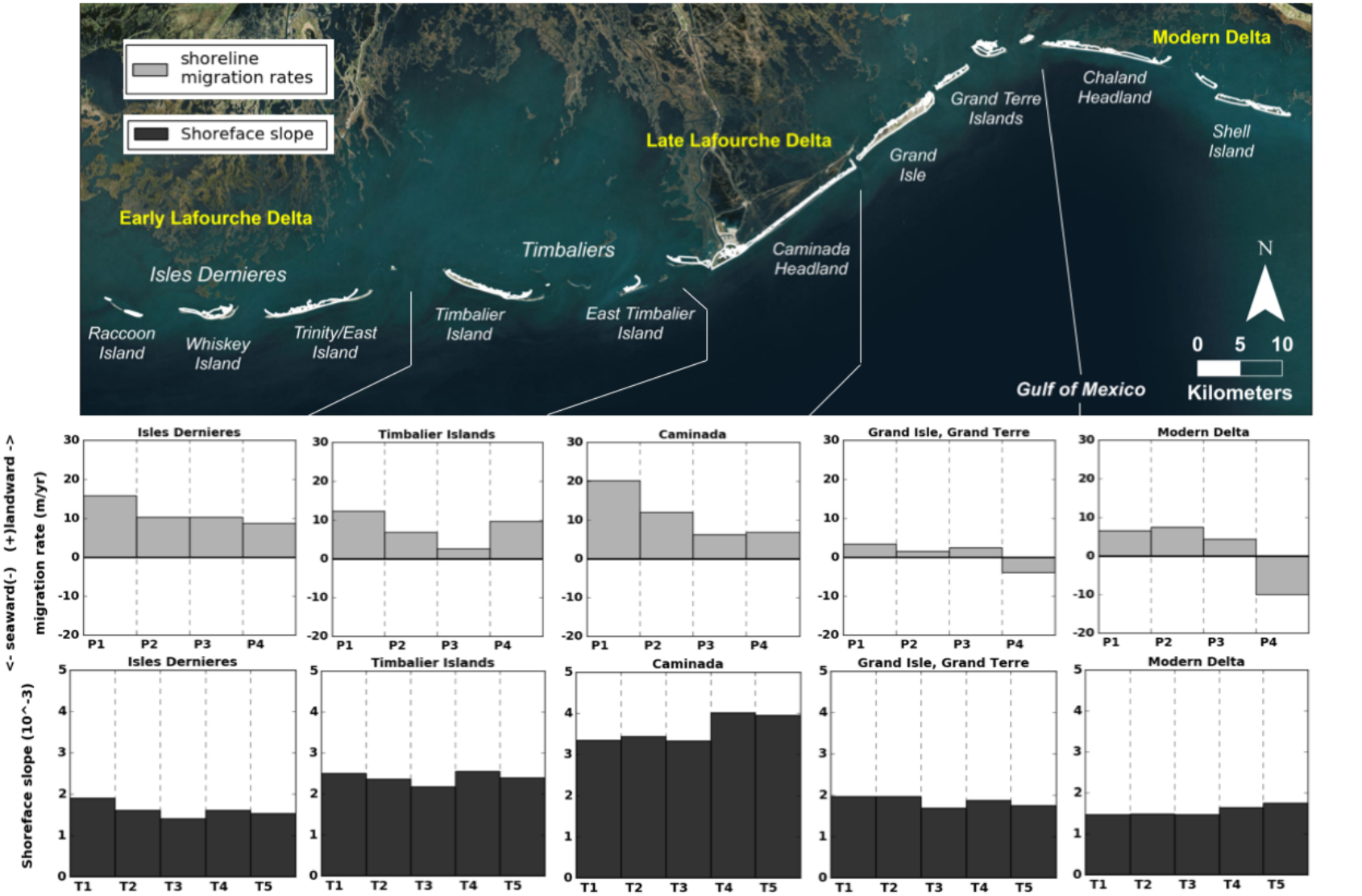

Figure 2: Shoreline migration rates (grey) and shoreface slopes (dark grey) for five regions of the Louisiana central coast; Isles Dernieres, Timbalier Islands, Caminada, Grand Isle/Grand Terre, and Modern Delta. Rates are separated into periods (P1: 1880s-1930s, P2: 1930s-1980s, P3: 1980s-2006, and P4: 2006-2015) and slopes are shown for each time (T1: 1880s, T2:1930s, T3:1980s, T4: 2006, and T5:2015). Note the reduction in shoreline migration rates in all regions and the steepest slopes are in the Caminada region.

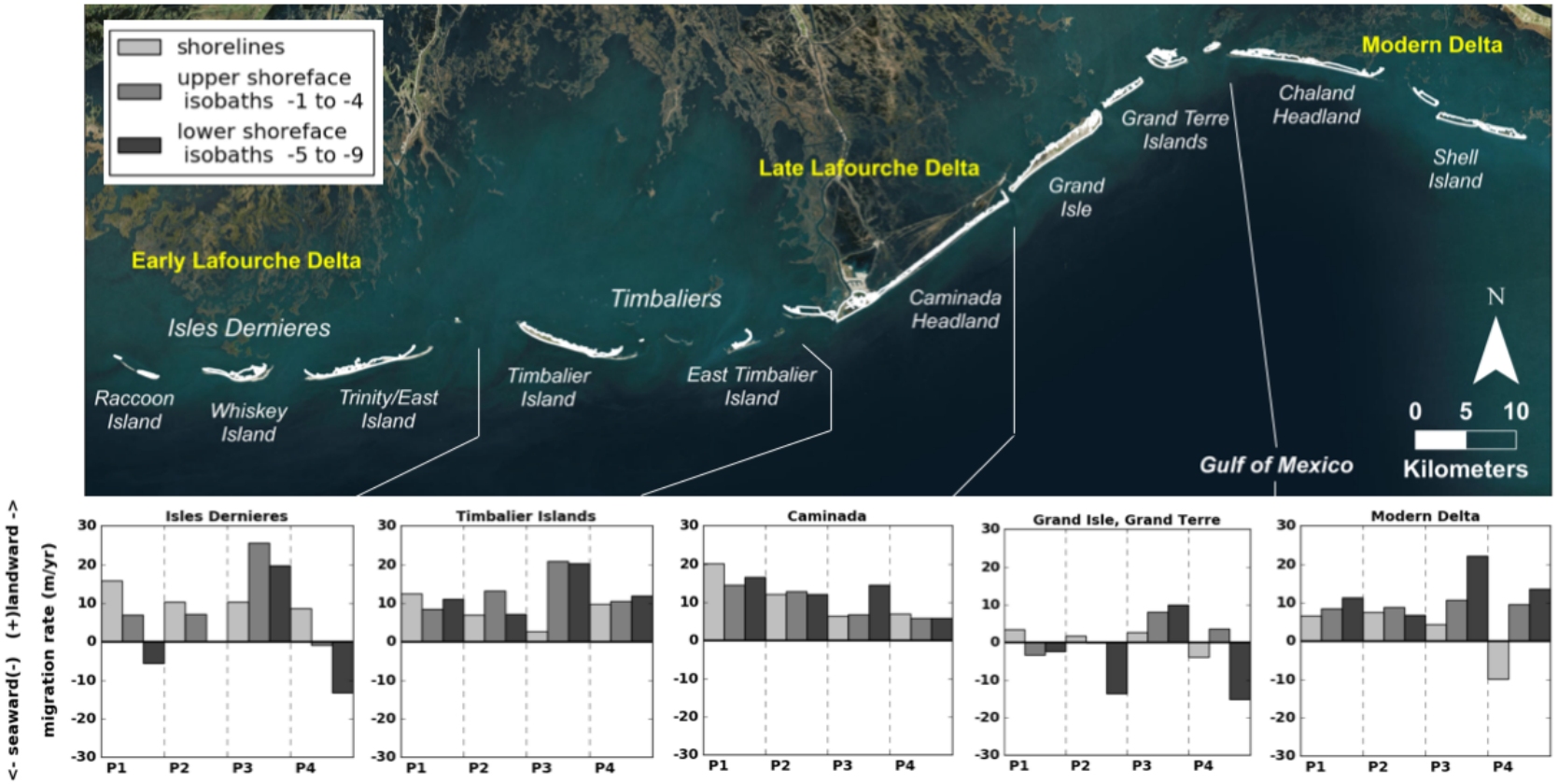

Figure 3: Shoreline migration rates (light grey) and upper shoreface (grey) and lower shoreface (dark grey) for five regions of the Louisiana central coast; Isles Dernieres, Timbalier Islands, Caminada, Grand Isle/Grand Terre, and Modern Delta. Rates are separated into periods (P1: 1880s-1930s, P2: 1930s-1980s, P3: 1980s-2006, and P4: 2006-2015). Note the increase in landward migration of the lower shoreface and P3 and the reduction in rates and/or seaward migration in P2 and P4.

The Timbalier Islands and Caminada Headland regions show landward migration of the shoreline and shoreface across all periods with the highest rates for Timbalier in period 3 and in period 1 for Caminada.

Grand Isle and Grand Terre lower shoreface switched from seaward in periods 1 and 2 to landward in period 3 and returned to seaward in period 4. The Modern Delta region shoreface migrated landward in all periods with the highest rates in period 3.

Regional: Summary and Discussion

An apparent trend in the shoreline migration results is that the shoreface migration has slowed for every region over the 135-year period. The shoreface slope do not show a clear trend with some regions increasing in slope and others decreasing. The slopes are also relatively stable without much change in the shoreface slopes over time. All regions show a steepening in 2006 (T4), reflecting the large-scale erosion during the 2005 hurricane season (Miner et al., 2009).

The Caminada Headland and Modern Delta are the two regions with the largest magnitude of change in shoreline migration rates are the same two sub-regions that have a steepening shoreface (Fig. 3). Both the Caminada Headland and Modern Delta, at least partially, are erosional headlands backed by marsh. In both cases, this marsh helps to keep the shoreline from migrating by trapping sediment, counteracting subsidence, and providing a platform for the barrier to rollover onto (Moore and Murray 2018). Both regions also benefitted from restoration and stabilization projects during this period, with beach/dune nourishment along Caminada (BA-45/BA-0143) and beach/dune nourishment projects (BA-35,

BA-40, BA-0110, BA-0111) and emergency berm creation after the 2010 oil spill (LA-0163) in the Modern Delta region.

Despite the beneficial marsh in the back barrier and the restoration of the beaches and dunes, the dominant process driving the regional steepening of the shoreface is the higher rates of landward migration of the lower shoreface rather than progradation of the upper shoreface. The differential (shoreface migration) rate is most prominent in period 3, which contains the active 2005 hurricane season. This suggests that in these two regions the lower shoreface is mainly driven by storm induced erosion. The other regions also had higher rates of landward migration of the lower shoreface during period 3, but there are other processes that offset the erosion. Timbalier Islands and Grand Isle Grand Terre, and Isle Dernieres are all downdrift recipients of sediments liberated from the erosional Caminada Headland region (Jaffe et al., 1997; Miner et al., 2009). The ebb tidal deltas and bights of these regions also have served a sediment sinks and act as depositional zones reducing the landward migration rates of the shoreface (Miner et al., 2009b).

Part 2: Local Case Studies of Barrier Island Shoreline and Shoreface Dynamics

2.1 Raccoon Island

Raccoon Island is located at the western end of the Isles Dernieres Island chain (Fig 1). The Isles Dernieres are the remains of the deposits of an abandoned delta lobe of the Mississippi River Delta complex that was active until ~400 years PB (Kulp et al. 2005). After an avulsion event in the Mississippi River the deposited sediment was reworked by marine processes eventually creating barrier islands (Penland et al. 1988a). Breaching and loss of sand to the back barrier and offshore, and migration into a deeper bay have reduced the robust continuous barrier of the late 1800s by 78% of the land area over a 100 year period (Mcbride et al., 1991; Miner et al., 2009; Fitzgerald et al. in Moore & Murray, 2018). The modern Isle Dernieres chain consists of Raccoon Island to the west, Whiskey Island in the center, and Trinity Island to the East. All the islands have undergone shoreline stabilization and restoration to reduce the rates of land loss.

Raccoon Island has had several attempts to prolong the subaerial exposure of the island starting with the construction of rock breakwaters in 1997 (TE-0029) to reduce the rate of shoreline erosion. The next project was constructed in 2007 following the widespread erosion brought on by the highly active 2005 hurricane season which includes Hurricanes Katrina, Cindy and Rita. Despite the stabilization efforts, Raccoon Island remains one of the most vulnerable islands in the south-central Louisiana coast.

Figure 4: Design of the TE-29 breakwaters and TE-48 breakwaters and marsh creation area (source: Coastal Protection and Restoration Authority of LA, Operations Division.)

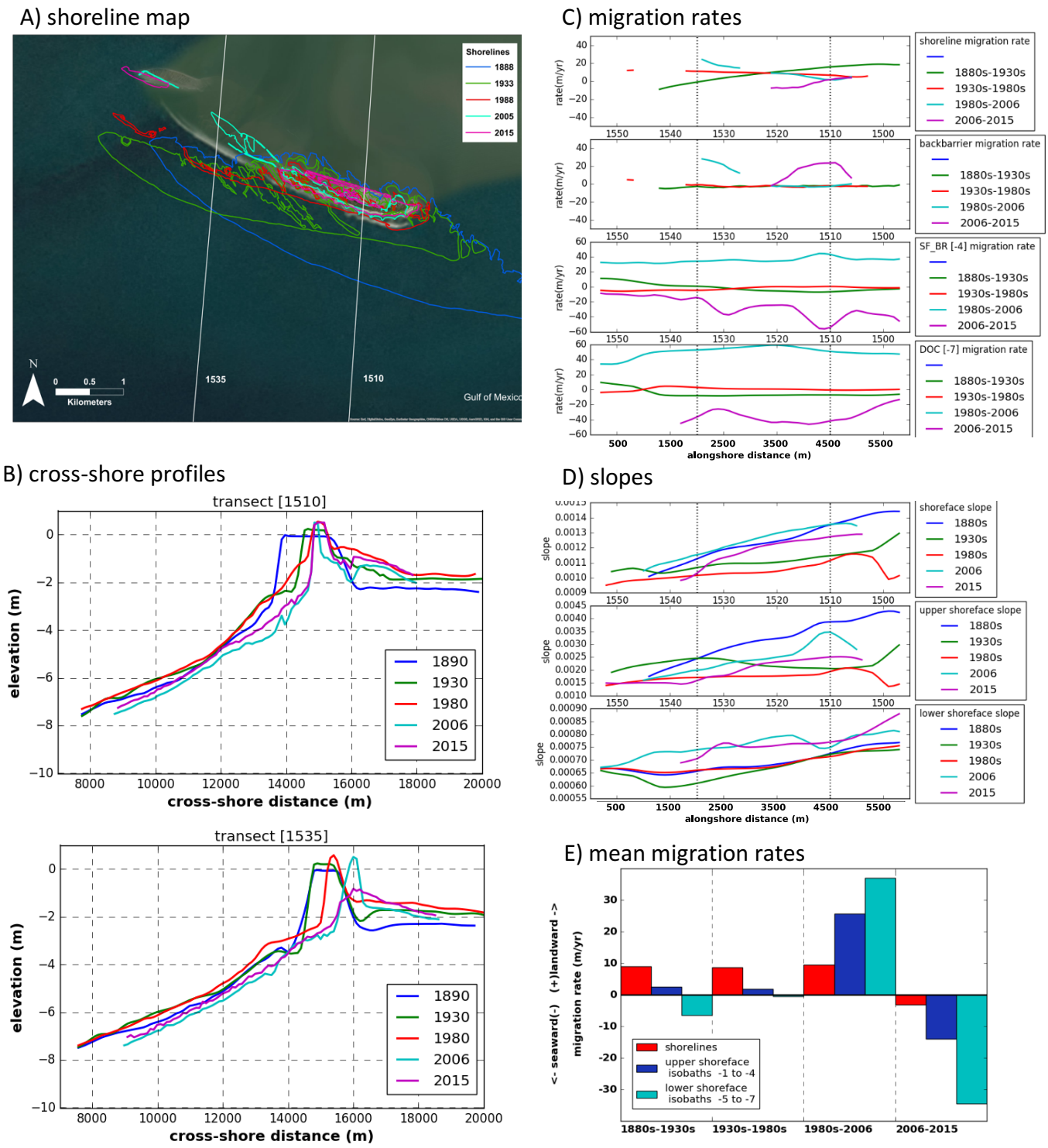

Figure 5: Raccoon Island barrier island change parameters including: A) shoreline change map, B) migration rates; b1) shoreline b2) back barrier, b3) shoreface break (-4m), b4) DOC (-7m), C) slopes; c1) shoreface slope, c2) upper shoreface slope, c3) lower shoreface slope. D) selected cross-shore profiles, E) mean migration rates for all the selected area.

Raccoon Island: Results

1880s - 1930s (Period 1)

During period 1, the Isle Dernieres barrier system was breached creating an inlet separating what is known today as Raccoon Island from Whiskey Island. The absence of a continuous shoreline and the presence of the inlet suppressed sediment bypassing facilitating the erosion of the up-drift portion of Raccoon Island transferring sediment via longshore transport processes to the west. This erosional event resulted in a landward shoreline migration rate of ~20 m/yr and the deposition on the western side resulted in spit progradation of ~10 m/yr (Fig 5C). The 1880s shoreface slopes were the steepest of all periods on the eastern side of the island with lower slopes on the western side (Fig 5D). By the 1930s, the shoreface slopes continue to relax as the island migrated landward on the eastern side and steepened on the western side as the island prograded. The landward migration of the shorelines and upper shoreface with a progradational lower shoreface (Fig. 5E) is evident in the change in the upper section (0m to -2m) of the (1510) profiles without much change on the lower shoreface (Fig 5B).

1930s - 1980s (Period 2)

Period 2 was the least active with a mean landward migration of the shoreline (~9m/yr) and relatively little change on the shoreface (Fig. 5E). The shoreface slope and upper shoreface slope both relaxed, as the shoreline retreated (Fig. 5D), and the back barrier eroded causing the barrier island to thin (Fig. 5C). The barrier was segmented when the spit on the western side was breached (Fig. 5A and C).

1980s – 2006 (Period 3)

During period 3, rock breakwaters (TE-29) were constructed in 1997 along the shoreline of the eastern side of the island (Fig. 4). As a result, the shoreline near the breakwaters remained relatively unchanged but the western side of the island migrated landward at ~20 m/yr (Fig. 5C). The effect of the breakwaters is apparent in the upper shoreface of profile 1510 (Fig. 5B). The shoreline remained in place while the rest of the profile migrated landward leading to a steeper upper shoreface slope (Fig. 5B, C, and D). Conversely, profile 1535 shows significant retreat of the upper shoreface and shoreline (Fig. 5B). Overall, the lower shoreface migrated landward at a higher rate than the upper shoreface (Fig. 5E) resulting in shoreface steepening. The upper shoreface steepened proximal to the breakwaters, as seen in the 4m isobaths migration rates (Fig. 5C), and in the change between 1980s and 2006 in the 1510 profiles (Fig. 5B).

2006 – 2015 (Period 4)

During period 4, a restoration/stabilization project (TE-48) that took place in 2007 with the construction of additional breakwaters to the west, followed by a marsh creation project in the back-barrier. This project is evident in the seaward shoreline migration (Fig. 5C) as well as the localized increase in landward back barrier migration rates (Fig. 5C). The shoreface slopes relaxed as the upper and lower shoreface migrated seaward (e.g. prograding) at rates of ~15 m/yr and ~30 m/yr respectively (Fig. 5D and E). The 4m isobaths migration rates were highest proximal to the breakwaters and decreased to the west (Fig. 5C) indicating a depositional zone on the upper shoreface.

Raccoon Island: Summary and Discussion

Over the past 135-years**,** Raccoon Island has transitioned from a robust barrier to fragmented barrier and is in the process of transgressive submergence. Beginning in 1997, mitigation projects have attempted to preserve the island. The construction of the breakwaters temporarily arrested the landward migration of the shoreline on the east end of the island (Fig. 5C). The migration rate of the west end accelerated due to a reduction in the longshore transport of sediment from east to west that supplemented the shoreline in period 1 and 2 (Fig. 5A and C). The spit fragmented in period 2 and became mostly submerged in by period 4 (Fig. 5A). The shoreline change from in period 1 illustrates the unimpeded barrier migration trajectory where the updrift end of the island was preferentially eroded and the downdrift shoreline was nourished by the liberated sediments. During period 3, the thinning of the island and the breaching of the spit are symptoms of the reduction in the sediment available to nourish the island.

The interchanging of the shoreface from a relatively stable state (P1 and P2) to erosional (P3) and next to progradational (P4) indicates that the shoreface is storm dominated whereby the shoreface recovers (post-storm) during a quiescent period (P4). The processes responsible for this recovery are in part due to longshore transport occurring in the littoral zone, and shoreface transport for areas along middle and lower shoreface.

The difference in shoreline and shoreface migration rates, by definition, controls the resulting slopes. A reduction in shoreline rate and an increase in shoreface rates yields a steeper shoreface and an increase in shoreline rates and reduction in shoreface rates yields and more relaxed shoreface. For example, relaxation of the slope due to the shoreline migrating at

a higher rate than the lower shoreface as seen in periods 1 and 2 (Fig. 5C and D). Conversely, the construction of breakwaters led to a localized steepening of the upper shoreface in period 3 due to the reduced shoreline migration (breakwaters) and storm induced erosion/migration of the shoreface. This shoreface erosion at this location may have occurred without the existence of the breakwaters, but the shoreline would have also migrated landward resulting in less change to the slope. This localized steepening may be comparable to a dredge pit that serves as a sediment trap after excavation. The 4m isobaths migration rates show a peak in seaward direction at this location, indicating the higher rates of deposition here, while to the west, rates appear reduced (Fig. 5C). This process could further reduce local sediment budgets downdrift, causing a sediment sink post storm erosion, whereby deposition is trapped starving the downdrift shoreface and barrier.

2.2 Chaland Pass to Grand Bayou Pass (Bay Joe Wise)

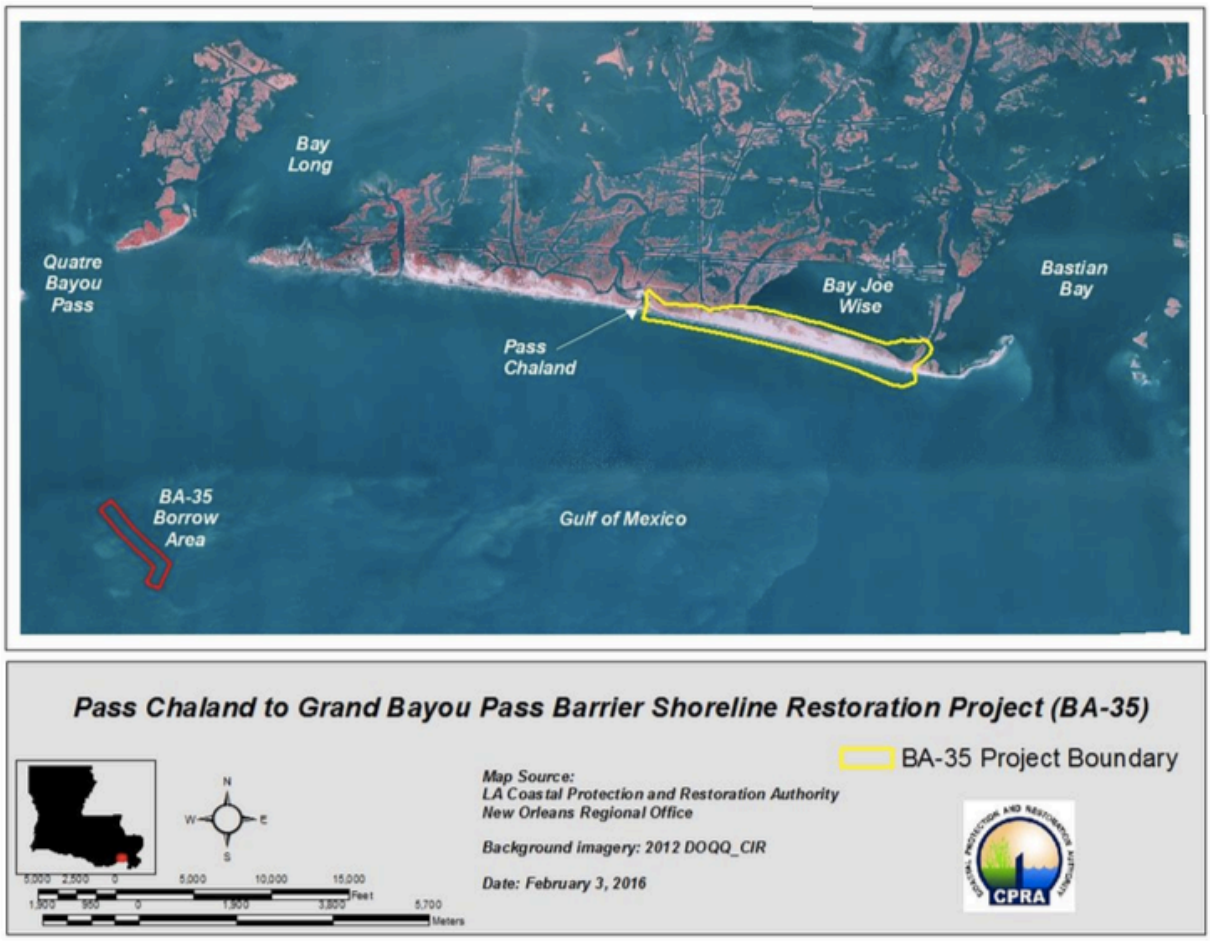

Figure 6: Pass Chaland to Grand Bayou Pass Barrier Shoreline Restoration Project map showing the project footprint (from Hymel et al. 2017).

The Chaland Pass to Grand Bayou Pass (Bay Joe Wise) project is located west of the modern Mississippi River delta and consists of a series of discontinuous sandy coastlines intercepted by tidal inlets and relict distributary channels and backed by a series marsh platforms and relict inter-distributary bays. This area has become increasing vulnerable and susceptible to storm induced breaching and erosion due insufficient sediment supply,

subsidence and an overall loss of sandy environments (dunes and beach) sediments (Hymel and Richard 2017).

The Chaland Pass area has undergone several restoration and stabilization efforts in an attempt in reestablish the continuity of the barriers through supplementing and constructing beaches and dunes to improve the resilience to storms. Beginning with the BA-38-1 Pass Chaland project in 2007 and BA-38-2 in Pelican Island portion in 2012. In 2009, the Pass Chaland to Grand Bayou Pass (Bay Joe Wise) Barrier Shoreline Restoration (BA-35) was constructed. This effort included beach and dune creation to reestablish a continuous shoreline to prevent the erosion into Bay Joe Wise which would maintain habitat in the bay, protect the interior marsh, and support the longshore processes that can beneficially supplement down-drift shorelines. BA-35 used 1.9×10^6 m^3 of sediment to build 170 ha of beach, dune, and marsh, and over 300m of shoreline (Hymel and Richard 2017).

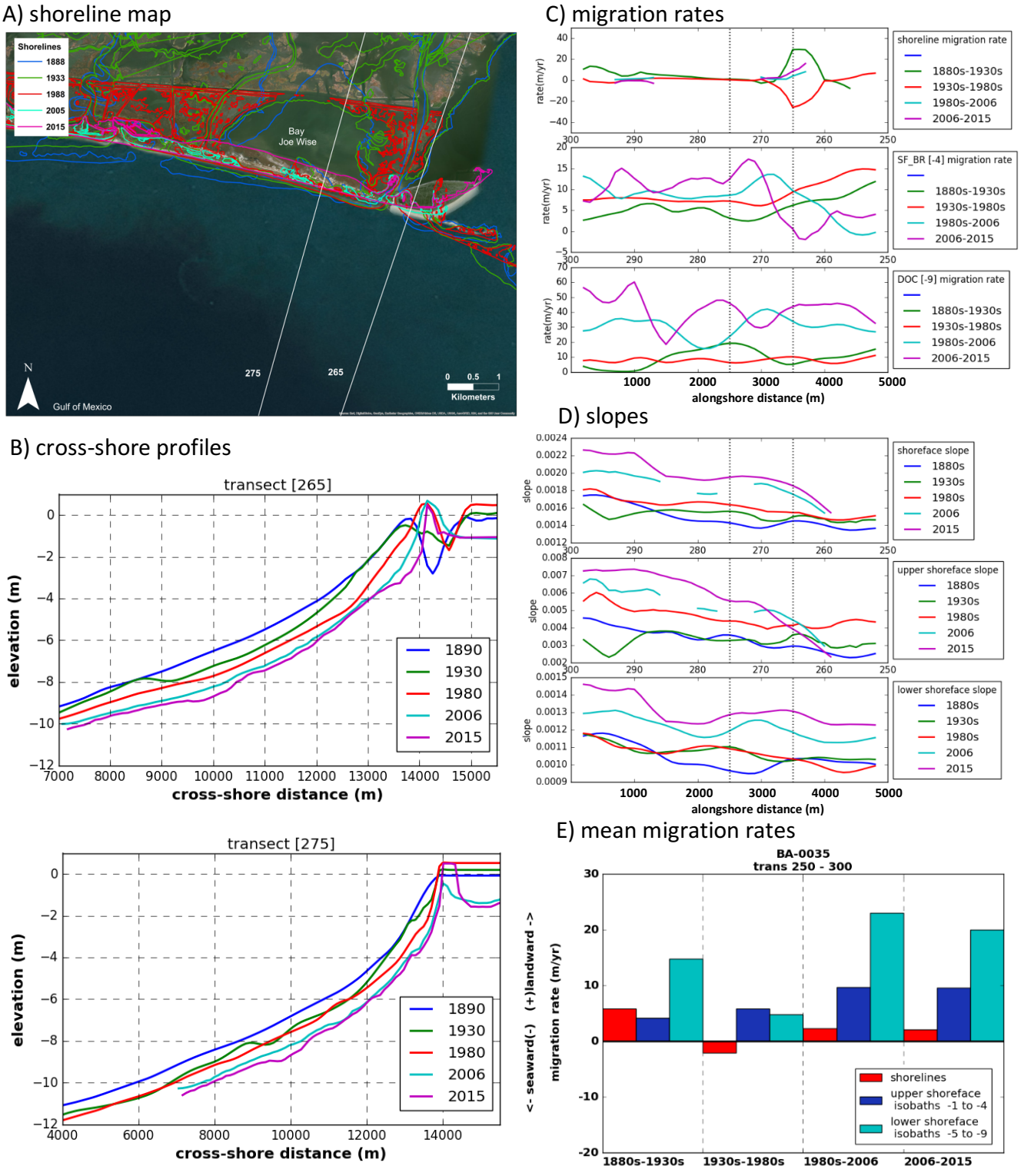

Figure 7: BA-35 barrier restoration project area historic barrier evolution parameters including; shoreline migration rates, shoreface break migration rates, shoreface slope, upper shoreface slope and lower shoreface slope. Note the increasing shoreface slope over time.

Pass Chaland to Grand Bayou Pass: Results

1880s - 1930s (Period 1)

During period 1, the west side the shoreline migrated landward (~10 m/yr) (Fig. 7A and C). On the east side, Grand Bayou Pass migrated to the east resulting in the erosion of the inner marsh where the channel bifurcates. This event is reflected in the localized increase in the landward shoreline migration rates (>20m/yr) (Fig. 7A). Higher landward migration of the lower shoreface (Fig. 7E) is evident in transects 265 and 275 profiles (blue to green lines) (Fig. 7B).

1930s - 1980s (Period 2)

In period 2, Grand Bayou Pass was constricted as the spit on the east encroached onto the inlet and resulted in the seaward migration of the shoreline (Fig. 7A and C). This progradation event is evident in profile 265 where the upper shoreface (~13,750m cross-shore distance) is below 0m for the 1880s (blue) and 1930s (green) and then emerges (~0.5 m) in the 1980s (red) (Fig. 7B). The mean migration rates for period 2 along the shoreface show a slight increase in the landward rate of the upper shoreface and a decrease in the landward migration rate of the lower shoreface compared to period 1 (Fig. 7E). Slope analysis shows that the upper shoreface slope increased across the entire reach while the lower shoreface maintained a similar slope to the previous period (Fig. 7D).

1980s – 2006 (Period 3)

In period 3, the island was breached (fragmentation in shoreline rate results) in several locations due to storm induced erosion during the 2005 hurricane season. The mean rate of shoreline retreat was (>5m/yr) but these rates do not include any areas where the shoreline no longer exists along that transect. Although the mean shoreline rate was moderate the physical

change on the shoreline was dramatic it was just in the form of shoreline submergence rather than migration. The most significant changes in this period were along the shoreface as the mean rates for the lower shoreface increased to greater than 23 m/yr (Fig. 7E) which resulted in a steepening of all shoreface slopes (Fig. 7B and D).

2006 – 2015 (Period 4)

After the widespread erosion from the 2005 hurricanes the BA-35 project was implemented in 2009 constructing beach and dune using 1.9 x 10^6 m^3 of sand. The results of this effort are evident in the 2015 shorelines (Fig. 7A) (magenta) as a continuous beach and back barrier across the front of Bay Joe Wise. The upper portion of profile 275 shows a drop in the 2006 elevation (cyan) due to the breach and a reemergence in 2015 (magenta) due to the restoration project (Fig. 7B). The shoreface continued to retreat at almost the same rates as it did in period 3 with the upper and lower shoreface migrating landward at a rate of ~10m/yr and ~20m/yr respectively, resulting in an overall steepening of the shoreface (Fig. 7D and E).

Pass Chaland to Grand Bayou Pass: Summary and Discussion

The results of the Pass Chaland to Grand Bayou Pass area analysis illustrate how the shoreline rates are complicated by the reorganization of the inlet in periods 1 and 2 and by the breaching and restoration efforts in periods 3 and 4 (Fig. 7A and C). The island breaching and shoreline segmentation that occurred in period 3 due to the storm, is not reflected in the shoreline statistics. This breaching should be recognized as a significant morphological change that has implications on the resilience of the back-barrier marsh. The BA-35 project successfully restored the sandy beach enclosing the seaward side of Bay Joe Wise, but the

addition of sediment to the shoreline has also increased the slope of the shoreface as the shoreface has continued to migrate landward.

The most significant results of the Pass Chaland case study are that the shoreface has migrated landward in all periods leading to a steeper shoreface. This trend has continued into period 4 at similar rates as the stormier period 3 which is the opposite of many other areas where the shoreface migration rates reduced during period 4. Although the BA-e35 restoration successfully enclosed the mouth of Bay Joe Wise, the continued steepening of the shoreface even in the quiescent period 4 suggest that this trend will continue. If these rates continue, the lower shoreface will migrate landward (~20 m/yr) at a higher rate than the upper shoreface (~10 m/yr) resulting in the increase in shoreface slope. This steepening could be contributing to the reduction in sand on subaerial portion of the headland by reducing the erodible portion shoreface for a given wave height, limiting overwash potential (Moore et al., 2010).

Discussion

Although literature indicates that the rates of shoreline migration and barrier thinning are linked to the shoreface slope (Bruun 1962; Wolinsky and Murray 2009; Moore et al. 2010), the direct causal relationship is not discernable along the south-central Louisiana coast over decadal time scales. The direct effects of decadal variation in the shoreface slope have less of an impact than other factors such as storms, subsidence, and mitigation projects have on the corresponding variations in shoreline migration rates. More data on shorter time-intervals would help to isolate the effects of shoreface slope resulting from these other factors. The magnitude of change of the shoreface slopes over the 135-year period may not have been sufficient to exert a distinct effect on the shoreline when analyzed on a regional scale.

Lower shoreface

The behavior of the shoreface as indicated by the mean migration rates reveals inter-regional differences that give clues to the trajectory of the shoreface and the interplay between the processes driving shoreface and shoreline change. The higher rates of shoreface retreat during period 3 which were influenced by the 2005 hurricane season, corroborate the hypothesis that the lower shoreface is active and responds with widespread erosion to storm disturbance (Miner et al., 2009b; Miner et al., 2009). Not only is the lower shoreface sensitive to storm activity, but the geometry of the shoreface in the alongshore direction can influence the response of the shoreface during quiescent times (see chapter 2). This pattern can be observed in the return of the lower shoreface to progradational in the Isle Dernieres and Grand

Isle and Grand Terre regions in contrast to the continued landward migration of the Timbalier, Caminada, and Modern Delta regions (Fig. 3).

Upper shoreface

The fluctuations of shoreface slope that are occurring are mostly on the more active upper shoreface (Hallermeier 1980), as seen in the Raccoon Island example. In the Chaland Pass example, the entire shoreface is steepening over time as the lower shoreface is migrating landward at higher rates. One difference between these two locations is likely the result of the proximity of Ship Shoal to Raccoon Island which partially protects the island shoreface from the impacts of large storm events. Ship Shoal attenuates larger waves while smaller waves still reach the shoreline resulting in more active upper shoreface and less active lower shoreface.

The Raccoon Island shoreface erosion was most active during the stormy period 3 resulting in steeper shoreface slopes. Diminished shoreface erosion and localized deposition in periods 2 and 4 led to some reduction in slope in the calmer periods.

Even though there is a recovery of the shoreface and a relaxing of the slope in some areas there is not a response in the migration rates of the shorelines that can be separated from the other processes, such as storms, that dominate the morphologic change of the system. For these variations in shoreface slope to have significant impacts on the magnitude of change in shoreface slope will have to increase. This could be the future scenario for areas like the Chaland Headland where the trend over the 135-year period is an increase in the rate of steepening with few signs of recovery.

Shorelines

Regardless of whether the steepness of the slope is contributing to a reduction in landward shoreline migration rates, the difference in shoreline and shoreface migration rates, by definition, controls the resulting slopes. A reduction in shoreline rate and an increase in shoreface rates yields a steeper shoreface (Chaland) and an increase in shoreline rates and reduction in shoreface rates yields and more relaxed shoreface (Raccoon).

The regional comparison of shoreline migration rates and shoreface slopes indicate that the two zones that have the largest magnitude of reduction of landward migration rates (>15m/yr reduction) are Caminada and Modern Delta. These two zones are the locations with the most extensive back barrier marsh. This marsh may have reduced the rate of landward migration of the shoreline resulting in a steeper shoreface.

Sediment Supply

None of the barriers islands are sustaining subaerial exposure except for Grand Isle which has benefitted by the combination of stabilization projects, proximity to Barataria Bight, and receiving nourishment from the erosion of Caminada Headland. Moore et al. (2010) found that for a barrier to reach a steady state of equilibrium (maintain geometry) the barrier trajectory converges with the substrate slope as the barriers mature (Moore et al. 2010; Moore and Murray 2018). In this case, the barriers must be able to keep pace long enough to reach that state. Two factors are limiting the possibilities of attaining this steady state, sediment supply and substrate composition. Moore et al. (2010) found that as the barrier migrates landward the shoreface is incising into the substrate and liberating sediment that nourishes the

barrier, but the composition of the substrate determines how much of that material is lost as fines are entrained in the water column and cannot supplement the barrier (Moore and Murray 2018). In the MRDP, the substrate is made up of deltaic deposits with a low percentage of sand (~15%, Georgiou et al., 2011) that are mostly lost from the area as the shoreface is eroded leading to a net loss of sediment (Miner et al., 2009).

The monitoring of shoreface migration rates and trajectories can aid in the creation and updating of a regional sediment budget that can be used to aid the allocating limited resources for barrier island restoration projects.

Conclusions:

1. Regional analysis of shoreface slope and shoreline migration rates do not show a discernable direct coupling in south-central Louisiana barrier islands over the 135-year period.
2. Although some of the broad conclusions about their connectivity are clouded by the storm activity and anthropogenic interventions, there are clear advantages to tracking these parameters as another tool to aid in the understanding regional long-term trajectories of the coast.
3. The Raccoon Island and Chaland Headland case studies show the how these tools include the shoreface to aid in the comprehensive understanding of barrier trajectory through the interpretation of changes in long-term barrier island evolution parameters.

References:

Aagaard, T., & Sørensen, P. (2012). Coastal profile response to sea level rise: A process-based approach. *Earth Surface Processes and Landforms*, *37*(3), 354–362. https://doi.org/10.1002/esp.2271

Barbier, E. B., Hacker, S. D., Kennedy, C., Koch, E. W., Stier, A. C., & Silliman, B. R. (2011). The value of estuarine and coastal ecosystem services. *Ecological Monographs*, *81*(2), 169–193.

Barras, J., Beville, S., Britsch, D., Hartley, S., Hawes, S., Johnston, J., … Suhayda, J. (2004). Historical and Projected Coastal Louisiana Land Changes : 1978-2050. *World*, *334*(January), 45. Retrieved from http://www.louisianaspeaks-parishplans.org/projectattachments/001246/NewHistoricalland.pdf

Barrell, J. (1912). Criteria for the recognition of ancient delta deposits. *GSA Bulletin*, *23*(1), 377–446. Retrieved from http://dx.doi.org/10.1130/GSAB-23-377

Bilskie, M. V., Hagen, S. C., Alizad, K., Medeiros, S. C., Passeri, D. L., Needham, H. F., & Cox, A. (2016). Dynamic simulation and numerical analysis of hurricane storm surge under sea level rise with geomorphologic changes along the northern Gulf of Mexico. *Earth's Future*, (April), n/a-n/a. https://doi.org/10.1002/2015EF000347

Bruun, P. (1962). *Sea-level Rise as a Cause of Shore Erosion*. Florida Engineering and Industrial Experiment Station. Retrieved from https://books.google.com/books?id=UJ_iHAAACAAJ

Byrnes, M. R., Berlinghoff, J. L., Griffee, S. F., Underwood, S. G., & Lee, D. M. (2017). Louisiana Barrier Island Comprehensive Monitoring Program (BICM): Phase 2 - Shoreline Compilation and Change Assessment. Prepared for : Louisiana Coastal Protection and Restoration Authority Prepared by : Louisiana Barrier Island Comprehensive Monitorin, (February), 41 p. plus appendices.

Cooper, J. A. G., & Pilkey, O. H. (2004). Sea-level rise and shoreline retreat: Time to abandon the Bruun Rule. *Global and Planetary Change*, *43*(3–4), 157–171. https://doi.org/10.1016/j.gloplacha.2004.07.001

Couvillion, B. R., Beck, H. J., Schoolmaster, D., & Fischer, M. R. (2016). *Land Area Change in Coastal Louisiana (1932 to 2016)*.

Coastal Protection and Restoration Authority of Louisiana. (2017). *Louisiana's Comprehensive Master Plan for a Sustainable Coast.* Coastal Protection and Restoration Authority of Louisiana. Baton Rouge, LA

Davis, R. A., & FitzGerald, D. M. (2004). *Beaches and Coasts*. *Estuarine, Coastal and Shelf Science*. Blackwell Science, Oxford, England. https://doi.org/10.1016/j.ecss.2004.11.006

Dean, R. G. (1977). *Equilibrium Beach Profiles: U.S. Atlantic and Gulf Coasts*. Center for Apllied Coastal Research. Retrieved from https://books.google.com/books?id=_bMRywAACAAJ

Dean, R. G. (1991). Equilibrium Beach Profiles : Characteristics and Applications. *Journal of Coastal Research*, *7*(1), 53–84. https://doi.org/10.2307/4297805

Fearnley, S. M., Miner, M. D., Kulp, M., Bohling, C., & Penland, S. (2009). Hurricane impact and recovery shoreline change analysis of the Chandeleur Islands, Louisiana, USA: 1855 to 2005. *Geo-Marine Letters*, *29*(6), 455–466. https://doi.org/10.1007/s00367-009-0155-5

FitzGerald, D. M., Fenster, M. S., Argow, B. A., & Buynevich, I. V. (2008). *Coastal Impacts Due to Sea-Level Rise*. *Annual Review of Earth and Planetary Sciences* (Vol. 36).

https://doi.org/10.1146/annurev.earth.35.031306.140139
Frazier, D. (1967). *Recent Deltaic Deposits of Mississippi River: Their Development and Chronology*. *Aapg Bulletin - AAPG BULL* (Vol. 51). https://doi.org/10.1306/5D25C219-16C1-11D7-8645000102C1865D
Georgiou, I. Y., FitzGerald, D. M., & Stone, G. W. (2005). The Impact of Physical Processes along the Louisiana Coast. *Journal of Coastal Research*, *Sp. Issue*(Figure 1), 72–89. Retrieved from http://www.jstor.org/stable/10.2307/25737050
Hallermeier, R. J. (1980). A profile zonation for seasonal sand beaches from wave climate. *Coastal Engineering*, *4*, 253–277. https://doi.org/https://doi.org/10.1016/0378-3839(80)90022-8
Hymel, M. K., & Richard, B. J. (2017). 2016 Operations , Maintenance , and Monitoring Report Pass Chaland to Grand Bayou Pass Barrier Shoreline Restoration (BA-35).
Jaffe, B. E., List, J. H., & Sallenger, A. H. (1997). Massive sediment bypassing on the lower shoreface offshore of a wide tidal inlet - Cat Island Pass, Louisiana. *Marine Geology*, *136*(3–4), 131–149. https://doi.org/10.1016/S0025-3227(96)00050-3
Kulp, M. A., Fitzgerald, D. M., & Penland, S. (2005). Sand-rich Lithosomes of the Holocene Mississippi River Delta Plain. In *River Deltas* (pp. 277–294).
List, J. H., Jaffe, B. E., Sallenger, A. H., Williams, S. J., Mcbride, R. A., & Penland, S. (1994). *Louisiana Barrier Island Erosion Study: Atlas of Sea-Floor Changes from 1878 to 1989*.
List, J. H., Sallenger, A. H., Hansen, M. E., & Jaffe, B. E. (1997). Accelerated relative sea-level rise and rapid coastal erosion: testing a causal relationship for the Louisiana barrier islands. *Marine Geology*, *140*(3–4), 347–365. https://doi.org/10.1016/S0025-3227(97)00035-2
Lorenzo-Trueba, J., & Ashton, A. D. (2014). Rollover, drowning, and discontinuous retreat: Distinct modes of barrier response to sea-level rise arising from a simple morphodynamic model. *Journal of Geophysical Research: Earth Surface*, *119*(6), 1310–1321. https://doi.org/10.1002/2013JF003034.Received
Martinez, L., Brien, S. O., Bethel, M., & Penland, S. (2009). Louisiana Barrier Island Comprehensive Monitoring Program (BICM) Volume 2 : Shoreline Changes and Barrier Island Land Loss 1800 ' s - 2005, *2*.
Mcbride, R. A., Penland, S., Hiland, M. W., Williams, S. J., Westphal, K. A., Jaffe, B. E., & Sallenger, A. H. (1991). Analysis of Barrier Shoreline Change in Louisiana from 1853 to 1989.
Miner, M. D., Kulp, M. A., FitzGerald, D. M., Flocks, J. G., & Weathers, H. D. (2009). Delta lobe degradation and hurricane impacts governing large-scale coastal behavior, South-central Louisiana, USA. *Geo-Marine Letters*, *29*(6), 441–453. https://doi.org/10.1007/s00367-009-0156-4
Miner, M. D., Kulp, M. A., FitzGerald, D. M., & Georgiou, I. Y. (2009). Hurricane-associated ebb-tidal delta sediment dynamics. *Geology*, *37*(9), 851–854. https://doi.org/10.1130/G25466A.1
Moore, L. J., List, J. H., Williams, S. J., & Stolper, D. (2010). Complexities in barrier island response to sea level rise: Insights from numerical model experiments, North Carolina Outer Banks. *Journal of Geophysical Research*, *115*(F3), F03004 1-27. https://doi.org/10.1029/2009JF001299
Moore, L. J., & Murray, A. B. (2018). *Barrier Dynamics and Response to Changing Climate*.

Niedoroda, A. W., & Swift, D. J. P. (1991). Handbook of Coastal and Ocean Engineering. In J. B. Herbich (Ed.) (pp. 736–769). Houston: Gulf Publishing Company.

Nordstrom, K. F. (2014). Living with shore protection structures: A review. *Estuarine, Coastal and Shelf Science*, *150*(PA), 11–23. https://doi.org/10.1016/j.ecss.2013.11.003

Penland, S., Boyd, R., & Suter, J. R. (1988a). Delta Plain : a Model for Barrier Shoreline and. *Journal of Sedimentary Petrology*, *58*(6), 932–949.

Penland, S., Boyd, R., & Suter, J. R. (1988b). Transgressive depositional systems of the Mississippi Delta plain; a model for barrier shoreline and shelf sand development. *Journal of Sedimentary Research*. https://doi.org/10.1306/212F8EC2-2B24-11D7-8648000102C1865D

Ranasinghe, R., & Stive, M. J. F. (2009). Rising seas and retreating coastlines. *Climatic Change*, *97*(3), 465–468. https://doi.org/10.1007/s10584-009-9593-3

Stone, G. W., & McBride, R. A. (1998). Louisiana barrier islands and their importance in wetland protection: forecasting shoreline change and subsequent response of wave climate. *Journal of Coastal Research*. Retrieved from http://www.jstor.org/stable/10.2307/4298843

Swift, D. J. P. (1975). Barrier-island genesis: evidence from the central atlantic shelf, eastern U.S.A. *Sedimentary Geology*, *14*(1), 1–43. https://doi.org/10.1016/0037-0738(75)90015-9

Wolinsky, M. A., & Murray, A. B. (2009). A unifying framework for shoreline migration: 2. Application to wave-dominated coasts. *Journal of Geophysical Research: Earth Surface*, *114*(1), 1–13. https://doi.org/10.1029/2007JF000856

VITA

Benjamin Beasley was born in 1977 in Montgomery, Alabama. He graduated from high school at Parkway West High School in St. Louis, Missouri in 1995. After moving to New Orleans in 2012, he began attending the University of New Orleans and completed a Bachelor of Science in Earth and Environmental Sciences in May of 2016. In the fall of 2016, he returned to the University of New Orleans to pursue a Master of Science in Earth and Environmental Sciences which he completed in August of 2018.